



ALMA MATER STUDIORUM  
UNIVERSITÀ DI BOLOGNA

Department of Physics and Astronomy "A. Righi"

Second cycle degree

Physics

# Tensor Perturbations

Supervisor:  
Prof. Roberto Balbinot

Defended by:  
Luca Morelli

Co-Supervisor:  
Dott. Fabio Finelli



## **Abstract**

## Notations and conventions

# Contents

Abstract . . . . .	iii
Notations and conventions . . . . .	iv
<b>I The homogeneous universe</b>	<b>1</b>
<b>1 The Friedmann Robertson Walker Universe</b>	<b>3</b>
1.1 The geometry of the universe . . . . .	3
1.1.1 The Friedmann Robertson Walker metric . . . . .	4
1.1.2 Dynamical effects in the Robertson Walker universe . . . . .	9
1.2 The Friedmann equations . . . . .	11
1.2.1 Cosmic fluids . . . . .	11
1.2.2 The Friedmann equations . . . . .	12
1.2.3 The $\Lambda$ CDM model . . . . .	15
<b>II The inhomogeneous universe</b>	<b>19</b>
<b>III CMB physic</b>	<b>21</b>
<b>2 Anisotropies of the CMB</b>	<b>23</b>
2.1 Angular power spectrum . . . . .	23
2.1.1 Multipole expansion . . . . .	25
2.1.2 From perturbations to anisotropies . . . . .	26
2.2 Time evolution of anisotropies . . . . .	27
2.2.1 Polarization from Compton scattering . . . . .	29
2.2.2 Multipole expansion of the Boltzmann equation . . . . .	33
2.2.3 Polarization power spectrum Check convention . . . . .	34
2.3 Tensor perturbations effects on the CMB . . . . .	35

2.3.1	Coupling of tensors to anisotropies . . . . .	35
2.3.2	Multipole expansion of tensor induced anisotropies . . . . .	37
2.4	Approximate solutions for the dynamics of the anisotropies . . . . .	38
2.4.1	The tight coupling approximation . . . . .	39
2.4.2	Improved tight coupling approximation . . . . .	39
<b>3</b>	<b>Spectral Distortions</b>	<b>41</b>
3.1	The thermalization problem . . . . .	41
3.1.1	Thermalization scales . . . . .	44
3.2	Modeling spectral distortions . . . . .	45
3.2.1	Shapes of spectral distortions . . . . .	45
3.2.2	Amplitudes of spectral distortions . . . . .	48
3.2.3	Injected, deposited energy and heating rate . . . . .	49
3.2.4	Branching ratios and the Green's function approach . . . . .	51
3.3	Silk dumping . . . . .	53
3.3.1	Mixing of blackbodies . . . . .	53
3.3.2	Comptonization of mixed blackbodies . . . . .	56
3.3.3	Mixing of polarized blackbodies . . . . .	57
3.3.4	Dissipation of acoustic waves . . . . .	59
<b>A</b>	<b>Differential geometry tools</b>	<b>61</b>
A.1	Maximally symmetric spaces . . . . .	61
<b>B</b>	<b>Thermodynamics tools</b>	<b>65</b>
B.1	Phase space distribution and thermodynamics observable . . . . .	65
B.1.1	Small chemical potential approximation . . . . .	65
B.2	Scalar perturbed Liouville operator . . . . .	66
B.3	Collision term . . . . .	68
B.4	Tensor perturbed Liouville operator . . . . .	68

# I

## The homogeneous universe





# Chapter 1

## The Friedmann Robertson Walker Universe

Cosmology is based upon two basics principles:

- **the Copernican Principle**, or that all the observers are on equal footing;
- **the Cosmological Principle**, which states that the universe, at the largest scales, is homogeneous and isotropic.

These principles may not seem to be consistent with physical reality: clearly the core of a star is very different from empty space or even from the interior of planets, but in order to describe the whole universe we need to make some simplifying assumptions. Observations, for example of the distribution of galaxies or of the cosmic microwave background radiation, show that at large scales, on average, the universe looks the same in all directions. From the Copernican Principle we then get that all observers should see an isotropic universe, thus we can claim that all points of the universe should also look the same. Again we should stress that these are just assumptions that, at some large scale, we think can become adequate to approximate the description of space, allowing us to reduce significantly the degrees of freedom that we have to study.

### 1.1 The geometry of the universe

We now have to translate the proprieties of isotropy and homogeneity to the language of General Relativity, namely differential geometry and manifolds.

Notice that the two above principles refer only to the universe, or better, to space at a fixed time, therefore it is space which is really isotropic and homogeneous, while time has no particular symmetries.

Hence, we will assume that space is **maximally symmetric**, which means that it possesses the maximum number of independent Killing vectors. In fact, homogeneity guarantees 3 Killing vectors, associated to the 3 possible space translations, while isotropy guarantees other 3 Killing vectors, associated to the 3 rotations around a point, and the maximum number of independent Killing vectors for a 3D manifold is indeed 6 (this is

proven in Appendix A.1). In the next sections we will study first how to describe a space-time with the above proprieties, then we will work out the dynamics that the Einstein field equations give to it.

### 1.1.1 The Friedmann Robertson Walker metric

We will now proceed constructing charts (coordinates) that are the more convenient to describe the assumed geometry. The main goal of this section is to find the most general form of the metric of an isotropic and homogeneous universe.

To start, consider a space-like hypersurface  $\Sigma$  (a volume in this case), which is a slice of the spacetime manifold, corresponding to space (the universe) at a fixed time. On this hypersurface we choose one chart with coordinates  $x^\mu = (0, x^1, x^2, x^3)$ .

For each point  $P \in \Sigma$  we pick a vector  $\vec{n}$  that is orthogonal to  $\Sigma$  (it should be orthogonal to each vector of the tangent space, in  $P$ , of the submanifold defined by  $\Sigma$ ) such that those are normalized to  $-1$  (since they must be time-like).

In each point  $P$ , the following Cauchy problem defines a unique geodesic, for which  $\vec{n}$  is the tangent vector,

$$\begin{cases} (\nabla_{\vec{n}} \vec{n})^\mu = \frac{d^2 x^\mu}{dt^2} + \Gamma_{\nu\lambda}^\mu \frac{dx^\nu}{dt} \frac{dx^\lambda}{dt} = 0, \\ \left. \frac{dx^\mu}{dt} \right|_P = n^\mu|_P, \\ x^\mu(0) = x^\mu|_P. \end{cases} \quad (1.1)$$

We can extend our initial chart, in a neighborhood of  $\Sigma$ , assigning to each point  $Q$  the coordinates  $x^\mu = (t, x^1, x^2, x^3)$ , where  $t$  is the value (in  $Q$ ) of the parameter of the geodesic passing through  $Q$ , and  $(0, x^1, x^2, x^3)$  are the coordinates of the point  $P$ , from which the geodesic starts. These coordinates will eventually fail once some geodesics, from our construction, will meet and intersect.

We now want to describe the metric of our spacetime manifold using one of these charts. To do so we will take the chart induced basis of each tangent space  $(\partial_t, \partial_1, \partial_2, \partial_3)$  and then label them:

$$\partial_t = \vec{n}, \quad \partial_i = \vec{Y}_{(i)},$$

where  $\partial_t$  is by construction the normal vector field we have defined, since  $\vec{n}$  is tangent to each geodesic by (1.1) and then is parallel transported along them.

Using this basis, the first component of the metric reads, by our initial construction and because scalar products of parallel transported vectors is preserved by metric connection,

$$g_{tt} = g(\partial_t, \partial_t) = n^\mu n_\mu = -1. \quad (1.2)$$

On  $\Sigma$ , from our construction hypothesis  $\vec{n} \perp \Sigma$ , the time-spacial mixed components read

$$g_{ti} = g(\partial_t, \partial_i) = n_\mu Y_{(i)}^\mu = 0. \quad (1.3)$$

We can prove that this holds also outside  $\Sigma$  by evaluating its covariant derivative along

one of the geodesics we constructed

$$\begin{aligned}
 n^\nu \nabla_\nu (n_\mu Y_{(i)}^\mu) &= n^\nu n_\mu \nabla_\nu (Y_{(i)}^\mu) + Y_{(i)}^\mu n^\nu \nabla_\nu (n_\mu) \\
 &= n^\nu n_\mu \nabla_\nu (Y_{(i)}^\mu) \\
 &= Y_{(i)}^\nu n_\mu \nabla_\nu (n^\mu) \\
 &= \frac{1}{2} (Y_{(i)}^\nu n_\mu \nabla_\nu (n^\mu) + Y_{(i)}^\nu n_\mu \nabla_\nu (n^\mu)) \\
 &= \frac{1}{2} (Y_{(i)}^\nu n_\mu \nabla_\nu (n^\mu) + Y_{(i)}^\nu n_\mu \nabla_\nu (g^{\mu\lambda} n_\lambda)) \\
 &= \frac{1}{2} (Y_{(i)}^\nu n_\mu \nabla_\nu (n^\mu) + Y_{(i)}^\nu n_\mu \nabla_\nu (g^{\mu\lambda}) n_\lambda + Y_{(i)}^\nu n_\mu g^{\mu\lambda} \nabla_\nu (n_\lambda)) \\
 &= \frac{1}{2} (Y_{(i)}^\nu n_\mu \nabla_\nu (n^\mu) + Y_{(i)}^\nu n^\lambda \nabla_\nu (n_\lambda)) \\
 &= \frac{1}{2} Y_{(i)}^\nu \nabla_\nu (n^\lambda n_\lambda) = 0,
 \end{aligned}$$

in which we used (in order): the geodesic equation  $n^\nu \nabla_\nu (n_\mu) = 0$ , that coordinates vectors commute, so that  $[\vec{n}, \vec{Y}_{(i)}]^\mu = n^\nu \nabla_\nu (Y_{(i)}^\mu) - Y_{(i)}^\nu \nabla_\nu (n^\mu) = 0$ <sup>1</sup>, the metric connection condition  $\nabla g = 0$ , and last that, being  $n^\mu n_\mu = -1$ , its derivative vanishes.

Summing up the above results, we can write the metric, from (1.2) and (1.3), as

$$ds^2 = -dt^2 + g_{ij} dx^i dx^j.$$

In this expression the absence of the mixed terms  $dt dx^i$  reflects that there exist a family of hypersurfaces, defined by  $t = \text{const}$ , that are all orthogonal to the vector field  $\vec{n}$ . These represent the evolved universe at different times.

The spatial components of the metric now depend on all the coordinates of the chart we have introduced. If we consider how time evolution could affect the spatial terms we can deduce that all the components  $g_{ij}$  should scale in the same way, otherwise we could have different scaling in different directions, which is against the idea that space is isotropic. We will write explicitly the time dependence as

$$ds^2 = -dt^2 + a^2(t) g_{ij} dx^i dx^j.$$

Let's now take into account that each space hypersurface is a maximally symmetric submanifold. As showed in Appendix A.1, maximally symmetric manifolds have the peculiar propriety that, due to their high number of symmetries, the Riemann tensor reduces, in 3 dimensions, to

$${}^{(3)}R_{ijkl} = \frac{{}^{(3)}R}{6} (g_{ik} g_{jl} - g_{il} g_{jk}),$$

in which the  ${}^{(3)}$  is used to signal that these are tensors referred to the submanifold  $\Sigma$  and  ${}^{(3)}R$  is the Ricci scalar. The Ricci tensor thus reads:

$${}^{(3)}R_{ij} = \frac{{}^{(3)}R}{6} (3g_{ij} - g^{lk} g_{il} g_{jk}) = \frac{{}^{(3)}R}{3} g_{ij}. \quad (1.4)$$

With this relation, we want to determine the metric without the Einstein field equations. To simplify the metric, we can note that, being maximally symmetric, each space submanifold will also have spherical symmetry. This allows us to write the metric in spherical

---

<sup>1</sup>The Christoffel symbols cancel out, due to symmetric connection, leaving only partial derivatives.

coordinates as

$$ds^2 = -dt^2 + a(t)^2 [e^{2\beta(r)} dr^2 + e^{2\gamma(r)} r^2 (d\theta^2 + \sin^2 \theta d\phi^2)],$$

where  $\beta(r)$ ,  $\gamma(r)$  are some unknown functions, that depend only on the radial coordinate due to spherical symmetry. Note that we exploited the exponential in order to preserve the signature. Lastly, the angular part,  $d\Omega^2 = d\theta^2 + \sin^2 \theta d\phi^2$ , must scales with an overall factor  $e^{2\gamma}$ , in order to maintain sphere to be perfectly round.

We can simplify this metric even more by scaling the radial coordinate

$$r \rightarrow e^{-\gamma(r)} r, \quad dr \rightarrow \left(1 - r \frac{d\gamma}{dr}\right) e^{-\gamma(r)} dr,$$

in this way the metric becomes

$$ds^2 = -dt^2 + a^2(t) \left[ \left(1 - r \frac{d\gamma}{dr}\right)^2 e^{2(\beta(r)-\gamma(r))} dr^2 + r^2 (d\theta^2 + \sin^2 \theta d\phi^2) \right].$$

Since  $g_{rr}$  must always be non-negative, we can define a function  $\alpha(r)$ , such that  $e^{2\alpha} = \left(1 - r \frac{d\gamma}{dr}\right)^2 e^{2(\beta(r)-\gamma(r))}$ , so that the metric reads

$$ds^2 = -dt^2 + a^2(t) [e^{2\alpha(r)} dr^2 + r^2 (d\theta^2 + \sin^2 \theta d\phi^2)].$$

Now, we can evaluate the Christoffel symbols of the metric restricted to the universe submanifold (because with this construction the time component has no dynamics):

$$\begin{aligned} {}^{(3)}\Gamma_{rr}^r &= \frac{d\alpha}{dr}, & {}^{(3)}\Gamma_{r\theta}^\theta &= \frac{1}{r}, & {}^{(3)}\Gamma_{\theta\theta}^r &= -re^{-2\alpha}, & {}^{(3)}\Gamma_{rr}^r &= \frac{\cos \theta}{\sin \theta}, \\ {}^{(3)}\Gamma_{r\phi}^\phi &= \frac{1}{r}, & {}^{(3)}\Gamma_{\phi\phi}^r &= -re^{-2\alpha} \sin^2 \theta, & {}^{(3)}\Gamma_{\phi\phi}^\theta &= -\sin \theta \cos \theta, \end{aligned} \quad (1.5)$$

all the others are zero or deducible from the symmetries of the above.

We then obtain the non-vanishing components of the Riemann tensor are:

$$\begin{aligned} {}^{(3)}R_{\theta r \theta}^r &= re^{-2\alpha} \frac{d\alpha}{dr}, \\ {}^{(3)}R_{\phi r \phi}^r &= re^{-2\alpha} \sin^2 \theta \frac{d\alpha}{dr}, \\ {}^{(3)}R_{\phi \theta \phi}^\theta &= (1 - e^{-2\alpha}) \sin^2 \theta. \end{aligned} \quad (1.6)$$

Lastly, we can get the Ricci tensor:

$${}^{(3)}R_{rr} = \frac{2}{r} \frac{d\alpha}{dr}, \quad {}^{(3)}R_{\theta\theta} = e^{-2\alpha} \left[ r \frac{d\alpha}{dr} - 1 \right] + 1, \quad {}^{(3)}R_{\phi\phi} = \sin^2 \theta R_{\theta\theta}. \quad (1.7)$$

Combining the expression for the Ricci tensor (1.4) and the one above (1.7), we end up with two differential equations that can be solved to determine the metric

$$\begin{aligned} {}^{(3)}R_{rr} &= \frac{{}^{(3)}R}{3} g_{tt} \Rightarrow \boxed{\frac{2}{r} \frac{d\alpha}{dr} = \frac{{}^{(3)}R}{3} e^{2\alpha}} \\ {}^{(3)}R_{ij} &= \frac{{}^{(3)}R}{3} g_{ij} \Rightarrow \boxed{e^{-2\alpha} \left[ r \frac{d\alpha}{dr} - 1 \right] + 1 = \frac{{}^{(3)}R}{3} r^2}. \end{aligned}$$

Since we have two equations for one unknown, substituting the first equation into the second one, we can obtain an initial condition for the former

$$\frac{d\alpha}{dr} = \frac{{}^{(3)}R}{6} r e^{2\alpha}, \quad e^{-2\alpha} \left[ \frac{{}^{(3)}R}{6} r^2 e^{2\alpha} - 1 \right] + 1 = \frac{{}^{(3)}R}{3} r^2.$$

To solve this differential equation we start by defining  $k = \frac{{}^{(3)}R}{6}$ , and then we integrate

$$\int e^{-2\alpha} d\alpha = \int k r dr \Rightarrow e^{-2\alpha} = -kr^2 + C,$$

then, to determine  $C$  we plug this solution into the initial condition

$$\begin{aligned} 2kr^2 &= e^{-2\alpha} \left[ kr^2 e^{2\alpha} - 1 \right] + 1 = kr^2 - e^{-2\alpha} + 1 \\ &= kr^2 + kr^2 - C + 1 = 2kr^2 - C + 1, \quad \Rightarrow \quad C = 1. \end{aligned}$$

In this way we have obtained the **Friedmann Robertson Walker metric** (FRW metric)

$$ds^2 = -dt^2 + a^2(t) \left[ \frac{dr^2}{1 - kr^2} + r^2(d\theta^2 + \sin^2 \theta d\phi^2) \right], \quad (1.8)$$

notice that, to obtain this metric, we never used the Einstein field equation, but only geometrical proprieties of spacetime, deduced from the cosmological principle, therefore this metric is totally generic once we assume the cosmological principle.

The coordinates  $(t, r, \theta, \phi)$  are called **comoving coordinates**, since these precise choice makes manifest the isotropy and homogeneity of the universe, that wouldn't be manifest in a moving reference frame with respect to the universe content (the cosmic fluid that we will use to model it). In this metric appear two parameters

- $a(t)$ , the **cosmic scale factor**, which measure how the "size" of the universe change with time;
- $k$ , the **curvature constant**, that is proportional to the Ricci scalar of each universe submanifold and thus measures the curvature of space.

These parameters can be rescaled as follows, without affecting the metric (1.8),

$$r \rightarrow \lambda r, \quad a \rightarrow \lambda^{-1} a, \quad k \rightarrow \lambda^{-2} k,$$

this allows to give dimensions of a length arbitrarily to  $r$  or to  $a$ .

We will now give some interpretation to the curvature constant that appears in the Friedmann Robertson Walker metric (1.8).

First, it is useful to use the scale invariance of the metric to reduce the possible values of this parameter so that it is just its sign to determine the curvature. Rescaling as follows

$$r \rightarrow \sqrt{|k|} r, \quad a \rightarrow \frac{a}{\sqrt{|k|}}, \quad k \rightarrow \frac{k}{|k|},$$

$k$  can now only assume the following values  $\{-1, 0, +1\}$ .

Let's now discuss the geometry associated to each value of  $k$ , we will focus just on the spatial metric  $d\sigma^2 = \frac{dr^2}{1 - kr^2} + r^2(d\theta^2 + \sin^2 \theta d\phi^2)$ .

- **Flat universe**, for  $k = 0$ , the metric reduces to usual metric of  $\mathbb{R}^3$  in spherical coordinates

$$d\sigma^2 = dr^2 + r^2(d\theta^2 + \sin^2 \theta d\phi^2)$$

which correspond to a flat universe.

- **Closed universe**, for  $k = +1$ , the metric can be reduced to a more familiar one introducing

$$d\chi = \frac{dr}{\sqrt{1-r^2}} \Rightarrow r = \sin \chi,$$

$$d\sigma^2 = d\chi^2 + \sin^2 \chi (d\theta^2 + \sin^2 \theta d\phi^2),$$

which clearly shows that the radial coordinate is bounded<sup>2</sup> ( $r \in [0, +1]$ ) and the metric is the one of a 3-dimensional sphere.

- **Open universe**, for  $k = -1$ , the metric can be better understood by introducing

$$d\chi = \frac{dr}{\sqrt{1+r^2}} \Rightarrow r = \sinh \chi,$$

$$d\sigma^2 = d\chi^2 + \sinh^2 \chi (d\theta^2 + \sin^2 \theta d\phi^2),$$

which shows that  $r$  is not bounded, and the metric takes the form of the one of a 3-dimensional hyperboloid.

The value of  $k$  will be determined by the energy content of the universe, through the Einstein field equations, this will be the goal of the next section.

Since in the following sections we will need the metric connection and the Ricci tensor, we are going just to calculate them now.

The Christoffel symbols of the Robertson Walker metric (1.8) are

$$\begin{aligned} \Gamma_{11}^0 &= \frac{a\dot{a}}{1-kr^2}, & \Gamma_{11}^1 &= \frac{kr}{1-kr^2}, \\ \Gamma_{22}^0 &= a\dot{a}r^2, & \Gamma_{33}^0 &= a\dot{a}r^2 \sin^2 \theta, \\ \Gamma_{01}^1 &= \Gamma_{02}^2 = \Gamma_{03}^3 = \frac{\dot{a}}{a}, & \Gamma_{22}^1 &= -r(1-kr^2), \\ \Gamma_{33}^1 &= -r(1-kr^2) \sin^2 \theta, & \Gamma_{12}^2 &= \Gamma_{13}^3 = \frac{1}{r}, \\ \Gamma_{33}^2 &= -\sin \theta \cos \theta, & \Gamma_{23}^2 &= \cot \theta, \end{aligned} \quad (1.9)$$

the ones that are not listed are zero or obtainable from the symmetry of the connection. From the above Christoffel symbols, the non-zero components of the Ricci tensor are

$$\begin{aligned} R_{00} &= -3\frac{\ddot{a}}{a}, \\ R_{11} &= \frac{a\ddot{a} - 2\dot{a} + 2k}{1-kr^2}, \\ R_{22} &= r^2(a\ddot{a} - 2\dot{a} + 2k), \\ R_{33} &= r^2(a\ddot{a} - 2\dot{a} + 2k) \sin^2 \theta. \end{aligned} \quad (1.10)$$

---

<sup>2</sup>This behavior is signaled by the fact that in the previous chart the metric was singular for  $r = 1$ .

### 1.1.2 Dynamical effects in the Robertson Walker universe

With the Robertson Walker metric (1.8) in our hand it is time to study the consequences of having allowed spacetime to have a dynamics. In this section we will work with an arbitrary cosmic factor, however we will also use as reference our universe in which we observe an expansion described by an increasing  $a(t)$ . Keep in mind that, from now on, we will use the convention that at  $t = t_{\text{today}}$  the cosmic scale factor is unitary.

#### Hubble Law

Let's start by evaluating the distance between two points: FRW metric gives

$$d(t) = a(t) \int_{r_1}^{r_2} \frac{dr}{\sqrt{1 - kr^2}}.$$

Notice that the first factor  $a(t)$  multiplies a time independent integral giving an overall time dependence to the distance. This means that distances can change overtime: in the case of our universe they increase resulting in the expansion of the universe. This suggests that the comoving coordinates are not really physical, since they represent fixed points that appear to be moving. We thus define the **physical coordinates** by multiplying the comoving ones by the cosmic scale factor, this allows to describe a non-zero physical velocity for an object at fixed comoving coordinates

$$\mathbf{x}_{\text{phy}} \stackrel{\text{def}}{=} a(t)\mathbf{x} \quad \Rightarrow \quad \mathbf{v}_{\text{phy}} \stackrel{\text{def}}{=} \dot{\mathbf{x}}_{\text{phy}} = \frac{\dot{a}}{a}\mathbf{x} + a(t)\mathbf{v}.$$

This is exactly what Hubble in 1929 [7] observed by studying the motion of far galaxies: a linear relation between observed velocities and the distance between us and these galaxies. The factor of proportionality is nowadays measured to be  $(\dot{a}/a)(t_0) = H_0 \approx 70 \text{ km s}^{-1} \text{ Mpc}^{-1}$  and it is called **Hubble parameter**, this tells us that for each Megaparsec of distance an object appears to be moving with a physical velocity of 70 km/s, due to the expansion of the universe. Indeed, by assuming a negligible peculiar velocity of the observed galaxy (typically hundreds of km/s) the physical velocity reads

$$\mathbf{v}_{\text{phy}} = H_0 \mathbf{x} \tag{1.11}$$

which is called the **Hubble law**. Note that there is no obstacle for the physical velocity of a far enough object to exceed the speed of light: however this does not contradict special relativity since this is an effect that arises in our reference frame which is only locally inertial. For two objects at the same arbitrary distance from us, their relative velocity will always be less than the speed of light.

#### Cosmological redshift

All our observations, from astronomical objects, come in the form of light or, more recently, gravitational waves. This means that the notion of physical distances and velocities could not be enough to describe all the effects that could affect our observations. We will therefore study the *null geodesics* of FRW metric. These are described by

$$dt = \pm a(t) \frac{dr}{\sqrt{1 - kr^2}}$$

that allows for the comoving distance between two objects to be related to the time needed by light to travel from one to the other. Now, suppose that a far object emits a periodic pulse of light each  $\delta t_{\text{em}}$  seconds and let's allow for an arbitrary time between consecutive observations  $\delta t_{\text{obs}}$  on the Earth. The above relation allows us to find the latter from the former. Indeed, if at some time  $t_0$  a first signal is emitted and then received by us at some time  $t_1$ , so that<sup>3</sup>

$$\int_{t_1}^{t_0} \frac{dt}{a(t)} = \int_0^{r_1} \frac{dr}{\sqrt{1 - kr^2}},$$

then a second pulse of light we would be emitted at  $t_0 + \delta t_{\text{em}}$  and received at  $t_1 + \delta t_{\text{obs}}$ , hence giving

$$\int_{t_1 + \delta t_{\text{obs}}}^{t_0 + \delta t_{\text{em}}} \frac{dt}{a(t)} = \int_0^{r_1} \frac{dr}{\sqrt{1 - kr^2}}.$$

Note that in both the above expressions the right-hand side is time independent and determined only by the comoving coordinates of the emitting and receiving objects. Equating the above and by splitting the second integral, we get

$$\int_{t_0}^{t_1} \frac{dt}{a(t)} = \int_{t_0 + \delta t_{\text{obs}}}^{t_1 + \delta t_{\text{em}}} \frac{dt}{a(t)} = \int_{t_0 + \delta t_{\text{em}}}^{t_0} \frac{dt}{a(t)} + \int_{t_0}^{t_1} \frac{dt}{a(t)} + \int_{t_1}^{t_1 + \delta t_{\text{obs}}} \frac{dt}{a(t)}$$

that, by assuming  $\delta t_{\text{em}}$  and  $\delta t_{\text{obs}}$  to be small (so that the remaining integral can be approximated by the integrand by  $\delta t$ ) we find the time between consecutive observations from the one between consecutive emissions:

$$\frac{\delta t_{\text{em}}}{\delta t_{\text{obs}}} = \frac{a(t_{\text{em}})}{a(t_{\text{obs}})}. \quad (1.12)$$

This means that, as the universe expands,  $a(t)$  increases and the elapsed time between consecutive observations becomes greater than the time between emissions.

This may seem a less important effect, however, when considering the wave nature of light, what we call **redshift** arises and becomes an essential tool for our observations. Consider  $\delta t$  as the period related to a specific wave of light (or a gravitational wave since both move on null geodesics), this time is proportional to its wavelength ( $\lambda = c\delta t$ ): ultimately this means that the effect described above results in a difference between the emitted wavelength and the observed one.

Redshift of far objects is measured by the **redshift parameter** as

$$z \stackrel{\text{def}}{=} \frac{\lambda_{\text{obs}} - \lambda_{\text{em}}}{\lambda_{\text{em}}} = \frac{1 - a(t_{\text{em}})}{a(t_{\text{em}})} \quad \Rightarrow \quad 1 + z = \frac{1}{a(t_{\text{em}})}, \quad (1.13)$$

where we used that  $\lambda(t) \propto a(t)$  and the convention  $a(t_{\text{obs}}) = 1$ . This shows that as the universe expands the light that comes from far objects is shifted, in its spectrum, towards red wavelengths. Further they are, more time for light is needed to reach us and  $t_{\text{em}}$  gets pushed away from today increasing the observed redshift. This connection allows for us to refer to time in terms of redshifts: today corresponds to  $z = 0$ ,  $z = 1$  corresponds to when the universe was half its current size and as  $z$  increases we go back in time.

Lastly, let us mention how redshift is measured. This is accomplished by studying the spectrum of the observed galaxies: for each object we can predict its absorption lines (by knowing its chemical composition) that for far objects appear all "*redshifted*" in the same way. By comparison with the spectrum of the same gasses on the Earth we obtain  $z$ .

---

<sup>3</sup>We used the  $-$  sign since the motion occurs from the galaxy to us at the center of the reference frame.



## 1.2 The Friedmann equations

We now want to determine the dynamics of the parameters appearing in the Friedmann Robertson Walker (1.8) metric knowing the energy content of the universe. The connection between the metric and the energy is given by the *Einstein field equations*

$$R_{\mu\nu} - \frac{1}{2}Rg_{\mu\nu} = 8\pi GT_{\mu\nu}, \quad (1.14)$$

where it appears the energy-momentum tensor  $T^{\mu\nu}$ .

### 1.2.1 Cosmic fluids

The simplest model for the content of the universe is a *perfect fluid* of energy and matter. A perfect fluid, in general, is described by an energy-momentum tensor given by

$$T^{\mu\nu} = (\rho + p)U^\mu U^\nu + pg^{\mu\nu}, \quad (1.15)$$

where  $\rho$  is the energy density of the fluid,  $p$  the pressure and  $U^\mu$  the 4-velocity of a particle of the fluid.

When we described the coordinates appearing in the FRW metric, we anticipated that those were comoving coordinates with respect to the content of the universe (so that in that reference frame the metric would be manifestly isotropic and homogeneous). In the reference frame associated to those coordinates, the fluid is at rest, thus its energy-momentum tensor takes the form

$$U^\mu = (1, 0, 0, 0), \quad \Rightarrow \quad T_{\mu\nu} = \begin{pmatrix} \rho & 0 & 0 & 0 \\ 0 & & & \\ 0 & g_{ij}p & & \\ 0 & & & \end{pmatrix}, \quad T^\mu{}_\nu = \text{diag}(-\rho, p, p, p) \quad (1.16)$$

Even before plugging everything in the Einstein equations, we can study the energy conservation of this fluid, which reads

$$\begin{aligned} 0 &= \nabla_\mu T^\mu{}_0 = \partial_\mu T^\mu{}_0 + \Gamma^\mu_{\mu\lambda} T^\lambda{}_0 - \Gamma^\lambda_{\mu 0} T^\mu{}_\lambda = \partial_0 T^0{}_0 + \Gamma^\mu_{\mu 0} T^0{}_0 - \Gamma^\lambda_{\mu 0} T^\mu{}_\lambda \\ &= -\dot{\rho} - 3\frac{\dot{a}}{a}\rho - 3\frac{\dot{a}}{a}p = -\dot{\rho} - 3\frac{\dot{a}}{a}(\rho + p), \end{aligned} \quad (1.17)$$

in which we used that  $T^\mu{}_\nu$  is diagonal, and the Christoffel symbols (1.9).

For simple fluids, it is usually assumed that they follow some simple equation of state, as

$$p = \omega\rho, \quad \omega = \text{constant}. \quad (1.18)$$

Inserting this into the conservation of energy equation (1.17) we find

$$\frac{\dot{\rho}}{\rho} = -3(1 + \omega)\frac{\dot{a}}{a},$$

that can be solved to obtain how the energy density of the fluid scales as the universe expands:

$$\int \frac{d\rho}{\rho} = -3(1 + \omega) \int \frac{da}{a} \quad \Rightarrow \quad \boxed{\rho = \rho_0 a^{-3(1+\omega)}}.$$

To better grasp the physics of our construction let's study some simple cases.

- **Dust:** this kind of fluid is defined as a set of collisionless, non-relativistic particles, that therefore will have zero pressure:

$$p_d = \omega_d \rho_d = 0, \quad \Rightarrow \quad \omega_d = 0 \quad \Rightarrow \quad \rho_d = \frac{E}{V} = \rho_0 a^{-3}.$$

We can appreciate how, for dust, the energy density scales with the volume ( $V \propto a^3$ ), keeping constant the total energy. This sort of fluid can be used to model groups of stars and galaxies, for which the pressure is negligible, compared to the energy density.

- **Radiation:** in this case we want to describe massless particles or ultra-relativistic ones, which can be approximated to be massless. We can obtain an equation of state for this fluid by first observing that the  $T^{\mu\nu}$  is traceless for E-M fields

$$T^\mu{}_\mu = F^{\mu\lambda} F_{\mu\lambda} - \frac{1}{4} g^\mu{}_\mu F^{\lambda\sigma} F_{\lambda\sigma} = 0,$$

at the same time equation (1.16) gives that

$$T^\mu{}_\mu = -\rho + 3P, \quad \Rightarrow \quad P_r = \frac{1}{3}\rho_r,$$

which implies  $\omega_r = \frac{1}{3}$ . Therefore, the energy density of radiation scales as

$$\rho_r = \rho_0 a^{-4},$$

that means that for radiation the total energy is not conserved. We interpret this as the fact that, while the universe expands, radiation gets redshifted.

- **Vacuum or dark energy:** this last type of cosmic fluid is quite a strange one, the equation of state for this fluid is

$$p_v = -\rho_v, \quad \Rightarrow \quad \omega_v = -1.$$

This means that the energy density, as well as the pressure, as the universe expands, remains constant. Sometimes this is not considered a content of the universe, and it is referred as the *cosmological constant*  $\Lambda$ :

$$\rho_v = \frac{\Lambda}{8\pi G}.$$

### 1.2.2 The Friedmann equations

Now that we know how to model the content of the universe, we can proceed to derive the equations governing the time evolution of spacetime.

First we want to modify a bit Einstein equations (1.14): from the trace of both sides we get

$$R - \frac{4}{2}R = 8\pi GT \quad \Rightarrow \quad R = -8\pi GT,$$

where  $T = T^\mu{}_\mu$ , plugging this result in the field equations (1.14), we can rewrite them as:

$$R_{\mu\nu} = 8\pi G \left( T_{\mu\nu} - \frac{1}{2} T g_{\mu\nu} \right).$$

From the Ricci tensor components of the FRW metric (1.10) and the energy momentum tensor (1.16) we can obtain two equations:

- the  $\mu\nu = 00$  component leads to

$$\begin{aligned} -3\frac{\ddot{a}}{a} &= 8\pi G \left[ -\rho - \frac{1}{2}(-\rho + 3p) \right] \\ &= 4\pi G(\rho + 3p); \end{aligned}$$

- the  $\mu\nu = ij$  components lead to

$$\begin{aligned} \frac{a\ddot{a} + 2\dot{a}^2 + 2k}{a^2} g_{ij} &= 8\pi G \left[ p g_{ij} - \frac{1}{2} g_{ij}(-\rho + 3p) \right] \\ &= 4\pi G(\rho - p) g_{ij}. \end{aligned}$$

Substituting the former into the latter we find

$$\begin{aligned} -\frac{4}{3}\pi G(\rho + 3p) + \frac{2\dot{a}^2 + 2k}{a^2} &= 4\pi G(\rho - p) \\ \frac{2\dot{a}^2 + 2k}{a^2} &= 4\pi G\frac{4}{3}\rho \\ \boxed{\left(\frac{\dot{a}}{a}\right)^2} &= \frac{8\pi G}{3}\rho - \frac{k}{a^2}, \end{aligned} \tag{1.19}$$

which is the **first Friedmann equation**, while from the 00 component alone we get the **second Friedmann equation**

$$\boxed{\frac{\ddot{a}}{a} = -\frac{4\pi G}{3}(\rho + 3p)} \tag{1.20}$$

The first, which is the one that is usually referred as the Friedmann equation, will determine the time evolution of the scale factor  $a(t)$ . To solve it, it is enough to know the dependence  $\rho(a)$ , that we previously discussed.

Usually, the first Friedmann equation (1.19) is expressed in terms of specific cosmological parameters that are more easily measurable:

- the **Hubble parameter**,  $H \stackrel{\text{def}}{=} \frac{\dot{a}}{a}$ , which measure the rate of expansion,
- the **critical density**,  $\rho_{\text{crit}} \stackrel{\text{def}}{=} \frac{3H^2}{8\pi G}$ , which is the energy density of a flat universe,
- the **density parameter**,  $\Omega = \frac{8\pi G}{3H^2}\rho \stackrel{\text{def}}{=} \frac{\rho}{\rho_{\text{crit}}}$ ,
- the **curvature parameter**,  $\Omega_k \stackrel{\text{def}}{=} \frac{k}{(aH)^2}$ .

In this way, equation (1.19) explicitly relates the matter content of the universe with its geometry (flat, open or closed). Indeed, inserting the above parameters in (1.19) it reads

$$\boxed{\Omega - 1 = \Omega_k = \frac{k}{H^2 a^2}}, \quad (1.21)$$

from which we can distinguish 3 distinct cases:

- $\rho < \rho_{\text{crit}} \quad \Leftrightarrow \quad \Omega < 1 \quad \Leftrightarrow \quad k < 0 \quad \Leftrightarrow \quad \text{open universe},$
- $\rho = \rho_{\text{crit}} \quad \Leftrightarrow \quad \Omega = 1 \quad \Leftrightarrow \quad k = 0 \quad \Leftrightarrow \quad \text{flat universe},$
- $\rho > \rho_{\text{crit}} \quad \Leftrightarrow \quad \Omega > 1 \quad \Leftrightarrow \quad k > 0 \quad \Leftrightarrow \quad \text{closed universe}.$

As we will see, observations suggest that now, for our universe,  $k \approx 0$ . Therefore, we will always consider flat geometry, in this case the dynamics of the universe is determined by

$$\left(\frac{\dot{a}}{a}\right)^2 = \frac{8\pi G}{3}\rho.$$

Depending on the different cosmic fluids the universe evolves mainly in three different ways.

- **Matter dominated universe:** in this case, the universe is approximated to contain only dust, therefore  $\rho = \rho_0 a^{-3}$ . Plugging this energy density into the above differential equation we get

$$\dot{a} = H_0 a^{-\frac{1}{2}} \quad \Rightarrow \quad a(t) = \left(\frac{3}{2}H_0 t\right)^{2/3},$$

where we introduced  $H_0 = H(t_0) = \sqrt{\frac{8\pi G}{3}\rho_0}$  and imposed  $a(0) = 0$ .

This kind of universe is expanding but at a slower and slower rate ( $\ddot{a} \leq 0$ ).

- **Radiation dominated universe:** now the universe is approximately filled only by radiation, therefore  $\rho = \rho_0 a^{-4}$ . The above differential equation now reads

$$\dot{a} = H_0 a^{-1} \quad \Rightarrow \quad a(t) = \sqrt{2H_0 t},$$

where again  $H_0 = H(t_0) = \sqrt{\frac{8\pi G}{3}\rho_0}$  and we imposed  $a(0) = 0$ .

Again, this universe is expanding at a slower and slower rate ( $\ddot{a} \leq 0$ ).

- **Empty universe:** lastly we consider an empty universe or in which vacuum energy dominates, therefore  $\rho = \frac{\Lambda}{8\pi G}$ , from which we get

$$\dot{a} = a\sqrt{\frac{\Lambda}{3}} \quad \Rightarrow \quad a(t) = a_0 e^{\sqrt{\frac{\Lambda}{3}}(t-t_0)},$$

in which we imposed  $a(t_0) = a_0$ .

Note that, among the cases, this universe is the only one that has an accelerating expansion ( $\ddot{a} \geq 0$ ). It is worth noting also that the first two cases admit a finite time (in our calculations  $t = 0$ ) for which the universe has no spatial extension ( $a(0) = 0$  generates a singularity). The empty universe does not admit it for any finite time.

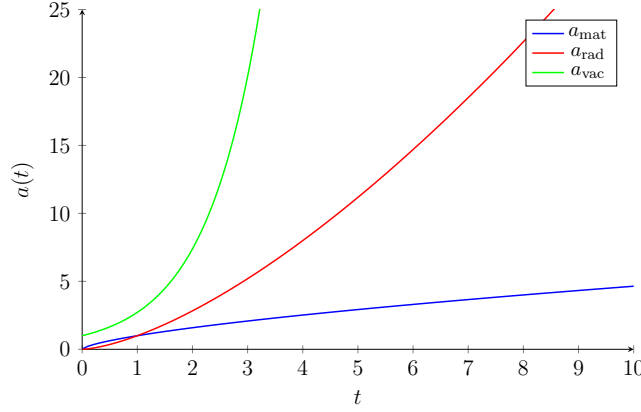


Figure 1.1: Comparison of the time evolution of the scale factor with the three different fluids in a flat universe.

### 1.2.3 The $\Lambda$ CDM model

With all the previous tools we introduced we are finally ready to describe the universe that we live in and its evolution. To draw the timeline of our universe we must start from today, from current observations of the cosmological parameters, and then trace back its history.

The first cosmological parameter that has been ever observed is the Hubble parameter, by Hubble himself. Current and more precise measurements of this parameter give

$$H_0 = (67.74 \pm 0.46) \text{ km s}^{-1} \text{ Mpc}^{-1}$$

which correspond to a critical density  $\rho_{\text{crit},0} = (8.62 \pm 0.12) \times 10^{-27} \text{ kg m}^3$ .

Nowadays, most of our knowledge on the cosmological universe comes from measures of the *CMB*, or the *Cosmic microwave background radiation*, which for now is just the relic of the photons that filled the universe at earlier times. In 1996, the *COBE* satellite [5] measured the spectrum of the CMB that turned out to be an almost perfect blackbody radiation at the temperature

$$T_0 = (2.7255 \pm 0.0006) \text{ K}, \quad (1.22)$$

this allows to estimate the number density and the energy density of these relic photons (section ???) that read

$$n_{\gamma,0} \approx 410 \text{ photons cm}^{-3}, \quad \rho_{\gamma,0} \approx 4.6 \times 10^{-34} \text{ g cm}^{-3}, \quad \Omega_{\gamma,0} = (5.38 \pm 0.15) \times 10^{-5}.$$

This turns out to be the main contribution to the overall photon contained in the universe. By the results of COBE, we also discovered that the CMB displays small temperature fluctuations  $\Delta T/T \approx 10^{-5}$  that, we will see, give us a tremendous amount of data about the history of the universe. For now, it is important that these measures suggest an upper bound for the spatial curvature of our universe today

$$|\Omega_{k,0}| < 0.005. \quad (1.23)$$

This shows that today only a small fraction of all the contribution to the Friedmann equation (1.21) is represented by curvature and therefore we consider our universe almost flat.

Together with photons, our universe is also filled by neutrinos that, being really light particles, behave almost as radiation (their speed is really close to  $c$ ) and therefore they contribute to the total radiation density<sup>4</sup>

$$\Omega_{r,0} = (9.02 \pm 0.21) \times 10^{-5}.$$

Clearly, also the ordinary matter of which we are made of (what we called dust that mainly is stars and gasses that fill the universe) must be taken into account: current measures from the CMB and the abundances of the lightest chemical elements in our universe show

$$\Omega_{b,0} = 0.0493 \pm 0.0006,$$

where the subscript  $b$  stands for baryons, which are the main ingredients of ordinary matter particles. From this data we can estimate the corresponding number density: assuming that the main contribute to ordinary matter is represented by protons (since they are more massive than electrons and the most abundant gas is hydrogen) we find

$$n_{n,0} \approx \frac{\rho_{m0}}{m_p} = \frac{\Omega_{b,0}\rho_{\text{crit},0}}{m_p} \approx 0.3 \times 10^{-6} \text{cm}^{-3}.$$

Comparing this to the density of photons we note that the latter is much higher, with a baryon-to-photon ratio

$$\eta_{b\gamma} \stackrel{\text{def}}{=} n_b/n_\gamma \approx 6 \times 10^{-10}. \quad (1.24)$$

Modern astrophysics hints that a further component must be accounted: **Dark matter** which is observed through the dynamics of galaxies or by other gravitational effect but doesn't seem to be affected by the other fundamental interactions. Again, the temperature perturbations of the CMB allows us to estimate the fraction of dark matter in our universe, which turn out to be

$$\Omega_{\text{cdm},0} \approx 0.27,$$

where  $cdm$  stands for *cold dark matter*, which means that we are assuming that it is described by the same equation of state of dust ( $\omega_d = 0$ ). In this way, the sum of baryon density and cold dark matter makes the total matter density of the universe

$$\Omega_{m,0} = 0.3153 \pm 0.0073.$$

Lastly we can note that, with all the above data, the Friedmann equation (1.21) is not satisfied

$$\sum_{\text{content}} \Omega_{i,0} - 1 \approx 0.68 \neq \Omega_{k,0} \approx \pm 0.0005$$

this suggests that another component of the content of the universe should be taken into account. Current observations of type 1 Supernovae hint that this last ingredient must be **dark energy** ( $\omega_v = -1$ ) with a corresponding density parameter

$$\Omega_{\Lambda,0} = 0.6847 \pm 0.0073.$$

---

<sup>4</sup>In this context radiation means that we describe this fraction of energy as a perfect fluid with  $\omega = 1/3$ .

Parameter	Meaning	Value
$H_0$	expansion rate	$67.74 \pm 0.46 \text{ km s}^{-1} \text{ Mpc}^{-1}$
$\rho_{\text{crit},0}$	critical density	$(8.62 \pm 0.12) \times 10^{-27} \text{ kg m}^{-3}$
$\Omega_{\gamma,0}$	photon density parameter	$(5.38 \pm 0.15) \times 10^{-5}$
$\Omega_{r,0}$	radiation density parameter	$(9.02 \pm 0.21) \times 10^{-5}$
$\Omega_{b,0}$	baryon density parameter	$0.0493 \pm 0.0006$
$\Omega_{\text{cdm},0}$	cold dark matter density par.	$\approx 0.27$
$\Omega_{m,0}$	total matter density parameter	$0.3153 \pm 0.0073$
$\Omega_{\Lambda,0}$	dark energy density parameter	$0.6847 \pm 0.0073$
$\Omega_{k,0}$	spatial curvature parameter	$ \Omega_{k,0}  < 0.005$
$t_0$	age of the universe	$\approx 13.8 \text{ Gyr}$
$t_{\text{eq}}$	time of matter-radiation eq.	$\approx 50,000 \text{ years}$
$t_{m\Lambda}$	time of matter-dark energy eq.	$\approx 10.2 \text{ Gyr}$

Table 1.1: Summary of parameters of the  $\Lambda$ CDM model today.

The above set of data (Tab. 1.1) is what we usually refer to as the  **$\Lambda$ CDM model** as from this information we can set initial conditions for the Friedmann equation and then study backwards, from today, the history of our universe. Comparing all the density parameters we presented we note that our universe today is vacuum dominated. Then, recalling that  $\rho_r \propto a^{-4}$ ,  $\rho_d \propto a^{-3}$  while  $\rho_v = \text{const}$ , we understand that this was not always the case. Indeed, as we go back in time the universe shrinks and the energy density of matter and radiation raise: the former, being more dominant today, is the first one to dominate over dark energy, while the latter dominates over both at earlier times. For this reason we usually subdivide the history in different eras, each one dominated by a different fluid and we assume that the transition occurred when the density parameter of a specific fluid became greater than all the others<sup>5</sup>.

The first transition that we encounter is between the current *Dark energy dominated era* and the *matter dominated era*, from the definition of the density parameters we easily get (here we are assuming the usual convention  $a_0 = 1$ )

$$\Omega_{\Lambda}(t) = \Omega_{\Lambda,0}, \quad \Omega_m(t) = \Omega_{m,0}a^{-3} \quad \Rightarrow \quad a_{m\Lambda} = \left(\frac{\Omega_{m,0}}{\Omega_{\Lambda,0}}\right)^{\frac{1}{3}} \approx 0.77,$$

when  $\Omega_{\Lambda}(t) = \Omega_m(t)$ . This allows us to obtain the redshift of the dark energy-matter transition  $z_{m\Lambda} \approx 0.3$ .

As we already described, proceeding backwards in time radiation starts to dominate: considering  $\Omega_r(t) = \Omega_{r,0}a^{-4}$  we find that the transition occurs at

$$a_{\text{eq}} = \frac{\Omega_{r,0}}{\Omega_{m,0}} \approx 2.9 \times 10^{-4} \quad \Rightarrow \quad z_{\text{eq}} \approx 3400,$$

where the subscript *eq* stands for matter-radiation equality.

Going further back in time the scale factor continues to decrease ( $a_{\text{rad}}(t) \propto \sqrt{t}$ ) and we reach a scale at which the universe was so small that quantum mechanics effects must

<sup>5</sup>Clearly, the dynamics of the universe must describe by a smooth function and this sharp transition approach let us simplify the calculations during a precise era in which we neglect all the subdominant fluids.

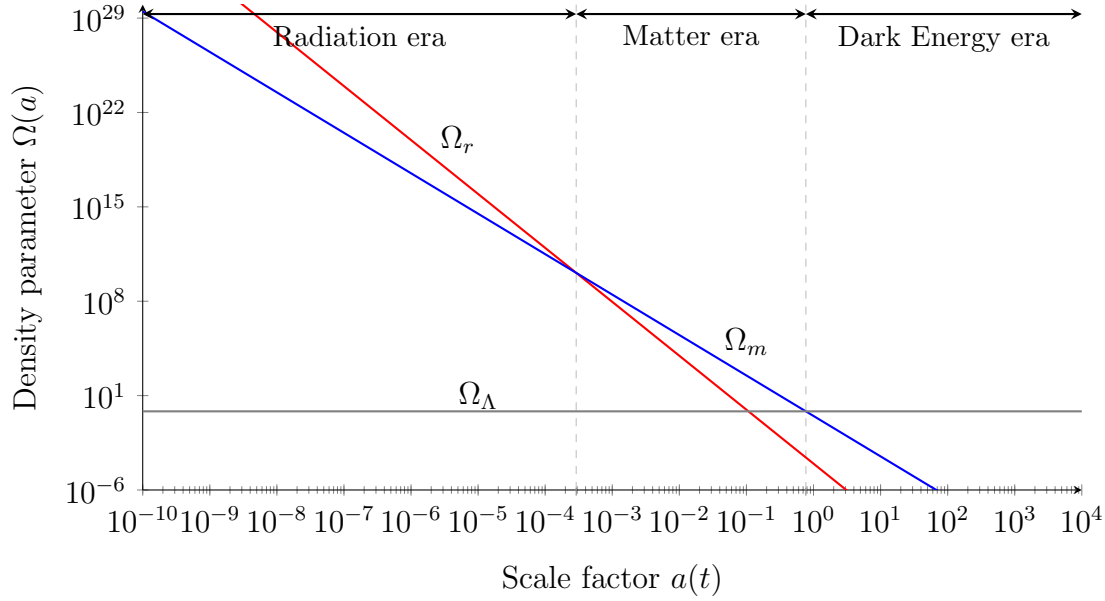


Figure 1.2: Evolution of the densities of matter, radiation and dark energy. In this plot the transitions between the main eras are showed.

be taken into account and a theory of *quantum gravity* is required. However, no-definitive solution for this problem has been found today.

For our purposes we will assume that the history of the universe started when  $a = 0$ , in this way we can convert our redshifts in comoving time. From the Friedmann equation (1.19)  $a(t)$  can be converted in a time by the following integral

$$H_0 t = \int_0^a \frac{da'}{\sqrt{\Omega_{r,0}a'^{-2} + \Omega_{m,0}a'^{-1} + \Omega_{\Lambda,0}a'^2 + \Omega_{k,0}}} \Rightarrow \begin{cases} t_0 \approx 13.8 \text{Gyrs}, \\ t_{\text{eq}} \approx 50\,000 \text{yrs}, \\ t_{m\Lambda} \approx 10.2 \text{Gyrs}. \end{cases}$$

This shows that, compared to the entire life of the universe ( $t_0$ ) the *radiation dominated era* lasted only for 50 000 years, while the *dark energy dominated era* is the closest to us, that started only a few billion years ago. Then the *matter dominated era* is the longest one of the three.



## II

# The inhomogeneous universe



# III

## CMB physic



# Chapter 2

## Anisotropies of the CMB

The *cosmic microwave background radiation*, as we explained in section 1.2.3, is one of the most valuable source of information that we got from the early universe. Its usefulness is encoded in its **anisotropies**: the small variations, in its temperature for example, from the perfectly homogeneous radiation that we would have in absence of perturbations. Anisotropies thus are a direct link to the perturbations that were generated in the early universe and allow us to obtain data from the earliest stages of the universe, such as inflation. To begin we will consider scalar perturbations, then we will also develop the same machinery for the tensor one.

### 2.1 Angular power spectrum

When we observe the *CMB* in the sky, we measure the temperature of photons coming from a specific direction  $\hat{\mathbf{n}}$  to us. As we know, this temperature is not perfectly the same from all directions, we call these tiny differences *anisotropies*:

$$T(\hat{\mathbf{n}}) = \bar{T} [1 + \Theta(\hat{\mathbf{n}})] \quad \text{with } \Theta(\hat{\mathbf{n}}) \stackrel{\text{def}}{=} \frac{\Delta T(\hat{\mathbf{n}})}{\bar{T}}$$

and where  $\bar{T}$  is the average temperature in the sky and  $\Delta T(\hat{\mathbf{n}})$  is the temperature fluctuation in the direction  $\hat{\mathbf{n}}$ . To compare the temperature at two distinct points in the sky we define the *two point correlation function*:

$$C(\hat{\mathbf{n}}, \hat{\mathbf{n}}') \stackrel{\text{def}}{=} \langle \Theta(\hat{\mathbf{n}}) \Theta(\hat{\mathbf{n}}') \rangle, \quad (2.1)$$

here the angle brackets denote an average over an ensemble of universes (It will be discussed later in this section how we can approximate this averaging process).

The most appropriate way to describe the temperature fluctuations, given that these are observed from the sky, is to expand  $\Theta$  in spherical harmonics

$$\Theta(\hat{\mathbf{n}}) = \sum_{\ell=0}^{\infty} \sum_{m=-\ell}^{\ell} a_{\ell m} Y_{\ell m}(\hat{\mathbf{n}}), \quad (2.2)$$

where the coefficients  $a_{\ell m}$ , also called **multipole moments**, are given by

$$a_{\ell m} = \int d\Omega \Theta(\hat{\mathbf{n}}) Y_{\ell m}^*(\hat{\mathbf{n}}).$$

Also, for the multipole moments we can define a two point correlation function

$$\langle a_{\ell m} a_{\ell' m'}^* \rangle = \delta_{\ell \ell'} \delta_{m m'} C_\ell, \quad (2.3)$$

where  $C_\ell$  is the **angular power spectrum** and again the angle brackets represent an ensemble average. Sometimes it is also used  $\mathcal{D}_\ell \stackrel{\text{def}}{=} \frac{\ell(\ell+1)}{2\pi} \bar{T}^2 C_\ell$ .

Note that combining (2.2) and (2.1) we obtain

$$\begin{aligned} C(\hat{\mathbf{n}}, \hat{\mathbf{n}}') &= \langle \Theta(\hat{\mathbf{n}}) \Theta(\hat{\mathbf{n}}') \rangle \\ &= \sum_{\ell=0}^{\infty} \sum_{m=-\ell}^{\ell} \sum_{\ell'=0}^{\infty} \sum_{m'=-\ell'}^{\ell'} \langle a_{\ell m} a_{\ell' m'}^* \rangle Y_{\ell m}(\hat{\mathbf{n}}) Y_{\ell' m'}^*(\hat{\mathbf{n}}') \\ &= \sum_{\ell=0}^{\infty} C_\ell \sum_{m=-\ell}^{\ell} Y_{\ell m}(\hat{\mathbf{n}}) Y_{\ell m}^*(\hat{\mathbf{n}}') \\ &\quad \downarrow \text{using } \sum_{m=-\ell}^{\ell} Y_{\ell m}(\hat{\mathbf{n}}) Y_{\ell m}^*(\hat{\mathbf{n}}') = \frac{2\ell+1}{4\pi} P_\ell(\cos \theta) \\ &= \sum_{\ell=0}^{\infty} C_\ell \frac{2\ell+1}{4\pi} P_\ell(\cos \theta), \end{aligned}$$

where  $P_\ell$  are the Legendre polynomials and  $\theta$  is the angle between  $\hat{\mathbf{n}}$  and  $\hat{\mathbf{n}}'$ . Invoking the orthogonality of the Legendre polynomials we can write

$$C_\ell = 2\pi \int_{-1}^1 d(\cos \theta) P_\ell(\cos \theta) C(\hat{\mathbf{n}}, \hat{\mathbf{n}}'), \quad (2.4)$$

this shows that the angular power spectrum encodes the same information as the two point correlation function (2.1), hence it measures the correlation between the temperature fluctuations at two points in the sky separated by an angle  $\theta$ .

We now want to understand how can we estimate the average over the ensemble of universes in the previous definitions. Note that, fixed  $\ell$ , we still get  $2\ell+1$  different values of  $a_{\ell m}$ , this allows us to estimate the angular power spectrum as

$$\hat{C}_\ell = \frac{1}{2\ell+1} \sum_{m=-\ell}^{\ell} |a_{\ell m}|^2. \quad (2.5)$$

One can show that this estimator is unbiased<sup>1</sup>, however its variance is non-zero:

$$\Delta \hat{C}_\ell \stackrel{\text{def}}{=} \sqrt{\langle (C_\ell - \hat{C}_\ell)^2 \rangle} = \sqrt{\frac{2}{2\ell+1}} C_\ell, \quad (2.6)$$

this error that systematically appears in this estimate is usually called **cosmic variance**. Cosmic variance will result in a larger error for smaller values of  $\ell$ , which corresponds to larger angular scales. This can be understood as a consequence of the fewer number of modes  $a_{\ell m}$  available at lower  $\ell$ .

---

<sup>1</sup>An estimator is said to be unbiased if its expected value is equal to the true value of the parameter being estimated.

### 2.1.1 Multipole expansion

In the previous section we considered the temperature fluctuations observed by us in the sky, therefore it was natural to assume that these were functions of the direction of observation  $\hat{\mathbf{n}}$ . In general however, we should consider that these anisotropies varies also with the position of the observer in spacetime. This broader view is needed since to predict the observations we will need to describe the evolution of the anisotropies throughout the whole universe. Therefore, we will now consider

$$\Theta(t, \mathbf{x}, \hat{\mathbf{p}}) \quad \text{with} \quad \begin{cases} t & \text{cosmic time,} \\ \mathbf{x} & \text{position of the anisotropy in space,} \\ \hat{\mathbf{p}} & \text{direction of motion of the photons.} \end{cases} \quad (2.7)$$

To come back to the observed anisotropies we just fix  $t$  at the present day,  $\mathbf{x}$  on the earth and we consider the direction of motion of the photons as the direction of observation (since it is the direction from which they come from).

In section 2.2 we will see that the evolution of the anisotropies is described by a linear differential equation (since we are working with first order perturbations). It is therefore useful to introduce here some expansions that will simplify these equations. First of all, we can simplify the spacial dependence moving to Fourier space

$$\Theta(t, \mathbf{x}, \hat{\mathbf{p}}) = \int \frac{d^3k}{(2\pi)^3} e^{i\mathbf{k}\cdot\mathbf{x}} \tilde{\Theta}(\mathbf{k}, t, \hat{\mathbf{p}}), \quad (2.8)$$

where  $\tilde{\Theta}$  is the Fourier transform of  $\Theta$ . In this way, we obtained a decomposition on plane waves that leaves  $\tilde{\Theta}$  depending on two vectors,  $\mathbf{k}$  and  $\hat{\mathbf{p}}$ . However, when dealing with the anisotropies generated only by *scalar perturbations*<sup>2</sup>, as we will see in section 2.2 the quantities that really matter are encoded in one of these two vectors and in the angle between them. This allows us to define

$$\mu = \frac{\mathbf{k} \cdot \hat{\mathbf{p}}}{k} \quad \Rightarrow \quad \tilde{\Theta}(t, \mathbf{k}, \mu) \quad \text{with } \mu \in [-1, 1].$$

This suggests us to that another useful expansion is the **Legendre polynomial expansion**:

$$\begin{aligned} \tilde{\Theta}(t, \mathbf{k}, \mu) &= \sum_{\ell=0}^{\infty} \frac{2\ell+1}{i^\ell} \tilde{\Theta}_\ell(t, \mathbf{k}) P_\ell(\mu), \\ \tilde{\Theta}_\ell(t, \mathbf{k}) &= \frac{i^\ell}{2} \int_{-1}^1 d\mu P_\ell(\mu) \tilde{\Theta}(t, \mathbf{k}, \mu), \end{aligned} \quad (2.9)$$

where  $P_\ell$  are the Legendre polynomials and  $\tilde{\Theta}_\ell$  are the **multipoles**.

The Legendre polynomials can be computed recursively using the Bonnet's formula

$$(\ell+1)P_{\ell+1}(\mu) = (2\ell+1)\mu P_\ell(\mu) - \ell P_{\ell-1}(\mu), \quad (2.10)$$

and knowing that  $P_0 = 1$ ,  $P_1 = \mu$  and  $P_2 = \frac{3\mu^2-1}{2}$ .

---

<sup>2</sup>For tensor perturbations this expansion is not appropriate anymore, this is discussed in section 2.3

### 2.1.2 From perturbations to anisotropies

It is now time to discuss how in general we connect the perturbations of the FRW universe to the angular power spectrum of the anisotropies that we observe in the *CMB*. Even though we will not study, in this work, the anisotropies themselves, this connection will be used, in a similar manner, when dealing with spectral distortions in the next chapter.

We are interested in evaluating  $\langle \tilde{\Theta}(\mathbf{k}, \hat{\mathbf{n}}) \tilde{\Theta}^*(\mathbf{k}', \hat{\mathbf{n}}') \rangle$ . This quantity is determined by two phenomena:

1. the initial amplitude of the perturbations generated during inflation, which from our point of view are random variables generated by vacuum fluctuations;
2. the evolution the anisotropies that we observe today and how they are sourced by the primordial perturbations: this process is clearly deterministic.

This consideration allows us to proceed in the following way: considering a generic primordial perturbation  $\delta(\mathbf{k})$ , we can decompose  $\tilde{\Theta}(\mathbf{k}, \hat{\mathbf{n}}) = \delta(\tilde{\Theta}/\delta)$ , now the ratio  $\tilde{\Theta}/\delta$  is completely independent of the initial amplitude of the perturbation (by initial conditions also  $\Theta$  is proportional to this amplitude) and won't contribute to the ensemble average. In this way we get

$$\begin{aligned} \langle \tilde{\Theta}(\mathbf{k}, \hat{\mathbf{n}}) \tilde{\Theta}^*(\mathbf{k}', \hat{\mathbf{n}}') \rangle &= \langle \delta(\mathbf{k}) \delta(\mathbf{k}') \rangle \frac{\tilde{\Theta}(\mathbf{k}, \hat{\mathbf{n}})}{\delta(\mathbf{k})} \frac{\tilde{\Theta}^*(\mathbf{k}', \hat{\mathbf{n}}')}{\delta^*(\mathbf{k}')} \\ &= (2\pi)^3 \delta^{(3)}(\mathbf{k} - \mathbf{k}') \mathcal{P}_\delta(k) \frac{\tilde{\Theta}(\mathbf{k}, \hat{\mathbf{n}})}{\delta(\mathbf{k})} \frac{\tilde{\Theta}^*(\mathbf{k}', \hat{\mathbf{n}}')}{\delta^*(\mathbf{k}')}, \end{aligned}$$

where we used the definition of the primordial perturbation power spectrum. In this expression the last two factors now depend only on the magnitude of  $\mathbf{k}$  and  $\mathbf{k}'$ .

Now, by inserting this result in the expression for the  $C_\ell$  (2.4) we find

$$\begin{aligned} C_\ell &= 2\pi \int_{-1}^1 d\mu P_\ell(\mu) \int \frac{d^3k}{(2\pi)^3} \int \frac{d^3k'}{(2\pi)^3} e^{i(\mathbf{k}-\mathbf{k}') \cdot \mathbf{x}} \langle \tilde{\Theta}(\mathbf{k}, \hat{\mathbf{n}}) \tilde{\Theta}^*(\mathbf{k}', \hat{\mathbf{n}}') \rangle \\ &= 2\pi \int \frac{d^3k}{(2\pi)^3} \mathcal{P}_\delta(k) \int_{-1}^1 d\mu P_\ell(\mu) \frac{\tilde{\Theta}(\mathbf{k}, \hat{\mathbf{n}})}{\delta(\mathbf{k})} \frac{\tilde{\Theta}^*(\mathbf{k}, \hat{\mathbf{n}})}{\delta^*(\mathbf{k})} \\ &= 2\pi \int \frac{dk}{(2\pi)^3} k^2 \mathcal{P}_\delta(k) \int_{-1}^1 d\mu P_\ell(\mu) \sum_{\ell', \ell''} \frac{\tilde{\Theta}_{\ell'}}{\delta} \frac{\tilde{\Theta}_{\ell''}^*}{\delta^*} (2\ell' + 1)(2\ell'' + 1) i^{\ell' - \ell''} \times \\ &\quad \times \int_0^{2\pi} d\phi \int_{-1}^1 d\cos\theta P_{\ell'}(\hat{\mathbf{n}} \cdot \hat{\mathbf{k}}) P_{\ell''}(\hat{\mathbf{n}}' \cdot \hat{\mathbf{k}}) \\ &\quad \downarrow \text{using } \int_0^{2\pi} d\phi \int_{-1}^1 d\cos\theta P_\ell(\hat{\mathbf{k}} \cdot \hat{\mathbf{n}}) P_{\ell'}(\hat{\mathbf{k}}' \cdot \hat{\mathbf{n}}') = \frac{4\pi}{2\ell + 1} P_\ell(\hat{\mathbf{n}} \cdot \hat{\mathbf{n}}') \delta_{\ell\ell'} \\ &= 8\pi^2 \int \frac{dk}{(2\pi)^3} k^2 \mathcal{P}_\delta(k) \sum_{\ell'=0}^{\infty} (2\ell' + 1) \left| \frac{\tilde{\Theta}_{\ell'}(\mathbf{k}, \hat{\mathbf{n}})}{\delta(\mathbf{k})} \right|^2 \int_{-1}^1 d\mu P_\ell(\mu) P_{\ell'}(\mu) \\ &\quad \downarrow \text{orthogonality } \int_{-1}^1 d\mu P_\ell(\mu) P_{\ell'}(\mu) = \frac{2}{2\ell + 1} \delta_{\ell\ell'} \\ &= 16\pi^2 \int \frac{dk}{(2\pi)^3} k^2 \mathcal{P}_\delta(k) \left| \frac{\tilde{\Theta}_\ell(\mathbf{k}, \hat{\mathbf{n}})}{\delta(\mathbf{k})} \right|^2 = \frac{2}{\pi} \int dk k^2 \mathcal{P}_\delta(k) \left| \frac{\tilde{\Theta}_\ell(\mathbf{k}, \hat{\mathbf{n}})}{\delta(\mathbf{k})} \right|^2, \end{aligned} \tag{2.11}$$



where  $\mu = \cos(\hat{\mathbf{n}} \cdot \hat{\mathbf{n}}')$  and we used the orthogonality of the Legendre polynomial and that  $\Theta$  is real.

Lastly, introducing the dimensionless power spectrum  $\Delta_\delta^2(k) \stackrel{\text{def}}{=} \frac{k^3}{2\pi^2} \mathcal{P}_\delta(k)$  we obtain:

$$C_\ell = 4\pi \int \frac{dk}{k} \Delta_\delta^2(k) \left| \frac{\tilde{\Theta}_\ell(\mathbf{k}, \hat{\mathbf{n}})}{\delta(\mathbf{k})} \right|^2. \quad (2.12)$$

We ended with a formula that relates the angular power spectrum to the power spectrum of the perturbations via the so-called **transfer function**  $|\frac{\tilde{\Theta}_\ell(\mathbf{k}, \hat{\mathbf{n}})}{\delta(\mathbf{k})}|$ , which describes how the perturbations generates anisotropies and that we have to find in the next sections.

## 2.2 Time evolution of anisotropies

In this section we want to develop the machinery needed to understand how the anisotropies of the *CMB* were generated by the primordial metric perturbations and, then, how they evolved until today. This gives us also the *transfer functions*, just by setting the amplitude of the perturbation to unity.

To tackle this problem we need to study the evolution of the phase space of photons in perturbed spacetime. Imposing the *newtonian gauge*, we can write the metric with only scalar perturbations as

$$ds^2 = -(1 + 2\Psi)dt^2 + a^2(t)(1 - 2\Phi)\delta_{ij}dx^i dx^j.$$

In appendix B.2 we showed that in this case the *Liouville operator* reads as in (B.5):

$$\hat{L}[f] = \frac{\partial f}{\partial t} + \frac{\partial f}{\partial x^i} \frac{\hat{p}^i}{a} - p \left( H - \frac{\partial \Phi}{\partial t} + \frac{\partial \Psi}{\partial x^i} \frac{\hat{p}^i}{a} \right) \frac{\partial f}{\partial p} + \text{second order terms},$$

where  $\hat{p}^i = \hat{p}^i p$  is the local 3-momentum.

In the above  $f = f(x^\mu, p^i)$ , however we know that at the background level the phase space distribution should depend only on  $(t, p)$  (due to homogeneity and isotropy of the universe). For this reason we should also decompose the distribution in:

$$f(x^\mu, \mathbf{p}) = \bar{f}(t, p) + \Upsilon(x^\mu, \mathbf{p}), \quad (2.13)$$

where  $\Upsilon$  is the perturbation of the phase space distribution function.

We can get an expression for this perturbation considering a *blackbody radiation* distribution with a fluctuating temperature  $T(x^\mu, \hat{\mathbf{p}}) = \bar{T}(1 + \Theta(x^\mu, \hat{\mathbf{p}}))$ .

Note that now  $\Theta$  depends on the time ( $t = x^0$ ) and position ( $x^i$ ) of observation, other than the direction of motion of the photons, which corresponds to the direction of observation  $\hat{\mathbf{n}}$  of section 2.1 (where the position and time of observation were fixed by the Earth position in spacetime). In this way, expanding in  $\Theta$  we find

$$\begin{aligned} f(x^\mu, p^i) &= \left[ \exp \left\{ \frac{p}{k_B \bar{T}(1 + \Theta)} \right\} - 1 \right]^{-1} \\ &\approx \frac{1}{e^{\frac{p}{k_B \bar{T}}} - 1} + \frac{e^{\frac{p}{k_B \bar{T}}}}{(e^{\frac{p}{k_B \bar{T}}} - 1)^2} \frac{p}{k_B \bar{T}} \Theta = \bar{f} - \Theta p \frac{\partial \bar{f}}{\partial p} \\ &\implies \Upsilon = -\Theta p \frac{\partial \bar{f}}{\partial p}. \end{aligned}$$

## Chapter 2. Anisotropies of the CMB

Expanding the distribution function also in the Liouville operator we get, at first order

$$\hat{L}[\Upsilon] = -p \frac{\partial \bar{f}}{\partial p} \left[ \frac{\partial \Theta}{\partial t} + \frac{\hat{p}^i}{a} \frac{\partial \Theta}{\partial x^i} - \frac{\partial \Psi}{\partial t} + \frac{\hat{p}^i}{a} \frac{\partial \Phi}{\partial x^i} \right], \quad (2.14)$$

where the first two terms describe free streaming (free motion of photons without scatterings) while the last two terms account for the effect of gravity.

To complete the Boltzmann equation we need to consider the first order collision term, describing Compton scatterings. A derivation of this term can be found in the book by Dodelson [4], the final result is:

$$C[\Upsilon]|_{\text{CS}} = -p \frac{\partial \bar{f}}{\partial p} n_e \sigma_T \left[ \Theta_0 - \Theta + \hat{\mathbf{p}} \cdot \mathbf{v}_b \right], \quad (2.15)$$

where  $\mathbf{v}_b$  is the **electron bulk velocity** and  $\Theta_0$  is the **anisotropy monopole**

$$\Theta_0(x^\mu) = \frac{1}{4\pi} \int d\Omega_{\hat{\mathbf{p}}} \Theta(x^\mu, \hat{\mathbf{p}}).$$

Let's appreciate that the collision term, assuming  $\mathbf{v}_b = 0$ , will vanish, and thus give equilibrium, if the anisotropies  $\Theta(\hat{\mathbf{p}}) = \Theta_0$ .

Equating the Liouville operator (2.14) with the collision term (2.15) we obtain

$$\frac{\partial \Theta}{\partial t} + \frac{\hat{p}^i}{a} \frac{\partial \Theta}{\partial x^i} - \frac{\partial \Psi}{\partial t} + \frac{\hat{p}^i}{a} \frac{\partial \Phi}{\partial x^i} = n_e \sigma_T \left[ \Theta_0 - \Theta + \hat{\mathbf{p}} \cdot \mathbf{v}_b \right] \quad (2.16)$$

which is the equation describing the dynamics of the *CMB anisotropies*. Assuming initially  $\Theta = 0$ , the perturbation of the metric  $\Psi$  and  $\Phi$  can still generate a final non-zero anisotropy. In this sense, perturbations are source terms for  $\Theta$ .

Since the above is a linear partial differential equation, it can be reduced to an ordinary differential equation by Fourier transforming the spatial coordinates. Introducing

$$\Theta(x^\mu) = \int \frac{d^3k}{(2\pi)^3} e^{i\mathbf{k} \cdot \mathbf{x}} \tilde{\Theta}(\mathbf{k}, t), \quad \mu \stackrel{\text{def}}{=} \cos \theta = \frac{\mathbf{k} \cdot \hat{\mathbf{p}}}{k},$$

respectively, the Fourier transform of  $\Theta$  and the cosine of the angle between  $\mathbf{k}$  and  $\hat{\mathbf{p}}$ , and assuming that  $\mathbf{v}_b$  is irrotational ( $\tilde{\mathbf{v}}_b = \hat{\mathbf{k}} \tilde{v}_b$ ) we obtain in momentum space:

$$\frac{\partial \tilde{\Theta}}{\partial t} + \frac{ik\mu}{a} \tilde{\Theta} + \frac{\partial \tilde{\Psi}}{\partial t} + \frac{ik\mu}{a} \tilde{\Phi} = n_e \sigma_T \left[ \tilde{\Theta}_0 - \tilde{\Theta} + \mu \tilde{v}_b \right].$$

The above collision term (2.15) however neglects the angular dependence of Compton scatterings, by accounting also for this (as explained in [4]) a new term appears:

$$\frac{\partial \tilde{\Theta}}{\partial t} + \frac{ik\mu}{a} \tilde{\Theta} + \frac{\partial \tilde{\Psi}}{\partial t} + \frac{ik\mu}{a} \tilde{\Phi} = n_e \sigma_T \left[ \tilde{\Theta}_0 - \tilde{\Theta} + \mu \tilde{v}_b - \frac{3\mu^2 - 1}{4} \tilde{\Theta}_2 \right], \quad (2.17)$$

where  $\tilde{\Theta}_2 \stackrel{\text{def}}{=} -\frac{1}{2} \int_{-1}^{+1} d\mu \frac{3\mu^2 - 1}{2} \tilde{\Theta}$  is the **anisotropy quadrupole momentum**. In the next sections we will discover that this momentum plays a leading role for many phenomena.

### 2.2.1 Polarization from Compton scattering

In the previous section we studied how the phase space of photons evolves in a perturbed spacetime. However, we have not yet considered that photons are spin 1 particles, and thus, to fully describe them, we also need to know their polarization.

To understand how polarization can be described, let's consider a monochromatic plane wave (which we could consider as a Fourier component of a generic wave). The electric and magnetic fields of such a wave, in empty space, are not independent, due to Maxwell equations, and thus we can just focus on the electric field.

If the wave is propagating along the  $\hat{\mathbf{z}}$  axis, its electric field can be written as

$$\mathbf{E}(z, t) = \text{Re} \left\{ (E_x \hat{\mathbf{x}} + E_y \hat{\mathbf{y}}) e^{ik(z-t)} \right\},$$

where  $E_x$  and  $E_y$  are the components of the electric field in complex space. Since they are complex numbers we can decompose them in the polar representation  $E_x = |E_x| e^{i\phi_x}$ ,  $E_y = |E_y| e^{i\phi_y}$ , in this way the monochromatic wave reads:

$$\mathbf{E}(z, t) = |E_x| \cos[k(z-t)] \hat{\mathbf{x}} + |E_y| \cos[k(z-t) + \phi] \hat{\mathbf{y}} \quad \text{with } \phi = \phi_y - \phi_x.$$

This shows that the electric field, at a fixed  $z = z_0$ , evolves drawing an ellipse in the  $xy$  plane. Note that this ellipse can degenerate depending on the values of  $|E_x|$ ,  $|E_y|$  and  $\phi$ :

- if  $\phi = 0, \pi$  or if one of the components  $E_x, E_y$  vanishes, the ellipse degenerates into a line, we call this case **linear polarization**;
- if  $\phi = \pm \frac{\pi}{2}$  and  $E_x = E_y$ , the ellipse degenerates into a circle, we call this case **circular polarization**.

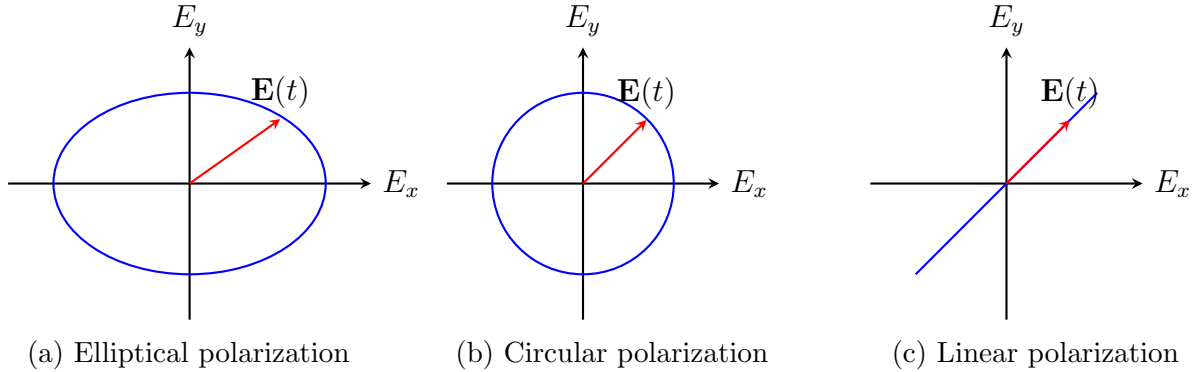


Figure 2.1: The plots of the electric field in the  $xy$  plane: each point of the plot corresponds to the electric field at a given time. In the first plot (a) the general elliptical polarization is represented, while in other two plots the electric field with circular (b) and linear polarization (a) are represented.

In general, the polarization describes how the electric field, of a wave, oscillates: indeed, figure 2.1 shows that for linear polarization, for example, the electric field oscillates in a precise direction. The polarization of a photon can be described the **Stokes parameters**:

$$\begin{aligned} I &\stackrel{\text{def}}{=} |E_x|^2 + |E_y|^2, & Q &\stackrel{\text{def}}{=} |E_x|^2 - |E_y|^2, \\ U &\stackrel{\text{def}}{=} 2|E_x||E_y| \cos \phi, & V &\stackrel{\text{def}}{=} 2|E_x||E_y| \sin \phi, \end{aligned} \quad (2.18)$$

where  $I$  is the intensity of the light while  $Q, U$  and  $V$  describe the polarization. Indeed, for linear polarized light  $U = V = 0$  while  $Q$  is related to the direction of oscillation. On the other hand, for circular polarization  $Q = U = 0$  while  $V \neq 0$ .

Circular polarization is not produced in the early universe, therefore we will set  $V = 0$ , so that we are describing only linearly polarized or unpolarized light.

Before proceeding, we should note that under rotations in the  $xy$  plane

$$E_x \rightarrow E_x \cos \theta - E_y \sin \theta, \quad E_y \rightarrow E_x \sin \theta + E_y \cos \theta,$$

the Stokes parameters will transform as

$$I \rightarrow I, \quad Q \pm iU \rightarrow e^{\pm 2i\theta} (Q \pm iU).$$

This transformation shows that the combination  $(Q \pm iU)$  transforms as a *spin-2 tensor* while  $I$  as a scalar. This observation will be crucial when we will need to decompose these modes. The above transformation makes also more clear the interpretation of the parameter  $U$ : from the above we have  $U' = \text{Im}[\exp(\pm 2i\theta)(Q \pm iU)]$ , thus for  $\theta = \pm\pi/2$  we have  $U' = \pm Q$ , showing that  $U$  is the difference of the components of  $\mathbf{E}$  along the bisectors of the  $x$  and  $y$  axis.

Now that we know how to describe polarized light, let's move to study how *Compton scattering* is influenced by polarization. Consider an electron, on which light can be scatter off, the interaction can absorb some components of the electric field, letting the other unchanged, modifying the polarization of the photon.

For example, an unpolarized photon moving along the  $x$  axis and deflected along the  $z$  axis, in the end, will have a polarization along the  $y$  axis. This is due to the simple fact that  $\mathbf{E}$  and  $\mathbf{B}$  must be orthogonal to the direction of motion and therefore any component along the  $z$  axis will be absorbed by the electron (as shown in figure 2.2 (a)).

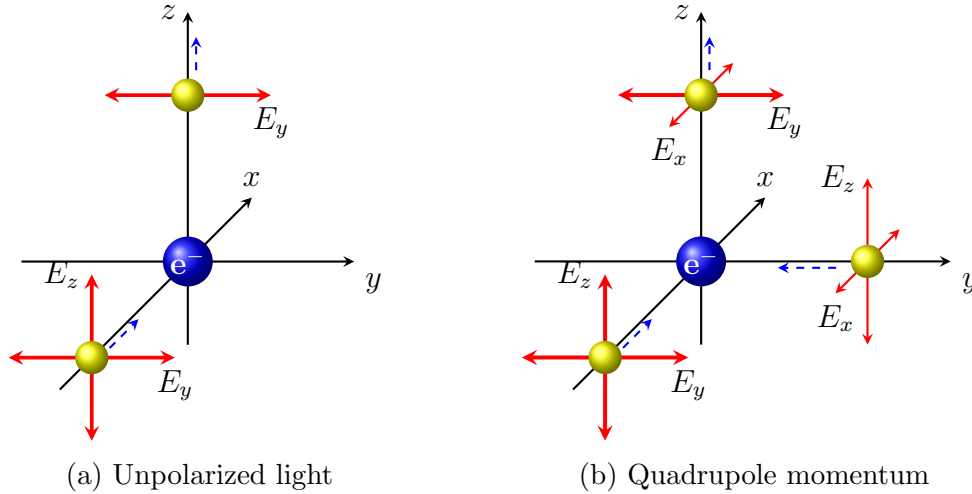


Figure 2.2: Graphical depiction Compton scatterings effects on polarized light. Figure (a) shows an unpolarized photon scattered by an electron resulting in a linearly polarized photon. Figure (b) instead shows how the presence of a quadrupole momentum can generate polarized photons by the scatterings: thicker vectors represents more intense electric fields, thus "hotter" photons.

In the general case, consider some incoming radiation with polarization  $\epsilon_i'^3$  which gets

---

<sup>3</sup> $\epsilon_i'$  are the versors onto which the  $\mathbf{E}$  decomposes.

scattered off by an electron. The deflected radiation will instead have a polarization  $\epsilon_i$ . Without loss of generality, we can orient our coordinate axis such that the outgoing radiation is travelling along the  $z$  axis and the polarization  $\epsilon_1 = \hat{\mathbf{x}}$  and  $\epsilon_2 = \hat{\mathbf{y}}$ . The parameter  $Q$ , after the scattering, can be estimated decomposing the incoming polarization on the outgoing one and then averaging over all possible incoming photons:

$$Q \propto \int d\Omega_{in} f_{in}(\hat{\mathbf{n}}') \sum_{i=1}^2 \left[ |\epsilon'_i \cdot \hat{\mathbf{x}}|^2 - |\epsilon'_i \cdot \hat{\mathbf{y}}|^2 \right],$$

where  $f_{in}$  is the phase space distribution of the incoming photons.

As a function of the polar incoming angles, the incoming polarization can be written as

$$\begin{aligned} \epsilon'_1(\theta', \phi') &= (\cos \theta' \cos \phi', \cos \theta' \sin \phi', -\sin \theta'), \\ \epsilon'_2(\theta', \phi') &= (-\sin \phi', \cos \theta', 0). \end{aligned}$$

Once inserted in the previous integral we find

$$\begin{aligned} Q &\propto \int d\Omega_{in} f_{in}(\hat{\mathbf{n}}') \left[ \cos^2 \theta' \cos^2 \phi' + \sin^2 \phi' - \cos^2 \theta' \sin^2 \phi' - \cos^2 \phi' \right] \\ &\propto \int d\Omega_{in} f_{in}(\hat{\mathbf{n}}') (\sin^2 \theta' \cos 2\phi') \propto \int d\Omega_{in} f_{in}(\hat{\mathbf{n}}') \left[ Y_{2,2}(\hat{\mathbf{n}}') + Y_{2,-2}(\hat{\mathbf{n}}') \right], \end{aligned}$$

where we recognized, in the last step, that  $\sin^2 \theta' \cos 2\phi'$  is proportional to the sum of two spherical harmonics<sup>4</sup>.

Now, considering perturbations of the temperature in  $f_{in}$ , as in (2.13), we discover that, since the integral picks the modes with  $\ell = 2$ , polarization will be generated through Compton scatterings by the quadrupole momentum  $\Theta_2$ . Similar calculations can lead to the same conclusion for the parameter  $U$ .

Intuitively, this can be understood considering two unpolarized photons, with different energies (thus temperatures when we consider an ensemble), travelling towards an electron from orthogonal directions: this simplified setting corresponds to a quadrupole momentum of the anisotropies. Then, a photon scattered in the  $z$  direction will then have one component of its electric field given by the first photon and the other component from the second photon, as represented in figure 2.2 (b). Since the two photons have different energies, the electric field components of the scattered photon will be different, giving a polarization to it.

To appropriately describe polarization in the context of anisotropies we must develop a proper framework. Let's start considering linear polarized light propagating in the  $z$  direction: the stokes parameter  $Q$  will therefore measure the difference of the energy density (recall  $\rho \propto \mathbf{E}^2$ ) associated to the electric field components  $E_x$  and  $E_y$ .

This radiation can be seen as the superposition of two gasses of photons: each one will be made by photons described by one of the two components of the electric field. Then, each gas will have its own phase space distribution:  $f_x$  and  $f_y$ . Note that if the two distributions are identical the light turns out to be unpolarized with respect to  $Q$ : indeed the two gasses would have the same temperature and thus the two components of  $\mathbf{E}$  would be equal, giving  $Q = 0$ <sup>5</sup>. Hence, we need to consider temperature anisotropies between

<sup>4</sup>Recall that  $Y_{\ell,\pm\ell}(\theta, \phi) = \frac{(\mp)^{\ell}}{2^{\ell}\ell!} \sqrt{\frac{(2\ell+1)!}{4\pi}} \sin^{\ell} \theta e^{\pm i\ell\phi}$  and therefore  $Y_{2,2} + Y_{2,-2} \propto \sin^2 \theta \cos 2\phi$ .

<sup>5</sup>For now, we just consider  $Q$  later on we will also find a way to describe  $U$ .

the two distributions: to better describe these we introduce a *phase space matrix*

$$\mathcal{F}_{\text{unpol}} \stackrel{\text{def}}{=} \begin{pmatrix} f_x(\bar{T}) & 0 \\ 0 & f_y(\bar{T}) \end{pmatrix} \xrightarrow{\text{polarization}} \mathcal{F} \stackrel{\text{def}}{=} \begin{pmatrix} f_x(\bar{T}[1 + \Theta_x]) & 0 \\ 0 & f_y(\bar{T}[1 + \Theta_y]) \end{pmatrix}, \quad (2.19)$$

where  $\Theta_x(x^\mu, \mathbf{n})$  and  $\Theta_y(x^\mu, \mathbf{n})$  are the fluctuations around the mean temperature  $\bar{T}$ . The total phase space distribution is then recovered by taking the trace of the above matrices  $f = \text{Tr}(\mathcal{F})/2$ , which corresponds to the average of the components.

From these two anisotropies we can define, recalling that  $T^4 \propto \rho \propto \mathbf{E}^2$ ,

$$\begin{aligned} \Theta_Q &\stackrel{\text{def}}{=} \Theta_x - \Theta_y \\ &= \frac{\Delta T_x - \Delta T_y}{\bar{T}} = \frac{\Delta \rho_x - \Delta \rho_y}{4\bar{\rho}} = \frac{(E_x^2 - \mathbf{E}^2) - (E_y^2 - \mathbf{E}^2)}{4\mathbf{E}^2} = \frac{Q}{4I}, \end{aligned} \quad (2.20)$$

where we used the approximation  $\Delta \rho / \rho \propto 4\Delta T / T$  for small perturbations.

The same holds for  $\Theta_U = U/(4I)$ , since we just need to rotate the axis to turn  $Q \rightarrow U$ , then we can repeat the above calculations and rotate everything back.

Lastly, we want to describe polarization by a single parameter, this can be done exploiting rotations. Suppose we have described chosen the axis such that  $Q \neq 0$  and  $U = 0$ , in this way  $\Theta_Q$  describes the anisotropies related to the "amplitude" of polarization and  $\Theta_U$  is not needed. To allow for a generic orientation of the axis we rotate the  $xy$  plane defining the amplitude  $\Theta_P$  to correspond to the previous  $\Theta_Q$ , which now instead reads

$$\Theta_Q = \Theta_P \cos 2\phi, \quad \text{while } \Theta_U = \Theta_P \sin 2\phi.$$

Note that the above discussion holds only for monochromatic waves. When dealing with a Fourier decomposition these two last formulae hold only in the limit  $\hat{\mathbf{n}} \cdot \hat{\mathbf{k}} \ll 1$ , with  $\hat{\mathbf{n}}$  direction of propagation of the full wave.

$\Theta_P$  will then evolve with its own Boltzmann equation: all the physics described previously is unchanged, however we need to account for Compton scattering effect on polarization. Indeed, we already discussed that the quadrupole  $\tilde{\Theta}_2$  will polarize scattered photons, therefore a collision term proportional to  $\Theta_2$  must be added to the Boltzmann equation (2.16). Furthermore, if polarization is not sourced, through Compton scattering the radiation will gradually become unpolarized. This means that now a term proportional to  $-\tilde{\Theta}_P$  must be added as a collision contribution. The final result, derived in [1], is the Boltzmann equation for the polarization anisotropy:

$$\frac{\partial \tilde{\Theta}_P}{\partial t} + \frac{ik\mu}{a} \tilde{\Theta}_P = -n_e \sigma_T \left[ \tilde{\Theta}_P + \frac{1}{2} \left( 1 - P_2(\mu) \right) \Pi \right], \quad (2.21)$$

where  $\Pi = \tilde{\Theta}_2 + \tilde{\Theta}_{P,2} + \tilde{\Theta}_{P,0}$  and  $P_2(\mu) = \frac{3\mu^2 - 1}{2}$  is the order 2 Legendre polynomial. Then, polarization will affect also the regular collision term for Compton scattering, hence equation (2.16) must be corrected:

$$\frac{\partial \tilde{\Theta}}{\partial t} + \frac{ik\mu}{a} \tilde{\Theta} + \frac{\partial \tilde{\Psi}}{\partial t} + \frac{ik\mu}{a} \tilde{\Phi} = n_e \sigma_T \left[ \tilde{\Theta}_0 - \tilde{\Theta} + \mu \tilde{v}_b - \frac{1}{4} P_2(\mu) \Pi \right]. \quad (2.22)$$

### 2.2.2 Multipole expansion of the Boltzmann equation

In section 2.2.1 we obtained the differential equations (2.22) and (2.21) governing the time evolution of the anisotropies in the CMB. To end our discussion of the time evolution of the anisotropies we want to expand these equations in multipoles.

Since the CMB is observed in the sky, spherical harmonics are the natural basis to use to project the anisotropies. The fact that the equations (2.22) and (2.21) depend only on  $\mu = \hat{\mathbf{p}} \cdot \hat{\mathbf{k}}$ , corresponds to a rotational symmetry of the system around one of these two vectors. By using spherical polar coordinates, such that the vector  $\hat{\mathbf{k}}$  lies on the  $z$  axis, the above symmetry corresponds to a rotational symmetry of the azimuthal angle  $\phi$ . Considering that  $Y_{\ell m} \propto e^{im\phi}$ , we immediately recognize that such symmetry is respected only by spherical harmonics with  $m = 0$  and these precisely corresponds to the Legendre polynomials. Therefore, for scalar perturbation, we can limit ourselves to a multipole expansion on the Legendre polynomials, without worrying of all the spherical harmonics.

By multiplying the (2.22) by the order  $\ell$  Legendre polynomial  $P_\ell(\mu)$  and integrating over  $\mu$ , we can exploit the orthogonality of the Legendre polynomials as follows.

- $\frac{\partial \tilde{\Theta}}{\partial t}$  and  $n_e \sigma_T \tilde{\Theta}$  depending on  $\mu$  in this expansion will give contributions corresponding respectively to  $\frac{\partial \tilde{\Theta}_\ell}{\partial t}$  and  $n_e \sigma_T \tilde{\Theta}_\ell$ .
- $\frac{\partial \tilde{\Psi}}{\partial t}$  and  $n_e \sigma_T \tilde{\Theta}_0$  have no  $\mu$  dependence, which corresponds to the zeroth order Legendre polynomial  $P_0(\mu) = 1$ , and thus they only contribute to the  $\ell = 0$  equation.
- $\tilde{\Phi}$  and  $n_e \sigma_T \tilde{v}_b$  are multiplied by  $P_1(\mu) = \mu$ , giving contributions only to  $\ell = 1$  equation, while  $\Pi$  is multiplied by  $P_2(\mu) = \frac{3\mu^2 - 1}{2}$ , contributing only to  $\ell = 2$  equation. Note that these terms must also be multiplied by a factor corresponding to the integral of their respective Legendre polynomial, since they don't contain any  $\tilde{\Theta}$  function to be expanded
- $\frac{ik\mu}{a} \tilde{\Theta}$  is instead more complicated since it is the product of two functions depending on  $\mu$ . Bonnet's formula (2.10) allows us to simplify the corresponding integral

$$\frac{i^\ell}{2} \int_{-1}^{+1} d\mu \mu P_\ell(\mu) \tilde{\Theta} = \frac{i^\ell}{2} \int_{-1}^{+1} d\mu \left[ \frac{\ell+1}{2\ell+1} P_{\ell+1}(\mu) + \frac{\ell}{2\ell+1} P_{\ell-1}(\mu) \right] \tilde{\Theta},$$

in this way this will give contributions to all the equations coupling them together.

Putting all of this together we obtain the following coupled system of differential equations

$$\dot{\tilde{\Theta}}_0 = -\frac{k}{a} \tilde{\Theta}_1 + \dot{\tilde{\Psi}} \quad (2.23a)$$

$$\dot{\tilde{\Theta}}_1 = \frac{k}{3a} \tilde{\Theta}_0 - \frac{2k}{3a} \tilde{\Theta}_2 + \frac{k}{3} \tilde{\Phi} - n_e \sigma_T \left[ \tilde{\Theta}_1 + \frac{\tilde{v}_b}{3} \right] \quad (2.23b)$$

$$\dot{\tilde{\Theta}}_\ell = \frac{\ell k}{(2\ell+1)a} \tilde{\Theta}_{\ell-1} - \frac{(\ell+1)k}{(2\ell+1)a} \tilde{\Theta}_{\ell+1} - n_e \sigma_T \left[ \tilde{\Theta}_\ell - \frac{\delta_{\ell,2}}{10} \Pi \right] \quad \ell \geq 2, \quad (2.23c)$$



Similarly, equation (2.21) will result in the following system of differential equations

$$\dot{\tilde{\Theta}}_{P0} = -\frac{k}{a}\tilde{\Theta}_{P1} - n_e\sigma_T\left[\tilde{\Theta}_{P0} - \frac{1}{2}\Pi\right] \quad (2.24a)$$

$$\dot{\tilde{\Theta}}_{P\ell} = \frac{\ell k}{(2\ell+1)a}\tilde{\Theta}_{P\ell-1} - \frac{(\ell+1)k}{(2\ell+1)a}\tilde{\Theta}_{P\ell+1} - n_e\sigma_T\left[\tilde{\Theta}_{P\ell} - \frac{\delta_{\ell,2}}{10}\Pi\right] \quad \ell \geq 1, . \quad (2.24b)$$

Equations (2.23) and (2.24) are not the full system of coupled equations, indeed these equations depend on the potential  $\tilde{\Psi}$  and  $\tilde{\Phi}$  and on the electron bulk velocity  $\tilde{v}_b$ . The differential equations governing these quantities must then be added to the ones above and solved all together.

Note that, in the above equations,  $\Psi$  and  $\Phi$  appears only in the equation with  $\ell = 0, 1$ : this means that primordial perturbations source directly only the first two momenta of the anisotropies. Then, since all the equations are coupled together, the dynamics of the anisotropies will give rise to the other momenta.

### 2.2.3 Polarization power spectrum Check convention

We already discussed that, in order to completely describe photons (thus the CMB), we also need to account for polarization. It is therefore natural to define a power spectrum for the polarization, which can be done similarly as for the temperature.

We want to expand in spherical harmonics the Stokes parameters  $Q$  and  $U$  (2.18), however we showed, in section 2.2.1 that under a rotation the combination  $Q \pm iU$  will transform as a spin 2 fields. This means that we cannot resort to the usual spherical harmonics decomposition, instead we must use **spin-weighted spherical harmonics**  $Y_{\ell m}^{\pm 2}$ . In this way we get

$$Q(\hat{\mathbf{n}}) \pm iU(\hat{\mathbf{n}}) = \sum_{\ell m} a_{\ell m}^{\pm 2} Y_{\ell m}^{\pm 2}(\hat{\mathbf{n}}).$$

It is then common to use modes that are projectable on the regular spherical harmonics: we start defining

$$a_{\ell m}^E \stackrel{\text{def}}{=} -\frac{a_{\ell m}^2 + a_{\ell m}^{-2}}{2}, \quad a_{\ell m}^B \stackrel{\text{def}}{=} \frac{a_{\ell m}^2 - a_{\ell m}^{-2}}{2i},$$

then we can recompose these modes as

$$E(\hat{\mathbf{n}}) = \sum_{\ell m} a_{\ell m}^E Y_{\ell m}(\hat{\mathbf{n}}), \quad B(\hat{\mathbf{n}}) = \sum_{\ell m} a_{\ell m}^B Y_{\ell m}(\hat{\mathbf{n}}). \quad (2.25)$$

The power spectra of the polarization can then be defined, as usual, as

$$\langle a_{\ell m}^E a_{\ell' m'}^{E*} \rangle \stackrel{\text{def}}{=} C_\ell^{EE} \delta_{\ell\ell'} \delta_{mm'}, \quad (2.26)$$

$$\langle a_{\ell m}^B a_{\ell' m'}^{B*} \rangle \stackrel{\text{def}}{=} C_\ell^{BB} \delta_{\ell\ell'} \delta_{mm'}, \quad (2.27)$$

$$\langle a_{\ell m} a_{\ell' m'}^{E*} \rangle \stackrel{\text{def}}{=} C_\ell^{TE} \delta_{\ell\ell'} \delta_{mm'}. \quad (2.28)$$



## 2.3 Tensor perturbations effects on the CMB

In the previous sections we focused on how the scalar perturbations interact with the CMB generating anisotropies. We will instead now study how tensor perturbations, namely gravitational waves produced during inflation, affects the evolution of the plasma of photons and what kind of anisotropies are sourced by them.

In appendix B.4 we showed that, considering tensor perturbed metric

$$ds^2 = -dt^2 + a^2(\delta_{ij}h_{ij})dx^dx^j,$$

the *Liouville operator* reads as in (B.8)

$$\hat{\mathbf{L}}[f] = \frac{\partial f}{\partial t} + \frac{\hat{p}^i}{a} \frac{\partial f}{\partial x^i} - \frac{1}{2} \frac{\partial f}{\partial t} \dot{h}_{ij} \hat{p}^i \hat{p}^j + \text{second order terms},$$

where  $p^i = p \hat{p}^i$  is the local 3-momentum of a photon and  $f$  the phase space distribution.

To obtain the equation describing the evolution of anisotropies, we must expand the photon phase space distribution on a blackbody radiation background ( $\bar{f}(t, p) + \Upsilon(x^\mu, \mathbf{p})$ ) and assume that the temperature is perturbed as  $T(x^\mu, \hat{\mathbf{p}}) = \bar{T}(1 + \Theta(x^\mu, \hat{\mathbf{p}}))$ . Proceeding in the same way as in section 2.2 with the above Liouville operator, we obtain the Liouville operator for the distribution perturbation

$$\hat{\mathbf{L}}[\Upsilon] = -p \frac{\partial \bar{f}}{\partial p} \left[ \frac{\partial \Theta}{\partial t} + \frac{\hat{p}^i}{a} \frac{\partial \Theta}{\partial x^i} + \frac{1}{2} \dot{h}_{ij} \hat{p}^i \hat{p}^j \right].$$

At this point we need to add the first order collision term associated to Compton scattering. For now let's consider the simplified form (2.15). Using Boltzmann equation and canceling out the common factor  $-p \frac{\partial \bar{f}}{\partial p}$  from both sides, as in section 2.2, we get the differential equation that describes the time evolution of the CMB anisotropies in presence of tensor perturbations

$$\frac{\partial \Theta}{\partial t} + \frac{\hat{p}^i}{a} \frac{\partial \Theta}{\partial x^i} + \frac{1}{2} \dot{h}_{ij} \hat{p}^i \hat{p}^j = n_e \sigma_T \left[ \Theta_0 - \Theta + \hat{\mathbf{p}} \cdot \mathbf{v}_b \right]. \quad (2.29)$$

Again, note that the tensor perturbations can be a source for the anisotropies, as for the scalar case.

### 2.3.1 Coupling of tensors to anisotropies

Previously, to expand equation (2.16), we Fourier transformed  $\Theta(t, \mathbf{x}, \hat{\mathbf{p}})$  and then expanded it in Legendre polynomials. However, this last step was justified (in section 2.2.2) by noting that the equations depended only on the cosine of angle between the direction of motion of the photon  $\hat{\mathbf{p}}$  and the wave number vector of the Fourier transform  $\mathbf{k}$ . This corresponded to a rotational symmetry around one of the above vectors that implied that Legendre polynomials were the appropriate basis to expand on. We shall now study equation (2.29), and its symmetries, to understand what will now be the right basis to use for this expansion.

## Chapter 2. Anisotropies of the CMB

To begin, let's recall that, being traceless transverse, in Fourier space  $h_{ij}$  can be separated in two independent polarizations

$$0 = \partial^i h_{ij} = \int \frac{d^3 k}{(2\pi)^3} e^{i\mathbf{k}\cdot\mathbf{x}} \tilde{h}_{ij} k^i \xrightarrow{\text{Traceless Symmetric}} \tilde{h}_{ij} = \tilde{h}_\times \mathbf{e}_{ij}^\times + \tilde{h}_+ \mathbf{e}_{ij}^+ = \begin{pmatrix} \tilde{h}_\times & \tilde{h}_+ & 0 \\ \tilde{h}_+ & -\tilde{h}_\times & 0 \\ 0 & 0 & 0 \end{pmatrix}.$$

Now, the only term in equation (2.29) that could give a more complicated angular dependence (that just  $\cos\theta$ ) is  $\dot{h}_{ij}\hat{p}^i\hat{p}^j$ : considering spherical polar coordinates  $(r, \theta, \phi)$  with  $\mathbf{k} \parallel \hat{\mathbf{z}}$ , once Fourier transformed, this term will be proportional to

$$\hat{\mathbf{p}} = (\sin\theta \cos\phi, \sin\theta \sin\phi, \cos\theta) \Rightarrow (\mathbf{e}_{ij}^\times + \mathbf{e}_{ij}^+) \hat{p}^i \hat{p}^j = \sin^2\theta (\cos 2\phi + \sin 2\phi).$$

This clearly shows that anisotropies coupled to tensor perturbations can no longer be decomposed on Legendre polynomials, since the azimuthal symmetry is now spoiled by the explicit dependence on  $\phi$ .

To individuate the appropriate basis for the spherical harmonics expansion, let's use the basis introduced by Hu and White in [6]

$$h_{ij} = -\sqrt{\frac{3}{2}}(h^{(+)}\mathbf{e}_{ij}^{(+)} + h^{(-)}\mathbf{e}_{ij}^{(-)}) \quad \text{with } \mathbf{e}^{(+)} = \begin{pmatrix} 1 & +i & 0 \\ +i & -1 & 0 \\ 0 & 0 & 0 \end{pmatrix} \quad \mathbf{e}^{(-)} = \begin{pmatrix} 1 & -i & 0 \\ -i & -1 & 0 \\ 0 & 0 & 0 \end{pmatrix}. \quad (2.30)$$

Comparing this definition and the previous basis, we can easily find the transformation between the two polarizations

$$\begin{aligned} h_+ &= -\sqrt{\frac{3}{2}}(h^{(+)} + h^{(-)}), & h^{(+)} &= \frac{1}{\sqrt{6}}(h_+ - ih_-), \\ h_- &= -i\sqrt{\frac{3}{2}}(h^{(+)} - h^{(-)}), & h^{(-)} &= -\frac{1}{\sqrt{6}}(h_+ + ih_-). \end{aligned}$$

Let's now project the versor  $\hat{\mathbf{p}}$ , defined as above, onto  $\mathbf{e}^{(\pm)}$ ,

$$\mathbf{e}_{ij}^{(\pm)} \hat{p}^i \hat{p}^j = \sin^2\theta [\cos^2\phi - \sin^2\phi \pm 2i \sin\phi \cos\phi] = \sin^2\theta e^{\pm i2\phi},$$

immediately we should recognize that this term is proportional to the spherical harmonics  $Y_{2,\pm 2}(\theta, \phi) = \frac{1}{4}\sqrt{\frac{15}{2\pi}} \sin^2\theta e^{\pm i2\phi}$ . This shows that the appropriate basis for the expansion of the anisotropies are the spherical harmonics  $Y_{\ell m}$  with  $m = \pm 2$ , since they all possess the same azimuthal symmetry  $Y_{\ell m} \propto e^{\pm i2\phi}$  as the tensor term in (2.29).

Following Hu and White [6] convention, we will use the following multipole expansion for the anisotropies

$$\Theta(t, \mathbf{x}, \hat{\mathbf{p}}) = \int \frac{d^3 k}{(2\pi)^3} e^{i\mathbf{k}\cdot\mathbf{x}} \sum_{\ell m} (-i)^\ell \sqrt{\frac{4\pi}{2\ell+1}} Y_{\ell m}(\hat{\mathbf{p}}) \tilde{\Theta}_\ell^{(m)}(t, \mathbf{k}), \quad (2.31)$$

in which we will only use the multipoles with  $m = \pm 2$ , for the reasons we just explained. Note that for  $m = 0$ , since  $Y_{\ell 0} = \sqrt{\frac{2\ell+1}{4\pi}} P_\ell(\cos\theta)$ , we recover the Legendre polynomials expansion used for scalar perturbations. In this case the sum over the  $2\ell + 1$  different

values of  $m$  will result in the correspondence  $\tilde{\Theta}_\ell^{(0)} = (2\ell + 1)\tilde{\Theta}_\ell$ .

Lastly, we shall note that the normalization of the new polarization (2.30) is such that

$$\begin{aligned} \frac{1}{2}\dot{\tilde{h}}_{ij}\hat{p}^i\hat{p}^j &= \frac{1}{2}\left(-\sqrt{\frac{3}{2}}\right)\left[\dot{\tilde{h}}^{(+)}\sin^2\theta e^{i2\phi} + \dot{\tilde{h}}^{(-)}\sin^2\theta e^{-i2\phi}\right] \\ &= -\sqrt{\frac{4\pi}{5}}\left[\dot{\tilde{h}}^{(+)}Y_{2,2}(\hat{\mathbf{p}}) + \dot{\tilde{h}}^{(-)}Y_{2,-2}(\hat{\mathbf{p}})\right], \end{aligned}$$

where the factor  $-\sqrt{\frac{4\pi}{5}}$  precisely corresponds to  $i^\ell\sqrt{\frac{4\pi}{2\ell+1}}|_{\ell=2}$ , which is also the factor that get all the others  $\tilde{\Theta}_2^{(2)}$  in the expansion. In this way the contribution of the tensor perturbation to the multipole expansion of equation (2.29), with  $\ell = 2$  and  $m = \pm 2$ , will be exactly  $\dot{\tilde{h}}^{(\pm)}$ .

### 2.3.2 Multipole expansion of tensor induced anisotropies

Knowing that tensor perturbations are projected in the sky onto spherical harmonics with  $m = \pm 2$  while scalar perturbations are projected onto spherical harmonics with  $m = 0$ , by their orthogonality, we can expand  $\Theta$  in multipoles using only  $Y_{\ell,\pm 2}$ . In this way we effectively decoupled the multipoles generated by tensor perturbations and the scalar ones.

First, we move to Fourier space where the equation describing anisotropies (2.29) reads

$$\frac{\partial \tilde{\Theta}}{\partial t} + i\frac{k \cos \theta}{a}\tilde{\Theta} - \sqrt{\frac{4\pi}{5}}\left[\dot{\tilde{h}}^{(+)}Y_{2,2}(\hat{\mathbf{p}}) + \dot{\tilde{h}}^{(-)}Y_{2,-2}(\hat{\mathbf{p}})\right] = n_e\sigma_T\left[\tilde{\Theta}_0 - \tilde{\Theta} + k\tilde{v}_b \cos \theta\right],$$

in which we assumed that  $\mathbf{v}_b$  is irrotational.

Now, the expansion in spherical harmonics (2.31) yields

$$\tilde{\Theta}_\ell^{(m)}(\mathbf{k}) = i^\ell\sqrt{\frac{2\ell+1}{4\pi}}\int d\Omega_{\hat{\mathbf{p}}}\tilde{\Theta}(\mathbf{x}, \hat{\mathbf{p}})Y_{\ell,m}^*(\theta, \phi),$$

therefore, upon integration of the equation above we can decompose it in a set of ordinary differential equations, one for each multipole  $\tilde{\Theta}_\ell^{(m)}$ .

However, similarly to what happened in section 2.2.2, we obtain from the second term on the left-hand side a contribution proportional to  $Y_{\ell m}^*(\theta, \phi)\cos\theta$ . The proprieties of spherical harmonics allows to simplify this term as follows

$$\cos\theta Y_{\ell m}(\theta, \phi) = \sqrt{\frac{4\pi}{3}}Y_{10}Y_{\ell m} = \sqrt{\frac{\ell^2 - m^2}{2\ell - 1}}Y_{\ell-1,m} + \sqrt{\frac{\ell^2 - m^2}{2\ell + 3}}Y_{\ell+1,m}$$

and upon integration we therefore also get contributions from other multipoles.

In this way equation (2.29) will be decomposed into

$$\dot{\tilde{\Theta}}_2^{(\pm 2)} = -n_e\sigma_T\tilde{\Theta}_2^{(\pm 2)} - \dot{\tilde{h}}^{(\pm)} \quad (2.32a)$$

$$\dot{\tilde{\Theta}}_\ell^{(\pm 2)} = \frac{k}{a}\left[\frac{\sqrt{\ell^2 - 4}}{2\ell - 1}\tilde{\Theta}_{\ell-1}^{(\pm 2)} - \frac{\sqrt{\ell^2 - 4}}{2\ell + 3}\tilde{\Theta}_{\ell+1}^{(\pm 2)}\right] - n_e\sigma_T\tilde{\Theta}_\ell^{(\pm 2)} \quad \ell \geq 3, \quad (2.32b)$$

where the contributions from  $\tilde{\Theta}_0$  and  $\tilde{v}_b$  are not appearing since they are multiplied by the  $m = 0$  spherical harmonics. Note that this time the primordial perturbations directly source a quadrupole momentum, that then can source the higher momenta.

As we discussed in section 2.2.1 the Compton scattering is influenced by the polarization of incoming and outgoing photons. For this reason we must add corrections to the above equations. To add the proper corrections we need also to describe the dynamics of the polarization.

Expanding the polarization in spherical harmonics as

$$(\Theta_Q \pm i\Theta_U)(\mathbf{x}, \hat{\mathbf{p}}) = \int \frac{d^3k}{(2\pi)^3} e^{i\mathbf{k}\cdot\mathbf{x}} \sum_{\ell m} (-i)^\ell \sqrt{\frac{4\pi}{2\ell+1}} Y_{\ell m}^{\pm 2}(\hat{\mathbf{p}}) (\tilde{E}_\ell^{(m)} \pm i\tilde{B}_\ell^{(m)}), \quad (2.33)$$

where  $Y_{\ell m}^{\pm 2}$  are again the *spin weighted spherical harmonics*. We already discussed that, while the free streaming of photons is not influenced by the polarization, the quadrupole of the anisotropies sources polarized light and then, when not produced, at equilibrium we should obtain unpolarized light. This means that the equation for the dynamics of polarization anisotropies should be the same of the regular  $\tilde{\Theta}^{(\pm 2)}$  plus source terms for  $\tilde{\Theta}_2$  and  $-\tilde{E}_\ell^{(\pm 2)}$ ,  $-\tilde{B}_\ell^{(\pm 2)}$ . The full derivation of these equations has been done by Hu and White in [6]; the final result reads

$$\begin{aligned} \dot{\tilde{E}}_\ell^{(\pm 2)} = \frac{k}{a} \left[ \frac{\ell^2 - 2}{\ell^2(2\ell - 1)} \tilde{E}_{\ell-1}^{(\pm 2)} - \frac{\pm 4}{\ell(\ell + 1)} \tilde{B}_\ell^{(\pm 2)} - \frac{\ell^2 - 2}{\ell^2(2\ell + 3)} \tilde{E}_{\ell+1}^{(\pm 2)} \right] + \\ - n_e \sigma_T \left[ \tilde{E}_\ell^{(\pm 2)} + \sqrt{6} \Pi^{(\pm 2)} \delta_{\ell,2} \right], \end{aligned} \quad (2.34a)$$

$$\begin{aligned} \dot{\tilde{B}}_\ell^{(\pm 2)} = \frac{k}{a} \left[ \frac{\ell^2 - 2}{\ell^2(2\ell - 1)} \tilde{B}_{\ell-1}^{(\pm 2)} - \frac{\pm 4}{\ell(\ell + 1)} \tilde{E}_\ell^{(\pm 2)} + \frac{\ell^2 - 2}{\ell^2(2\ell + 3)} \tilde{B}_{\ell+1}^{(\pm 2)} \right] + \\ - n_e \sigma_T \tilde{B}_\ell^{(\pm 2)}, \end{aligned} \quad (2.34b)$$

$$\text{with } \Pi^{(\pm 2)} = \frac{1}{10} \left[ \tilde{\Theta}_2^{(\pm 2)} - \sqrt{6} \tilde{E}_2^{(\pm 2)} \right].$$

In a similar way, also the equations for the anisotropies must be corrected, giving

$$\dot{\tilde{\Theta}}_2^{(\pm 2)} = n_e \sigma_T \left[ \Pi^{(\pm 2)} - \tilde{\Theta}_2^{(\pm 2)} \right] - \dot{\tilde{h}}^{(\pm)}, \quad (2.35a)$$

$$\dot{\tilde{\Theta}}_\ell^{(\pm 2)} = \frac{k}{a} \left[ \frac{\sqrt{\ell^2 - 4}}{2\ell - 1} \tilde{\Theta}_{\ell-1}^{(\pm 2)} - \frac{\sqrt{\ell^2 - 4}}{2\ell + 3} \tilde{\Theta}_{\ell+1}^{(\pm 2)} \right] - n_e \sigma_T \tilde{\Theta}_\ell^{(\pm 2)} \quad \ell \geq 3. \quad (2.35b)$$

Let's stop for a second to appreciate that the equations (2.35), (2.34a) and (2.34b) do not mix the  $\pm 2$  modes. Furthermore, for both values of  $m$  the equations read the same, this means that from now on we can study only the  $m = 2$  modes and then use the results to obtain the  $m = -2$  ones.

## 2.4 Approximate solutions for the dynamics of the anisotropies

All the differential equations we derived are pretty hard to solve analytically, since they are strongly coupled and in theory they are an infinite number (as much as the number

of multipoles). Usually we resort to numerical methods to obtain exact results, however some approximations can be useful to understand the general behavior of the CMB or even to simplify some numerical calculations.

### 2.4.1 The tight coupling approximation

At early times, when the plasma was denser and hotter, the mean free path of photons was very small and the rate of Compton scattering was very high. We will show that in this regime only the first two multipoles are relevant to describe fully the plasma. In this limit the anisotropies behave similarly to a fluid that can be fully described by just two parameters: its density and velocity field.

The guiding idea behind the tight coupling approximations is that the scatterings between baryons and photons, in this limit, is the only relevant interaction that determines the dynamics of the anisotropies. This is equivalent to consider the limit in which  $n_e \sigma_T \gg 1$ , which means that the mean free path ( $\propto \frac{1}{n_e \sigma_T}$ ) is very small. Starting from scalar perturbations, in equation (2.23c) we can drop the time derivative, since it is negligible with respect to the terms multiplied by  $n_e \sigma_T$ . In this way we are left with

$$\frac{\ell k}{(2\ell+1)a} \tilde{\Theta}_{\ell-1} - n_e \sigma_T \left[ \tilde{\Theta}_\ell - \frac{\delta_{\ell,2}}{10} \Pi \right] = -\frac{(\ell+1)k}{(2\ell+1)a} \tilde{\Theta}_{\ell+1},$$

from which we can note that the term  $\tilde{\Theta}_{\ell+1}$  is small compared to  $\tilde{\Theta}_{\ell-1}$ . This essentially prove that only the first few moments are relevant while higher multipoles are always smaller and smaller as  $\ell$  increases. In this limit, we can neglect all the multipoles with  $\ell \geq 2$ , we are thus left only with two only differential equations to be solved: equation (2.23a) and equation (2.23b) removing all  $\Theta_\ell$  with  $\ell \geq 2$  (still coupled to the rest of the plasma). Similar considerations are valid for the polarization equations (2.24a) and (2.24b), which can be simplified in the same way.

Also for tensor perturbations the tight coupling limit significantly simplifies the equations of motion. Reasoning as we have just done, from equations (2.35) and (2.34) we conclude that only the multipoles with  $\ell = 2$  are relevant. In this way, after having dropped the time derivatives, we are left with

$$n_e \sigma_T \left[ \frac{1}{10} \Pi^{(\pm 2)} - \tilde{\Theta}_2^{(\pm 2)} \right] \approx \dot{\tilde{h}}^{(\pm 2)}, \quad \tilde{E}_2^{(\pm 2)} \approx -\sqrt{6} \Pi^{(\pm 2)}, \quad \tilde{B}_2^{(\pm 2)} \approx 0,$$

that using the definition of  $\Pi^{(\pm 2)} = \frac{1}{10} [\tilde{\Theta}_2^{(\pm 2)} - \sqrt{6} \tilde{E}_2^{(\pm 2)}]$  gives

$$\tilde{\Theta}_2^{(\pm 2)} \approx -\frac{4\dot{\tilde{h}}^{(\pm 2)}}{3n_e \sigma_T}, \quad \tilde{E}_2^{(\pm 2)} \approx -\frac{\sqrt{6}}{4} \tilde{\Theta}_2^{(\pm 2)}, \quad \tilde{B}_2^{(\pm 2)} \approx 0. \quad (2.36)$$

This approximation will be particularly useful in the next chapter to study the spectral distortions associated to the dissipation of gravitational waves.

### 2.4.2 Improved tight coupling approximation

To conclude we want to present a simple way to improve the tight coupling approximation relaxing the approximation of stationary solutions, without spoiling the reduced number of

multipoles excited. For the purpose of this work, we are going to focus primarily on tensor perturbations as illustrated in [3]. Consider equations (2.35), (2.34a) and (2.34b) with conformal time: working in tight coupling approximation we can neglect every multipole except for the quadrupoles. In this way we get

$$\begin{aligned}\partial_\tau \tilde{\Theta}_2^{(\pm 2)} &= n_e \sigma_{Ta} \left[ \frac{9}{10} \tilde{\Theta}_2^{(\pm 2)} + \frac{\sqrt{6}}{10} \tilde{E}_2^{(\pm 2)} \right] - \partial_\tau \tilde{h}^{(\pm)}, \\ \partial_\tau \tilde{E}_2^{(\pm 2)} &= n_e \sigma_{Ta} \left[ \frac{2}{5} \tilde{E}_2^{(\pm 2)} + \frac{\sqrt{6}}{10} \tilde{\Theta}_2^{(\pm 2)} \right] - k \frac{2}{3} \tilde{B}_2^{\pm 2}, \\ \partial_\tau \tilde{B}_2^{(\pm 2)} &= n_e \sigma_{Ta} \tilde{B}_2^{(\pm 2)} + k \frac{2}{3} \tilde{E}_2^{\pm 2}.\end{aligned}$$

To solve these equations we should proceed with an ansatz: assume that the solution has the form  $\tilde{\Theta}_2^{(2)} = A_\Theta e^{ik\tau}$ ,  $\tilde{E}_2^{(2)} = A_E e^{ik\tau}$  and  $\tilde{B}_2^{(2)} = A_B e^{ik\tau}$  and that the gravitational perturbation is  $\tilde{h}^{(\pm)} = A_h e^{ik\tau}$ , where we dropped the  $\pm$  since the equations are the same for both cases.

In this way the above system of differential equations reduces to a system of linear equations for the coefficients

$$\begin{aligned}ik A_\Theta &= n_e \sigma_{Ta} \left[ \frac{9}{10} A_\Theta + \frac{\sqrt{6}}{10} A_E \right] - ik A_h, \\ ik A_E &= n_e \sigma_{Ta} \left[ \frac{2}{5} A_E + \frac{\sqrt{6}}{10} A_\Theta \right] - k \frac{2}{3} A_B, \\ ik A_B &= n_e \sigma_{Ta} A_B + k \frac{2}{3} A_E.\end{aligned}$$

Once solved this system we find, defining  $\xi \stackrel{\text{def}}{=} \frac{k}{n_e \sigma_{Ta}}$ ,

$$\begin{aligned}\frac{|A_\Theta|}{\frac{4}{3} \frac{|A_h|}{n_e \sigma_{Ta}}} &= \sqrt{\frac{1 + \frac{341}{36} \xi^2 + \frac{625}{324} \xi^4}{1 + \frac{142}{9} \xi^2 + \frac{1649}{82} \xi^4 + \frac{2500}{729} \xi^6}}, \\ \tan \phi_\Theta &= -\frac{11}{6} \xi \frac{1 + \frac{697}{99} \xi^2 + \frac{1250}{891} \xi^4}{1 + \frac{197}{18} \xi^2 + \frac{125}{54} \xi^4},\end{aligned}\tag{2.37a}$$

$$\begin{aligned}\frac{|A_E|}{\frac{4}{3} \frac{|A_h|}{n_e \sigma_{Ta}}} &= \frac{\sqrt{6}}{4} \sqrt{\frac{1 + \xi^2}{1 + \frac{142}{9} \xi^2 + \frac{1649}{82} \xi^4 + \frac{2500}{729} \xi^6}}, \\ \tan(\phi_E - \pi) &= -\frac{13}{3} \xi \frac{1 + \frac{121}{117} \xi^2}{1 - \xi^2 - \frac{50}{27} \xi^4},\end{aligned}\tag{2.37b}$$

$$\begin{aligned}\frac{|A_B|}{\frac{4}{3} \frac{|A_h|}{n_e \sigma_{Ta}}} &= \frac{\xi}{\sqrt{6}} \sqrt{\frac{1}{1 + \frac{142}{9} \xi^2 + \frac{1649}{82} \xi^4 + \frac{2500}{729} \xi^6}}, \\ \tan(\phi_B - \pi) &= -\frac{16}{3} \xi \frac{1 + \frac{121}{117} \xi^2}{1 - \frac{19}{3} \xi^2}.\end{aligned}\tag{2.37c}$$

Note that in the tight coupling limit  $\xi \ll 1$  and indeed the equations above reduce to the previous discussed approximations with  $\phi_E = \phi_B = \phi_\Theta = 0$ .

This approximation also shows that as we exit the tight coupling regimes and photons start to free stream ( $\xi \gg 1$ ) the anisotropies start to decay as  $\xi^{-1}$ , while the polarization decays even faster as  $\xi^{-2}$ .

# Chapter 3

## Spectral Distortions

As the *CMB* is composed by photons, it is reasonable to think that it should be described as some black body radiation. Indeed, the measurements from COBE/FIRAS satellite [5] showed that the CMB spectrum is very compatible with this assumption.

However, many physical processes could affect the spectrum of the CMB generating some **spectral distortions** that were not detectable by the previous experiments.

In the next sections we will discuss the theory of spectral distortions and the physical processes that could generate them. Our goal is to describe a particular process called **Silk dumping** that allows for dissipation of the primordial perturbation to generate the distortions

### 3.1 The thermalization problem

The CMB, nowadays, is the relic of the photon component of the primordial plasma that, at early times, filled the universe. For this reason, the spectrum that we observe today is influenced by the interactions occurring between the components of the plasma. Furthermore, several processes can inject energy that then, through different interactions, will be redistributed in the plasma, recovering equilibrium. The problem of determining how equilibrium is reached is usually referred as the **thermalization problem**.

To predict the final spectrum of the CMB, we need to understand how these interactions influenced the evolution of the phase space of the photons: as we already know, this is accomplished by the **Boltzmann equation**.

In the early universe, photons are mainly subject to scattering processes with electrons and light nuclei (Hydrogen and Helium). To describe these process it is useful to introduce the *dimensionless frequency*

$$x \stackrel{\text{def}}{=} \frac{\nu}{k_B T_z}, \quad T_z \stackrel{\text{def}}{=} T_0(1+z), \quad (3.1)$$

where  $T_0$  is the present temperature of photons and  $T_z$  is the temperature that would have a gas of decoupled photons at redshift  $z$ . In this way  $x$  is a *time invariant variable*, since the redshift  $\nu = \nu_0(1+z)$  cancels the time dependence of the temperature  $T_z$ , leaving only the today observed frequency and temperature. The use of this variable strongly simplifies the Boltzmann equation. Indeed, neglecting perturbations, the phase space distribution

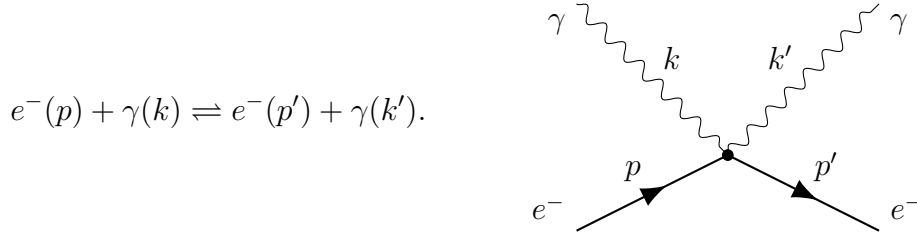
function is just a function of time and energy only. We can then use  $x$  as a measure of the energy of photons, since it is related to their frequency, so that the time independence of  $x$  allows to remove the momentum derivatives from the Liouville operator

$$\hat{L}[f] = \frac{df(t, x)}{dt} = \frac{\partial f}{\partial t} + \frac{dx}{dt} \frac{\partial f}{\partial x} = \frac{\partial f}{\partial t} = C[f].$$

Note that in this way, the phase space distribution is stationary if and only if the collision term vanishes. Physically this means that only scatterings can change the number of photons or their energies.

There are three main types of these interactions.

1. **Compton scattering:** this is the main actor in the thermalization of the CMB. In this process photons are scattered by electrons



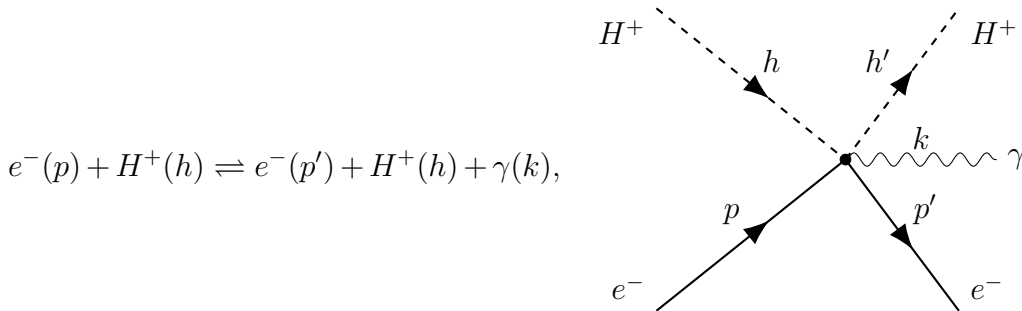
Each collision results in a transfer of energy between the photon component of the plasma and the electron component without changing the number of both. The collision term associated with this process is the **Kompaneets equation**, which reads

$$C[f] \Big|_{CS} = n_e \sigma_T \frac{k_B T_e}{m_e} x^{-2} \frac{\partial}{\partial x} \left[ x^4 \left( \frac{\partial f}{\partial x} + \frac{T_z}{T_e} f(1+f) \right) \right], \quad (3.2)$$

where  $n_e$  is the number of electrons per unit volume,  $\sigma_T$  the Thompson cross section and  $T_e$  is the temperature of the electrons.

The first term of the equation (3.2) account for the *Doppler effect* due to relative motions of the species in the plasma, while the second term describes the *recoil effect* and *stimulated recoil*.

2. **Bremsstrahlung:** this phenomenon arises when, during Coulomb scattering between electrons and ions ( $H^+$  of charge  $Ze$ ), an extra photon is produced



Note that this process, while transferring energy between different components of



the plasma, generates new photons. The corresponding collision term reads

$$C[f] \Big|_{CS} = n_e \sigma_T \frac{K_{BR} e^{-x_e}}{x_e^3} (1 - f(e^{x_e} - 1)), \quad (3.3)$$

$$K_{BR} \stackrel{\text{def}}{=} \frac{\alpha}{2\pi} \frac{\lambda_e^3}{\sqrt{6\pi} \theta_e^{7/2}} \sum_i Z_i^2 n_i \bar{g}_{ff}.$$

In the above we used the *dimensionless electron frequency*  $x_e = \nu/(k_B T_e)$ , the *dimensionless electron temperature*  $\theta_e \stackrel{\text{def}}{=} k_B T_e/m_e$  and the *fine structure constant*  $\alpha = e^2/(4\pi) \approx 137$ . We are also accounting for the possibility of having different gasses of ions, each with a number of ions per unit volume corresponding to  $n_i$ . Lastly, we used the electron Compton wavelength  $\lambda_e = 1/m_e \approx 2.43 \times 10^{-10}$  cm and the *thermally averaged Gaunt factor*

$$\bar{g}_{ff} \approx \begin{cases} \frac{\sqrt{3}}{\pi} \log \frac{2.25}{x_e}, & \text{for } x_e \leq 0.37, \\ 1 & \text{otherwise.} \end{cases}$$

3. **Double Compton scattering:** this process consists of a regular Compton scattering followed by the emission of a second photon by the scattered electron

$$e^-(p) + \gamma(k) \rightleftharpoons e^-(p') + \gamma(k_1) + \gamma(k_2).$$

Assuming that  $\gamma(k_2)$  is a soft photon, namely  $k_2 \ll m_e$ , (check ref 30 tagliazucchi) the collision term for this interaction reads

$$C[f] \Big|_{DCS} = n_e \sigma_T \frac{K_{DCS}}{x^3} [1 - f(e^{x_e} - 1)], \quad (3.4)$$

$$K_{DCS} \stackrel{\text{def}}{=} g_{DCS} \frac{4\alpha}{3\pi} \theta_\gamma^2 \int dx x^4 f(x) (1 + f(x)),$$

$$g_{DCS} \approx \frac{1 + 3/2x + 29/24x^2 + 11/16x^3 + 5/12x^4}{1 + 19.739\theta_\gamma - 5.5797\theta_e},$$

where we used the variables introduced for the previous interactions and the *dimensionless photon temperature*  $\theta_\gamma = T_z/???$ .

All these collision terms must then be combined to obtain the full *Boltzmann equation* for the photons.

We already argued that the stationary phase space solution is reached when  $C[f] = 0$ . Since the main driving interaction is the Compton scattering, the most relevant collision term to study is equation (3.2). This identically vanishes when

$$0 = \frac{\partial f}{\partial x} + \frac{T_z}{T_e} f(1 + f),$$

which upon integration gives the equilibrium distribution

$$f(\nu) = \frac{1}{\exp[\nu/(k_B T_e) + C] - 1},$$

that we clearly recognize as the Bose-Einstein distribution of a gas in thermal equilibrium with the electrons in the plasma and with a chemical potential determined by the integration constant  $C$ .

Note that the non-vanishing chemical potential at equilibrium is compatible with Compton scattering since such interaction conserves the number of photons. However, Bremsstrahlung and double Compton scattering involve the creation of new photons, thus a zero chemical potential is required to achieve equilibrium when considering all the interactions. In the end, we conclude that the above interactions will drive to phase space distribution to the well known **Planck distribution**

$$f(\nu) = \frac{1}{\exp[\nu/(k_B T_e)] - 1}.$$

### 3.1.1 Thermalization scales

In the previous section we described how Comptonization, or Compton interactions, leads the plasma of photons to the equilibrium distribution. We will now try to understand the timescale needed to reach equilibrium by this process.

In general, the Thomson timescale  $t_T = (n_e \sigma_T)^{-1}$  describes the time between consecutive scatterings, this timescale can be compared to the timescale associated with the expansion of the universe  $t_H = H^{-1}$  to understand when the time between scatterings becomes large enough for the number of these to be neglected.

To thermalize the plasma, scatterings by themselves are not enough, indeed we also need to transfer, by these interactions, energy. The Kompaneets equation (3.2) gives us the timescale for this transfer (ref cluba future steps)

$$t_{e\gamma} = \frac{m_e}{n_e \sigma_T k_B T_e} \approx \frac{4.9 \times 10^5}{n_e \sigma_T} \left( \frac{1100}{1+z} \right) \approx 1.2 \times 10^{29} (1+z)^{-4} s,$$

where we considered that before recombination  $T_e \approx T_\gamma \propto a^{-1}$  and the temperature of the plasma at recombination ( $z \approx 110$ ) is ???.

A comparison with the timescale of the expansion of the universe

$$t_H = H^{-1} \approx \begin{cases} 4.8 \times 10^{19} (1+z)^{-2} s & \text{radiation domination or } z > 3400, \\ 8.4 \times 10^{17} (1+z)^{-3/2} s & \text{matter domination,} \end{cases}$$

shows that the thermalization by Compton scattering becomes inefficient for  $z_{\mu y} \approx 5 \times 10^4$ . We should appreciate that this process becomes subdominant much before recombination.

As we discussed, also Bremsstrahlung and double Compton scatterings affect the thermalization of the photon plasma, mainly by changing the number of photons. The timescales associated with these processes can be read from the collision terms of these processes (3.3) and (3.4) and can be approximated as in (ref chluba future)

$$t_{\text{BR}} = \frac{t_T x_e^3}{K_{\text{BR}} (1 - e^{-x_e})} \approx 1.4 \times 10^{-6} \left( \frac{\bar{g}_{ff}}{3} \right) \left( \frac{\Omega_b h^2}{0.022} \right) \frac{x_e^3}{1 - e^{-x_e}} (1+z)^{-5/2} s,$$

$$t_{\text{DCS}} = \frac{t_T x^3 e^{2x}}{K_{\text{DCS}} (e^{x_e} - 1)} \approx 5.9 \times 10^{20} \frac{t_T x^3 e^{2x}}{e^{x_e} - 1} ???$$

Note that the timescales of these processes is also determined by the frequency  $x$  or  $x_e$  of the photons: in general these are efficient at high redshifts or for low frequency photons. Indeed, a comparison with Hubble timescale shows that at  $z_{\text{th}} \approx 2 \times 10^6$  both Bremsstrahlung and double Compton scattering become subdominant for high energy photons.

To proceed we should have in mind the following picture

1. For  $z > z_{\text{th}} \approx 2 \times 10^6$  all the discussed interactions are efficient and thus, as we argued in the previous section, the plasma can fully thermalize to a blackbody radiation.
2. For  $z_{\text{th}} \approx 2 \times 10^6 > z > z_{\mu y} \approx 5 \times 10^4$  Bremsstrahlung and double Compton scattering become subdominant, with respect to effect of the expansion of the universe on the photon plasma. Compton scattering is still efficient and thus photons and electrons can exchange energy, but the number of the former is almost fixed. This results in the possibility of generating *spectral distortions* since, as we showed previously, Compton scattering thermalizes with a non-zero chemical potential.
3. For  $z > z_{\mu y} \approx 5 \times 10^4$  also Compton scattering becomes inefficient and therefore obtaining a perfect blackbody spectrum through thermalization becomes even harder.

In the next sections we will focus on what kind of spectral distortions can be generated in these three phases and how they are generated.

## 3.2 Modeling spectral distortions

When dealing with spectral distortions, generated as we just described, we always decompose the full spectrum as

$$f(t, x) = B(x) + \Delta f(t, x),$$

where  $x = \nu/(k_B T_z)$  as before,  $B(x) \stackrel{\text{def}}{=} (e^x - 1)^{-1}$  is the *Planckian blackbody spectrum* and  $\Delta f(x, t)$  is the distortion. Every spectral distortion can then be further decomposed into a shape and an amplitude: the former one is determined by the physical process that generates the distortion while the latter measures how much the spectrum is distorted.

This decomposition is a direct consequence of the observations we derived studying the thermalization problem. Indeed, we showed that when all interactions are efficient a blackbody radiation is produced, then, as they become inefficient, deviations from blackbody spectrum can arise. It is thus natural to consider distortions as deviations from the blackbody spectrum.

### 3.2.1 Shapes of spectral distortions

To determine the precise shape of the spectral distortions  $\Delta f$  we must consider some energy injection in the plasma (in section ??? we will discuss the nature of these injections) that perturbed equilibrium. We know that at different redshifts photons can thermalize in different ways since different interactions are efficient.

### Temperature shift G

At  $z > z_{\text{th}} \approx 2 \times 10^6$  Compton scattering, Bremsstrahlung and double Compton scattering are all efficient and, as we now know, these allow for photons to fully thermalize again to a blackbody spectrum. However, since some energy was injected, the final spectrum will be at a different temperature from the starting one. Suppose that initially the plasma is at some temperature  $T_z$ , then, after the injection, the new temperature  $T_z + \Delta T$  is reached. This means that the final spectrum is

$$B\left(\frac{\nu}{T_z + \Delta T}\right) = B\left(\frac{x}{1 + \Delta T/T_z}\right) \approx B(x) - x \frac{\partial B(x)}{\partial x} \frac{\Delta T}{T_z} \stackrel{\text{def}}{=} B(x) + G(x) \frac{\Delta T}{T_z},$$

where we Taylor expanded assuming that the change of temperature was small compared to the temperature of the plasma. In this way we obtained the explicit expression for the spectral distortions generated at these redshifts.  $G(x)$  is the shape of the spectral distortion and it is usually called **temperature shift**

$$G(x) \stackrel{\text{def}}{=} -x \frac{\partial B(x)}{\partial x} = \frac{x e^x}{(e^x - 1)^2}. \quad (3.5)$$

The temperature shift is then multiplied by an amplitude to obtain the spectral distortion: in this case the amplitude is determined by the change of temperature  $\Delta T/T_z$ . Consequently, since  $T_z$  is defined with respect to a reference temperature observed today  $T_0$ , it is always possible to readjust  $T_0$  such that it coincides with the perturbed temperature today, in this way the temperature shift becomes essentially unobservable.

### Chemical potential $\mu$ distortion

For  $z_{\text{th}} > z > z_{\mu y}$  Bremsstrahlung and double Compton scattering are inefficient, thus the number of photons is almost fixed and only their energy can change through Compton scatterings. We already showed that from Kompaneets equation then follows that at equilibrium a Bose-Einstein distribution with a non-zero chemical potential<sup>1</sup> is generated (section 3.1). Expanding the resulting distribution for small chemical potential  $\mu/x \ll 1$  we find

$$f(x) = B(x + \mu) = (e^{x+\mu} - 1)^{-1} \approx B(x) + \frac{\partial B(x)}{\partial x} \mu = B(x) - \mu \frac{G(x)}{x},$$

which suggests that the shape of the so-called  $\mu$ -distortion should be  $G/x$  while its amplitude should be  $\mu$ . However, a simple calculation can show that such distortion would also change the number of photons

$$\int_0^\infty dx \frac{G(x)}{x} x^2 = \int_0^\infty dx \frac{x^2 e^x}{(e^x - 1)^2} = 2\zeta(2) \neq 0^2,$$

while we know that when only the Compton scattering is dominant this must remain unchanged.

<sup>1</sup>Note that in the following the chemical potential uses the convection  $f(x, \mu) = (e^{x+\mu} - 1)^{-1}$  which is different from the usual definition by a factor  $-1/(k_B T)$ .

<sup>2</sup>Recall that in general  $n = \int f(p, t) d^3 p$ .

We can remove this undesired behavior considering also a temperature shift: this extra distortion allows us to adjust the final number density of photons to be fixed.

$$\begin{aligned}
 M(x) &\stackrel{\text{def}}{=} -G(x) \left( \frac{1}{x} - \alpha_\mu \right) \\
 0 &= \int_0^\infty dx \, x^2 M(x) = \int_0^\infty dx \, (-x^2 + \alpha_\mu x^3) \frac{e^x}{(e^x - 1)^2} = \int_0^\infty dx \, (x^2 - \alpha_\mu x^3) \frac{d}{dx} \frac{1}{e^x - 1} \\
 &= \int_0^\infty dx \, (-2x + \alpha_\mu 3x^2) \frac{1}{e^x - 1} = \sum_{k=0}^\infty \int_0^\infty dx \, (-2x + \alpha_\mu 3x^2) e^{-x(k+1)} \\
 &= \sum_{k=0}^\infty \left( -\frac{2}{(k+1)^2} + \alpha_\mu \frac{6}{(k+1)^3} \right) = -2\zeta(2) + 6\alpha_\mu \zeta(3) \\
 &\implies \alpha_\mu = \frac{\zeta(2)}{3\zeta(3)} \approx 0.4561.
 \end{aligned} \tag{3.6}$$

With this correction we finally have a  **$\mu$ -disortion** given by

$$\Delta f(x) = \mu M(x) \stackrel{\text{def}}{=} -\mu G(x) \left( \frac{1}{x} - 0.4561 \right).$$

### Compton y distortion

Lastly, for  $z < z_{\mu y}$  also Compton scattering becomes inefficient in transferring energy, this means that equilibrium is not fully reached by Comptonization. In this case we can obtain a shape for the spectral distortions by exploiting the Kompaneets equation (3.2)

$$\frac{\partial f}{\partial t} = n_e \sigma_T \frac{k_B T_e}{m_e} x^{-2} \frac{\partial}{\partial x} \left[ x^4 \left( \frac{\partial f}{\partial x} + \frac{T_z}{T_e} f(1 + f) \right) \right].$$

Recall that here we exploited the time independence of  $x$  to rewrite  $\hat{L}[f] = \frac{\partial f}{\partial t}$ .

Considering an initial blackbody distribution  $B(x)$ , this equation gives us an estimate for the change of phase space distribution over a small lapse of time  $\Delta t$

$$\Delta f \approx n_e \sigma_T \frac{k_B T_e}{m_e} x^{-2} \frac{\partial}{\partial x} \left[ x^4 \left( \frac{\partial B(x)}{\partial x} + \frac{T_z}{T_e} B(x)(1 + B(x)) \right) \right] \Delta t.$$

Here, exploiting that  $-\frac{\partial B}{\partial x} = B(x)(1 + B(x)) = \frac{G(x)}{x} = \frac{e^x}{(e^x - 1)^2}$ , we can rewrite the above

$$\Delta f = y Y(x) \stackrel{\text{def}}{=} -y \frac{1}{x^2} \frac{\partial}{\partial x} \left( x^3 G(x) \right) = y G(x) \left( x \frac{e^x + 1}{e^x - 1} - 4 \right), \tag{3.7}$$

where  $Y$  is the shape of the so-called **y-distortion** and  $y = n_e \sigma_T k_B \frac{T_e - T_z}{m_e} \Delta t$  is its amplitude.

Observe that this distortion already conserves the number density of photons, since

$$\int_0^\infty dx \, x^2 Y(x) = \int_0^\infty dx \, x^2 G(x) \left( x \frac{e^x + 1}{e^x - 1} - 4 \right) = 0,$$

and therefore no extra temperature shift is needed this time.

Note that an inefficient Compton scattering interaction is not the only way to generate a y-distortion. Indeed, by Taylor expanding at second order in  $\Delta T/T_z$  a temperature shift we can produce a distortion with the same shape as a y-distortion.

$$\begin{aligned}
 B\left(\frac{x}{1 + \Delta T/T_z}\right) &\approx B(x) + \frac{\partial}{\partial \frac{\Delta T}{T_z}} \left( e^{\frac{x}{1 + \Delta T/T_z}} - 1 \right)^{-1} \frac{\Delta T}{T_z} + \frac{1}{2} \frac{\partial^2}{\partial \frac{\Delta T}{T_z}^2} \left( e^{\frac{x}{1 + \Delta T/T_z}} - 1 \right)^{-1} \left( \frac{\Delta T}{T_z} \right)^2 \\
 &\approx B(x) + x \frac{e^x}{(e^x - 1)^2} \frac{\Delta T}{T_z} - \frac{1}{2} \frac{e^x x}{(e^x - 1)^2} \left[ x - \frac{2e^x}{e^x - 1} + 2 \right] \left( \frac{\Delta T}{T_z} \right)^2 \\
 &= B(x) + G(x) \frac{\Delta T}{T_z} - \frac{1}{2} \frac{x e^x}{(e^x - 1)^2} \left[ \frac{x(e^x - 1) - 2x e^x}{e^x - 1} - 2 \right] \left( \frac{\Delta T}{T_z} \right)^2 \\
 &= B(x) + G(x) \frac{\Delta T}{T_z} + \frac{1}{2} [Y(x) + 2G(x)] \left( \frac{\Delta T}{T_z} \right)^2. \tag{3.8}
 \end{aligned}$$

We can see that, overall, a temperature shift of amplitude  $\Delta T/T_z + (\Delta T/T_z)^2$  and a y-distortion of amplitude  $1/2 \times (\Delta T/T_z)^2$  are generated.

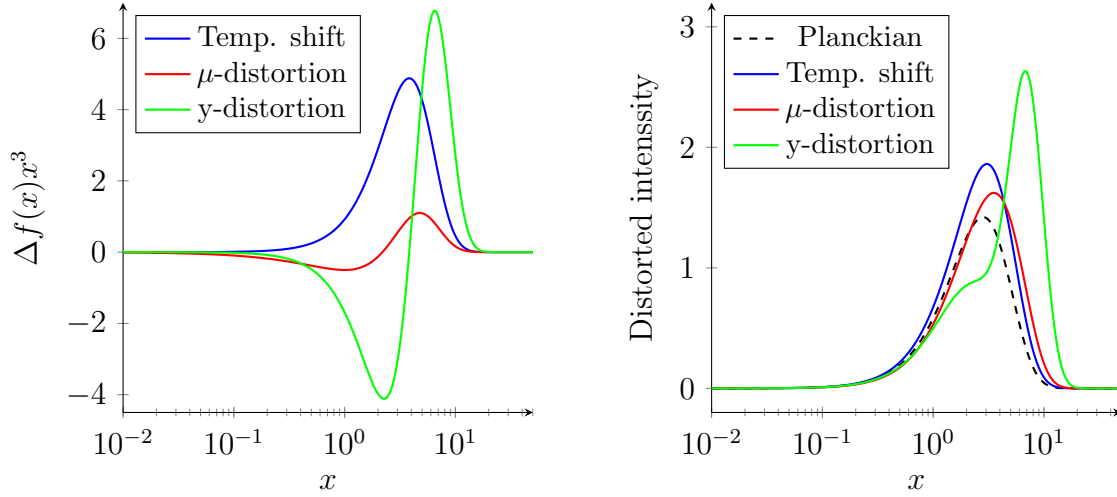


Figure 3.1: Shapes of the spectral distortions plotted by their intensity  $I \propto \int dx f(x)x^3$ .

The plot on the left shows the intensity shapes of the three spectral distortions with unitary amplitudes. The plot on the right shows the full Planckian intensity and the three distorted spectra (Planckian + distortion).

A more refined discussion should also consider non-thermal processes, such as atomic transitions, that could generate spectral distortions. Since these processes are less relevant for our purpose, but they still contribute to the full energy balance of spectral distortions, we will define the **residual distortion**  $R(x)$  that will account for those. In the end numerical methods will allow also to determine this distortion.

### 3.2.2 Amplitudes of spectral distortions

Now that we know which are the main types of spectral distortions that we expect to observe in the *CMB* and their shapes, we want to understand how their respective amplitudes can be obtained and what is their meaning.

In the previous section we derived the form of the different amplitudes as functions of temperatures or of the chemical potential. However, when studying the effects of energy injections in the plasma, it is useful to relate the amplitudes to the injected energy. This can easily be accomplished by considering that the injected energy will contribute to the corresponding spectral distortion. In this way, recalling that  $\rho = \int d^3p f(p, t) E = 4\pi(k_B T_z)^4 \int dx f(x) x^3$  since  $E = p = \nu$  and  $x = \nu/(k_B T_z)$ , we can write

$$\left. \frac{\Delta\rho_\gamma}{\rho_\gamma} \right|_g = g \frac{\int dx G(x) x^3}{\int dx B(x) x^3} = 4g \quad \Rightarrow \quad \boxed{g = \frac{1}{4} \left. \frac{\Delta\rho_\gamma}{\rho_\gamma} \right|_g} \quad \text{Temp. Shift,} \quad (3.9)$$

$$\left. \frac{\Delta\rho_\gamma}{\rho_\gamma} \right|_\mu = \mu \frac{\int dx M(x) x^3}{\int dx B(x) x^3} = \frac{\mu}{1.401} \quad \Rightarrow \quad \boxed{\mu = 1.401 \left. \frac{\Delta\rho_\gamma}{\rho_\gamma} \right|_\mu} \quad \mu\text{-distortion,} \quad (3.10)$$

$$\left. \frac{\Delta\rho_\gamma}{\rho_\gamma} \right|_y = y \frac{\int dx Y(x) x^3}{\int dx B(x) x^3} = 4y \quad \Rightarrow \quad \boxed{y = \frac{1}{4} \left. \frac{\Delta\rho_\gamma}{\rho_\gamma} \right|_y} \quad y\text{-distortion.} \quad (3.11)$$

Let's stop for a while to appreciate the physical meaning of each of these amplitudes. Indeed, in the above, we can even consider energy extraction from the plasma, therefore some physical considerations are needed. From our discussion on the shapes it is already clear that  $g$  is just a measure of the change of temperature of the blackbody radiation (equation (3.5)), in this way some energy extraction would correspond to a decrease of the temperature ( $g < 0$ ). In the same way  $\mu$ , from equation (3.6), is the chemical potential: physically its appearance means that the photon plasma hasn't the same number of particle that a blackbody radiation at the same temperature would have. In particular, since the chemical potential measures the energy necessary to change the number of particles:

- $\mu > 0$  distortions generated by an energy injection, since we now have *more energetic but fewer photons* compared to a blackbody radiation at the same temperature;
- $\mu < 0$  is the result of an energy extraction that just lowered the energy of each photon leaving *more photons* than the corresponding blackbody radiation.

Lastly, considering that a y-distortion is produced when thermalization is not completely reached, we can distinguish between  $y > 0$ , when some energy is still being (inefficiently) transferred from electrons to photons, and  $y < 0$ , when the opposite occurs. In the former case scatterings cause *Comptonization*, while in the latter they cause *Compton cooling*.

Usually only energy injections will occur in the early universe, as most of the processes tend to heat the plasma. Even though they can happen through some more exotic processes, energy extractions will be considered negligible and only positive amplitudes will be considered.

### 3.2.3 Injected, deposited energy and heating rate

In the previous sections we argued that spectral distortions are generated by injection of energy in the photon plasma when some scattering process has become inefficient. However, this description is still not accurate enough: indeed, after the injection, the energy can be subject to other processes (e.g. adiabatic cooling due to the expansion

of the universe or production of non-interacting particles) that can change the amount of energy that generates spectral distortions.

To refine our description of the injected energy we must differentiate between **injected energy** and **deposited energy**. The former is the energy that a certain process transfer to the plasma, while the latter is the energy that heat the plasma and contributes to the spectral distortions.

For each process that injects energy in the channel  $c$  (which describes the form of the heat), we define the **deposition function**  $f_c(z)$ . This function describes, at a given redshift, the fraction of injected energy that is deposited in the plasma. We can further decompose this function into an **injection efficiency function**  $f_{\text{eff}}(z)$  and a **deposition fraction**  $\chi_c(z)$ . The former describes how much energy is deposited regardless the form and depends on the injecting process and on the universe conditions, while the latter accounts for the fraction deposited in each channel, with  $\sum_c \chi_c = 1$ . Overall we have

$$\left. \frac{dE}{dt dV} \right|_{\text{dep},c} = \left. \frac{dE}{dt dV} \right|_{\text{inj}} f_c(z) = \left. \frac{dE}{dt dV} \right|_{\text{inj}} f_{\text{eff}}(z) \chi_c(z) \stackrel{\text{def}}{=} \dot{Q}(z) \chi_c(z). \quad (3.12)$$

To understand the meaning of this decomposition consider a process that injects energy in the form of different kinds of particles. If some species do not interact electromagnetically (for example neutrinos) they will not be able to exploit Comptonization to transfer energy to the photon plasma: the injection efficiency function will account for this.

Furthermore, the injection efficiency does not correspond to the energy transferred by electromagnetic interactions. Indeed, as it happens during the Dark ages, when the scattering rate is too low to thermalize the plasma immediately, some injected energy is lost due to the adiabatic cooling caused by the expansion of the universe. However, at pre-recombinatory redshifts, scatterings are frequent enough to thermalize the plasma almost immediately. In this case it is usually employed the so-called *on-the-spot* approximation, for which no energy is lost due to a non-istantaneous deposition. For our purposes, since we will always consider high redshifts (as explained in section 3.1.1), we will always use this approximation.

Lastly, we should account for the possibility of heating the photon component of the plasma by energy transfers among the different species or even by some energy redistribution among the photons themselves. This can happen, for example, during adiabatic cooling of different species: different cooling rates results in energy transfers between the species to reestablish equilibrium. In this case no energy is injected but in the end spectral distortions can still be generated. To describe this last effect we define the **non-injected heating rate**  $\dot{Q}_{\text{non-inj}}$ , so that the heating rate of the photon plasma reads

$$\dot{Q} = \left. \frac{dE}{dt dV} \right|_{\text{dep},c} + \dot{Q}_{\text{non-inj}} = \dot{Q}(z) \chi_c + \dot{Q}_{\text{non-inj}}. \quad (3.13)$$

Now that we have a full picture of how energy is injected in the plasma of photons, let's connect the heating rate to the spectral distortion amplitudes that we obtained in section 3.2.2. We can relate the heating rate to the energy density using the Liouville



operator

$$\begin{aligned}
 \rho = \int d^3p f(p, t) E &\Rightarrow \dot{Q} = \int d^3p \frac{df}{dt} E = \int_0^\infty 4\pi p^2 dp \left( \frac{\partial f}{\partial t} - H p \frac{\partial f}{\partial p} \right) p \\
 &= \frac{\partial \rho}{\partial t} - 4\pi H \int_0^\infty dp \frac{\partial f}{\partial p} p^4 = \frac{\partial \rho}{\partial t} + 16\pi H \int_0^\infty dp f(p, t) p^3 \\
 &= \frac{\partial \rho}{\partial t} + 4H\rho = \frac{1}{a^4} \frac{\partial(a^4 \rho)}{\partial t},
 \end{aligned}$$

in this way we obtained a differential equation for the energy density  $\rho$ , for which  $\dot{Q}$  is a source term

$$\frac{\partial(a^4 \rho)}{\partial t} = a^4 \dot{Q}.$$

The general solution of this equation  $\rho(t)$  is made of a homogeneous solution  $\rho_z(t)$  and a particular solution  $\Delta\rho(t)$ . The homogeneous solution, obtained in absence of heating, is just the energy density of decoupled photons in the expanding universe  $\rho_z \propto a^{-4}$ . On the other hand, the particular solution  $\Delta\rho(t)$  is the energy density deviation from the homogeneous one, that we related in section 3.2.2 to the spectral distortion amplitudes. Upon integration, we find that the particular solution reads

$$\Delta\rho(t) = \frac{1}{a^4} \int dt' a^4 \dot{Q}(t') = \rho_z \int dt' \frac{\dot{Q}(t')}{\rho_z}$$

. We can now find an explicit expression for the left and side of equations (3.9), (3.10) and (3.11) by considering  $\Delta\rho = \Delta\rho_\gamma$  and  $\rho_{\text{gamma}} = \rho_z$

$$\frac{\Delta\rho_\gamma}{\rho_\gamma} = \int dt \frac{\dot{Q}}{\rho_\gamma} = \int dz \frac{\dot{Q}}{(1+z)H\rho_\gamma} = \int dz \frac{dQ/dz}{\rho_\gamma}, \quad (3.14)$$

where we used that  $dz = -H(1+z)dt$ .

Note that an alternative notation for the heating rate is sometimes used in the literature. Indeed, equation (3.14) implies that  $\dot{Q}/\rho_\gamma$  is (by the fundamental theorem of calculus) the time derivative of  $\Delta\rho_\gamma/\rho_\gamma$ . In this way, some papers refers to the heating rate as  $\frac{d}{dt} \frac{\Delta\rho_\gamma}{\rho_\gamma}$ . Hence, the two conventions are equivalent.

### 3.2.4 Branching ratios and the Green's function approach

In the previous section we reduced the problem of determining the distortions in the CMB spectrum to the task of integrating the heating rate over time (equation (3.14)). In section 3.1.1 we showed that different types of distortions arise in different epochs of the universe since different interactions are efficient. Hence, when dealing with the heating rate we must take into account the thermal state of the universe. This can be accomplished by introducing the **branching ratios**  $\mathcal{J}_a(z)$ : each of these functions describes the fraction of the deposited energy that contributes to a specific distortion  $a$  at redshift  $z$ . In this way, using the equation (3.14) with (3.9), (3.10) and (3.11) that we just derived in the previous section, we get that a given amplitude  $a$  can be evaluated as

$$a = C_a \frac{\Delta\rho_\gamma}{\rho_\gamma} \Big|_a = C_a \int dz \frac{dQ/dz}{\rho_\gamma} \mathcal{J}_a(z), \quad \text{for } a = g, \mu, y, , \quad (3.15)$$

where  $C_a$  is the constant that relates the amplitude of each distortion to the fraction of deposited energy, and they are  $C_g = 1/4$ ,  $C_\mu = 1.401$  and  $C_y = 1/4$ .

In this way we have split the general problem in two independent subproblems: determining the heating rate  $dQ/dz$ , which depends on the specific model that inject energy in the plasma, and solving for the branching ratios, which instead is independent of the injecting mechanism and is determined only by the thermal history of the universe.

Different approaches can be taken to obtain the branching ratios, we will now describe the main approximations and how to obtain the exact solution. From the discussion of section 3.1.1 one could get a brute approximation for the branching ratios as step functions that allows for a certain distortion to be produced only during its specific era.

$$\mathcal{J}_g(z) = \Theta_H(z - z_{\text{th}}), \quad \mathcal{J}_\mu(z) = \Theta_H(z_{\text{th}} - z)\Theta_H(z - z_{\mu y}), \quad \mathcal{J}_y(z) = \Theta_H(z_{\mu y} - z), \quad (3.16)$$

with  $z_{\text{th}} \approx 2 \times 10^6$  and  $z_{\mu y} \approx 5 \times 10^4$ . In this way we are assuming that the transition from one era to another is instantaneous, which clearly is not the case.

To improve this approximation we can consider that the chemical potential of the  $\mu$ -distortions is frequency dependent (some ref). This happens because, as we discussed in section 3.1, the collision term for Bremsstrahlung and double Compton scattering has frequency dependence, thus for low energy photons these two processes can still be efficient outside the  $\mu$ -era. Studying the full Boltzmann equation (as in ref) we can find an approximate solution of the frequency dependence of the chemical potential

$$\mu(x, t) \approx \mu_0 e^{-x_c(t)/x} e^{-(z/z_{\text{th}})^{5/2}},$$

where  $x_c$  is the critical frequency and  $z_{\text{th}}$  is the redshift at which the Compton scattering becomes inefficient. This suggests that the  $\mu$  branching ratio can be approximated by  $f(z) \stackrel{\text{def}}{=} e^{-(z/z_{\text{th}})^{5/2}}$ , giving in the end

$$\mathcal{J}_g(z) = 1 - f(z), \quad \mathcal{J}_\mu(z) = f(z), \quad \mathcal{J}_y(z) = f(z)\Theta_H(z_{\mu y} - z), \quad (3.17)$$

which describes a smooth  $g$ - $\mu$  transition and an instantaneous  $\mu$ - $y$  transition.

A further improvement is obtained by (ref 63 of lucca) considering a smooth  $\mu$ - $y$  transition and results in the following branching ratios:

$$\mathcal{J}_g(z) = 1 - f(z), \quad (3.18)$$

$$\mathcal{J}_\mu(z) = f(z) \left\{ 1 - \exp \left[ - \left( \frac{1+z}{5.8 \times 10^4} \right)^{1.88} \right] \right\}, \quad (3.19)$$

$$\mathcal{J}_y(z) = \left[ 1 + \left( \frac{1+z}{6 \times 10^{2.58}} \right) \right]^{-1}. \quad (3.20)$$

Note that in this last approximation the sum of all the branching ratios is not equal to one, this is due to the presence of the residual distortions we mentioned at the end of section 3.2.1.

Finally, we can derive an exact solution for the branching ratios. This is done by exploiting *Green's functions* methods to solve equation (3.14). To begin we consider the intensity associated with the photon plasma

$$I(x, z) \stackrel{\text{def}}{=} 2p^3 f(p, t) = (k_B T_z)^3 x^3 \left[ B(x) + G(x) + M(x) + Y(x) \right],$$

in which we used  $x \stackrel{\text{def}}{=} p/(k_B T_z)$ . Note that the intensity is the integrand function that gives the energy density of the plasma (upon integration over  $p$ ), here the factor 2 accounts for the two polarization of the photons. Now, the last three terms of the above are the intensity contributions associated to the spectral distortions, we thus define  $\Delta I$  as their sum.

Now, we want to find the Green's function  $G_{\text{th}}(x, z, z')$  that gives  $\Delta I(x, z)$  for an arbitrary heating rate as

$$\Delta I(x, z) = \int dz' G_{\text{th}}(x, z, z') \frac{dQ(z')/dz'}{\rho_\gamma(z')}.$$

This has been done by J. Chluba [2] by studying the full Boltzmann equation for photons and baryons. Then, as explained by M. Lucca [9], a direct comparison with equation (3.15) relates the full Green's function to each branching ratios

$$G_{\text{th}}(x, z = 0, z') = \frac{1}{4}x^3 G(x) \mathcal{J}_g(z') + 1.401x^3 M(x) \mathcal{J}_\mu(z') + \frac{1}{4}x^3 Y(x) \mathcal{J}_y(z'),$$

in this way one can on the different shapes of the distortions the full Green's function and obtain the branching ratios. Note that at this point a residual contribution can be added to obtain a measure of the residual distortion we introduced at the end of section 3.2.1.

### 3.3 Silk dumping

Primordial perturbations, when reentering the Hubble horizon after inflation, excite standing waves in the plasma that, depending on the phase of the wave, lead to different patches of photons to be hotter or colder than the average. Later on, these photons can diffuse in the baryon-photon plasma and mix together. In this way diffusion dissipates the standing waves and generates distortions in the *CMB spectrum*. This effect is called *Silk damping*.

Initially, the **mixing of blackbodies** at different temperatures (by diffusion) produces *y-distortions* in the overall spectrum of the CMB. Then, **comptonization** brings the equilibrium phase space distribution to a Bose-Einstein one (section 3.1), turning the initial distortions in  *$\mu$ -distortions*.

In the following sections we will describe these two processes in detail.

#### 3.3.1 Mixing of blackbodies

We already discovered that at high redshifts all the interactions in the primordial plasma bring the photons to a state of thermal equilibrium described by the Planck distribution

$$B(\nu, T) = \frac{1}{\exp[\nu/(k_B T_e)] - 1} = \left(e^x - 1\right)^{-1}, \quad \text{with } x = \frac{\nu}{k_B T_e}.$$

From this distribution we can evaluate the number density and the energy density of the photons in the radiation

$$\begin{aligned} n &\stackrel{\text{def}}{=} \frac{g}{(2\pi)^3} \int d^3p f(p, T) &\implies n &= b_R T^3, \\ \rho &\stackrel{\text{def}}{=} \frac{g}{(2\pi)^3} \int d^3p f(p, T) p &\implies \rho &= a_R T^4, \end{aligned}$$

### Chapter 3. Spectral Distortions

where  $a_R \stackrel{\text{def}}{=} \pi^2 k_B^4/15$  and  $b_R \stackrel{\text{def}}{=} 2k_B^3\zeta(3)/\pi^2$  while the number of internal degrees of freedom  $g = 2$  for photons.

From the first principle of thermodynamics and choosing as the intensive thermodynamic variable  $T$  we can then obtain the entropy density ( $s = S/V$ ) by

$$\begin{aligned} TdS &= TVds + Ts dV = TV \frac{\partial s}{\partial T} \Big|_V dT + Ts dV \\ &= d(\rho V) + PdV = Vd\rho + \rho dV + PdV = V \frac{\partial \rho}{\partial T} \Big|_V dT + \rho dV + \frac{1}{3}\rho dV \\ \Rightarrow \quad &\left( TV \frac{\partial s}{\partial T} \Big|_V - V \frac{\partial \rho}{\partial T} \Big|_V \right) dT = \left( \frac{4}{3}\rho + Ts \right) dV \quad \Rightarrow \quad \boxed{s = \frac{4}{3} \frac{\rho}{T} = \frac{4}{3} a_R T^3}, \end{aligned}$$

where we used the equation of state for radiation  $P = \frac{1}{3}\rho$  and the fact that the change of temperature and volume must be independent.

In general, Zeldovich [10] showed that the mixing of blackbody spectra results in the appearance of a y-distortion. This can easily be understood by Taylor expanding a Planck distribution whose temperature depends on the position in the plasma (so that this describes a different blackbody spectrum at each point in space) and then taking the spatial average. Considering a temperature  $\bar{T} + \Delta T(x)$ , with  $\Delta T \ll \bar{T}$  the expansion of  $B[x/(1 + \Delta T/\bar{T})]$  is a temperature shift expanded at the second order (equation 3.8): therefore the average yields

$$\begin{aligned} \left\langle B\left(\frac{x}{1 + (\Delta T/\bar{T})^2}\right) \right\rangle &\approx \left\langle B(x) + G(x) \frac{\Delta T}{\bar{T}} + \frac{1}{2}[Y(x) + 2G(x)] \left(\frac{\Delta T}{\bar{T}}\right)^2 \right\rangle \\ &= B(x) + G(x) \left\langle \frac{\Delta T}{\bar{T}} \right\rangle + \frac{1}{2}[Y(x) + 2G(x)] \left\langle \left(\frac{\Delta T}{\bar{T}}\right)^2 \right\rangle \\ \downarrow \left\langle \frac{\Delta T}{\bar{T}} \right\rangle &= 0, \quad B(x) + G(x) \left\langle \left(\frac{\Delta T}{\bar{T}}\right)^2 \right\rangle \approx B\left(\frac{x}{1 + \langle (\Delta T/\bar{T})^2 \rangle}\right), \\ &\approx B\left(\frac{x}{1 + \langle (\Delta T/\bar{T})^2 \rangle}\right) + \frac{1}{2}Y(x) \left\langle \left(\frac{\Delta T}{\bar{T}}\right)^2 \right\rangle, \end{aligned} \quad (3.21)$$

where we used that the mean of the temperature perturbations is zero, and we recognized a first order temperature shift distortion in the term that contained  $G(x)$ .

The above calculation thus shows that the mixing of blackbodies, not only results in a y-distortion, but also in a small increase in temperature to  $T_{\text{new}} = \bar{T}(1 + \langle (\Delta T/\bar{T})^2 \rangle)$ . We shall also recall that a y-distortion maintains unchanged the number of photons in the radiation: indeed the mixing consists just in a redistribution of "hotter" and "colder" photons. Hence, even though the temperature increases and thus one should expect a change in the number of photons, this happens only with respect to the number density of each blackbody, while the total number of photons remains unchanged.

Another way to see this phenomenon is by considering directly the mixing of two blackbodies at temperature  $T_1 = \bar{T} + \Delta T$  and  $T_2 = \bar{T} - \Delta T$  (now  $\Delta T$  is not a function of space anymore). Before the two blackbodies have mixed some photons will obey the first blackbody distribution while the others the second one: hence the initial energy density,

number density and entropy density are just the average of the two blackbodies:

$$\rho_{\text{initial}} = \frac{1}{2}a_R(T_1^4 + T_2^4) \approx a_R\bar{T}^4 \left[ 1 + 6\left(\frac{\Delta T}{\bar{T}}\right)^2 \right] > a_R\bar{T}^4, \quad (3.22)$$

$$n_{\text{initial}} = \frac{1}{2}b_R(T_1^3 + T_2^3) \approx b_R\bar{T}^3 \left[ 1 + 3\left(\frac{\Delta T}{\bar{T}}\right)^2 \right] > b_R\bar{T}^3, \quad (3.23)$$

$$s_{\text{initial}} = \frac{1}{2}\frac{4}{3}a_R(T_1^3 + T_2^3) \approx \frac{4}{3}a_R\bar{T}^3 \left[ 1 + 3\left(\frac{\Delta T}{\bar{T}}\right)^2 \right] > \frac{4}{3}a_R\bar{T}^3, \quad (3.24)$$

where for each quantity we Taylor expanded for  $\Delta T/\bar{T} \ll 1$  at the first order.

Note that all the three averages are larger than the densities that would have a single blackbody at the average temperature  $\bar{T}$ . These extra contributions, as we will see, are responsible for the creation of the distortions.

After the mixing we will have a single blackbody spectrum (plus distortions) with a new temperature  $T_{\text{final}}$ ; since the number of photons is unchanged (we only mix them) we can obtain this new temperature from the initial number density

$$T_{\text{final}} = \left( \frac{n_{\text{initial}}}{b_R} \right)^{1/3} \approx \bar{T} \left[ 1 + \left( \frac{\Delta T}{\bar{T}} \right)^2 \right],$$

similarly to what we found with the previous approach. The extra photons thus cause only an increase in the temperature because the y-distortion conserves the number of photons ( $\int dx x^2 Y(x) = 0$ ), hence only the blackbody part of the spectrum and the temperature shift, from the (3.21), contribute to the number density.

Now, the final temperature allows us to evaluate the final energy density

$$\rho_{\text{final}} = a_R T_{\text{final}}^4 \approx a_R \bar{T}^4 \left[ 1 + 4\left(\frac{\Delta T}{\bar{T}}\right)^2 \right] < \rho_{\text{initial}},$$

which we find to be smaller than the initial one. This is because some energy is now stored in the form of the y-distortion (that we haven't considered yet since we are only using the observable of a blackbody). Indeed, by comparing  $\rho - a_R \bar{T}^4$ , which (from equation 3.21) is the energy density associated to all the distortions (temperature shift + y-distortion), we discover that only 2/3 of this energy is then transferred in the new blackbody radiation at  $T_{\text{final}}$  (in the form of the temperature shift)

$$\rho_{\text{final}} - a_R \bar{T}^4 = 4\left(\frac{\Delta T}{\bar{T}}\right)^2 a_R \bar{T}^4 = \frac{2}{3} \left( \rho_{\text{initial}} - a_R \bar{T}^4 \right).$$

The remaining 1/3 of the energy corresponds to the contribution of the y-distortion

$$\frac{1}{3} \left( \rho_{\text{initial}} - a_R \bar{T}^4 \right) = 2\left(\frac{\Delta T}{\bar{T}}\right)^2 a_R \bar{T}^4 \propto \frac{1}{2} \left( \frac{\Delta T}{\bar{T}} \right)^2 \int dx x^3 Y(x).$$

Lastly, we can compute the final entropy density

$$s_{\text{final}} = \frac{4}{3}a_R T_{\text{final}}^3 \approx \frac{4}{3}a_R \bar{T}^3 \left[ 1 + 3\left(\frac{\Delta T}{\bar{T}}\right)^2 \right] = s_{\text{initial}}.$$

However, this holds only for the entropy associated to the new shifted blackbody spectrum and also the y-distortion should contribute to entropy. We can compute this contribution from the fraction of energy stored in the y-distortion  $\Delta\rho = 1/3(\rho_{\text{initial}} - a_R\bar{T}^4)$

$$\Delta s = \frac{\Delta\rho}{T} \approx 2a_R\bar{T}^3 \left( \frac{\Delta T}{\bar{T}} \right)^2.$$

This extra contribution is expected since, when mixing the two blackbodies, the entropy should increase as when we mix two fluids (the disorder increases), hence the initial entropy cannot be the same as the final.

To sum up what we discovered, mixing of blackbodies leads to a new spectrum that can be decomposed in two parts: a blackbody at a higher temperature  $T_{\text{new}} = \bar{T}(1 + \langle(\Delta T/\bar{T})^2\rangle)$  and a y-distortion. While the number of photons is conserved (since we are only mixing them) and fully accounted by the blackbody part, the energy and entropy are redistributed between the temperature shift of the blackbody and the y-distortion. Exactly, 2/3 of the energy associated to the distortions is directly transferred to the new blackbody (as a temperature increase), while the remaining 1/3 is stored in the y-distortion. The entropy associated to the blackbody is instead conserved, while a new contribution appears due to the y-distortion.

### 3.3.2 Comptonization of mixed blackbodies

The previously described mixing generates a y-distortion without considering the interactions in the plasma, this means that the y-distortion is produced at redshifts  $z > z_{\mu y} \approx 5 \times 10^4$  (see section 3.1). In the presence of Compton scatterings the resulting transfer of energy thermalizes the radiation to a Bose-Einstein distribution (or a Planckian if also Bremsstrahlung and double Compton scattering are efficient). When the Bose-Einstein distribution is produced, the y-distortion is converted into a  $\mu$ -distortion.

To obtain the amplitude of the new distortion generated we can proceed to consider the mixing of the two, previously introduced, blackbodies at  $T_1$  and  $T_2$ . We assume that after comptonization the temperature of the radiation changes from  $T_{\text{new}} = \bar{T}[1 + (\Delta T/\bar{T})^2]$  to  $T_{\text{BE}} = T_{\text{new}}(1 + t_{\text{BE}}) \approx \bar{T}[1 + t_{\text{BE}} + (\Delta T/\bar{T})^2]$ , where  $t_{\text{BE}} \ll 1$  measures the change in temperature. Now, the energy and number densities are fully described by the Bose-Einstein distribution, in appendix B.1.1 approximated formulae for these are evaluated in the limit of small chemical potential. Since comptonization conserves the number of photons (in section 3.1 we discussed that no extra photons are created by Compton scattering) we can compare the initial number density to the final one. Then, since the blackbodies are at very close temperatures, we can assume that they are almost in thermal equilibrium with the other components of the plasma. Hence, the exchange of energy between different species of the plasma is negligible and we can consider the energy density of the photons unchanged. Using equation (B.1) and (B.2) we can equate

the initial and final number and energy densities:

$$\begin{aligned}
 n_{\text{final}} &\approx b_R T_{\text{BE}}^3 \left( 1 - \mu \frac{\zeta(2)}{\zeta(3)} \right) \approx b_R \bar{T}^3 \left( 1 + 3t_{\text{BE}} + 3 \left( \frac{\Delta T}{\bar{T}} \right)^2 - \mu \frac{\zeta(2)}{\zeta(3)} \right) \\
 &= n_{\text{initial}} = b_R \bar{T}^3 \left[ 1 + 3 \left( \frac{\Delta T}{\bar{T}} \right)^2 \right], \\
 \rho_{\text{final}} &\approx b_R T_{\text{BE}}^4 \left( 1 - \mu \frac{\zeta(3)}{\zeta(4)} \right) \approx b_R \bar{T}^3 \left( 1 + 4t_{\text{BE}} + 4 \left( \frac{\Delta T}{\bar{T}} \right)^2 - \mu \frac{\zeta(3)}{\zeta(4)} \right) \\
 &= \rho_{\text{initial}} = b_R \bar{T}^3 \left[ 1 + 6 \left( \frac{\Delta T}{\bar{T}} \right)^2 \right].
 \end{aligned}$$

From the first equation we immediately obtain that  $t_{\text{BE}} = \mu \frac{\zeta(2)}{3\zeta(3)}$ , inserting this relation in the second equation we obtain

$$\mu = 2 \left( \frac{4\zeta(2)}{3\zeta(3)} - \frac{\zeta(3)}{\zeta(4)} \right)^{-1} \left( \frac{\Delta T}{\bar{T}} \right)^2 \approx 2.802 \left( \frac{\Delta T}{\bar{T}} \right)^2, \quad (3.25)$$

$$t_{\text{BE}} = \frac{2\zeta(2)}{3\zeta(3)} \left( \frac{4\zeta(2)}{3\zeta(3)} - \frac{\zeta(3)}{\zeta(4)} \right)^{-1} \left( \frac{\Delta T}{\bar{T}} \right)^2 \approx 1.278 \left( \frac{\Delta T}{\bar{T}} \right)^2. \quad (3.26)$$

Note that the same chemical potential can be obtained by considering a that all the energy stored in the  $y$ -distortion gets transferred to the  $\mu$ -distortion, using equation 3.10:

$$\mu = 1.401 \frac{\Delta \rho}{\rho} = 1.401 \frac{\frac{1}{3}(\rho_{\text{initial}} - a_R \bar{T}^4)}{a_R \bar{T}^4} = 1.4 \times \frac{6}{3} \left( \frac{\Delta T}{\bar{T}} \right)^2 \approx 2.802 \left( \frac{\Delta T}{\bar{T}} \right)^2.$$

To conclude let us write the total spectral distortion that we obtain after comptonization:

$$f(x) = B(x) + G(x) \left[ \left( \frac{\Delta T}{\bar{T}} \right)^2 + t_{\text{BE}} \right] - \mu \frac{G(x)}{x},$$

where, after the Planckian spectrum  $B$ , we have the total temperature shift (both from the mixing and the comptonization) and the  $\mu$ -distortion. Note the latter appears as  $-G/x$  and not at as  $M$ : this is because we assumed that the temperature changes during comptonization and then we imposed that the number of photons was conserved. Hence, the temperature shift  $t_{\text{BE}}$  already accounts also for the shift contained in  $M$ .

To conclude we shall indicate that, although our derivation used only the mixing of two blackbodies, considering an ensemble of  $n$  blackbodies the result can be generalized without spoiling our solution. Indeed, it is sufficient to replace  $(\Delta T/\bar{T})^2$  by  $\langle (\Delta T/\bar{T})^2 \rangle$  to account for the whole ensemble, as explained in [8] and hinted at the end of the previous section.

### 3.3.3 Mixing of polarized blackbodies

When dealing with the *CMB*, the mixing of blackbodies must take into account also that the radiation is polarized. To connect to section 2.2.1 we shall change our notation to be consistent to the usual definition of *CMB anisotropies*  $\Theta(x, t) \stackrel{\text{def}}{=} \Delta T/\bar{T}$ .



### Chapter 3. Spectral Distortions

We start by describing linearly polarized light, then the more general case will be deduced exploiting the following calculations. We start by introducing a *phase space matrix*

$$\mathcal{F}_{\text{unpol}} \stackrel{\text{def}}{=} \begin{pmatrix} B(x) & 0 \\ 0 & B(x) \end{pmatrix} \xrightarrow{\text{polarization}} \mathcal{F} \stackrel{\text{def}}{=} \begin{pmatrix} B(x/[1 + \Theta_{\parallel}]) & 0 \\ 0 & B(x/[1 + \Theta_{\perp}]) \end{pmatrix}, \quad (3.27)$$

where  $\Theta_{\perp}$  and  $\Theta_{\parallel}$  are the temperature fluctuations associated to photons that are polarized either in the perpendicular direction or in the orthogonal one and  $B(x)$  is the Planckian spectrum. The total phase space distribution is then recovered by taking the trace of the above matrices  $f = \text{Tr}(\mathcal{F})/2$ , which corresponds to the average of the two polarization. It is useful to rewrite the above in terms of the *Pauli matrices*  $\sigma_i$

$$\mathcal{F} = \frac{f_{\parallel} + f_{\perp}}{2} \begin{pmatrix} 1 & 0 \\ 0 & 1 \end{pmatrix} + \frac{f_{\parallel} - f_{\perp}}{2} \begin{pmatrix} 1 & 0 \\ 0 & -1 \end{pmatrix} = f_I \hat{1} + f_Q \sigma_3,$$

where  $f_{\parallel} \stackrel{\text{def}}{=} B(x/[1 + \Theta_{\parallel}])$  and  $f_{\perp} \stackrel{\text{def}}{=} B(x/[1 + \Theta_{\perp}])$ , while  $f_I$  is the distribution associated to the Stokes parameter  $I$ , and it corresponds to  $f$ , while  $f_Q$  is associated to  $Q$ .

With this framework we can proceed to expand (as in equation 3.21) the perturbation at the second order to obtain the distortions:

$$\begin{aligned} f_I &= \frac{f_{\parallel} + f_{\perp}}{2} \approx B(x) + G(x) \frac{\Theta_{\parallel} + \Theta_{\perp} + \Theta_{\parallel}^2 + \Theta_{\perp}^2}{2} + Y(x) \frac{\Theta_{\parallel}^2 + \Theta_{\perp}^2}{4}, \\ f_Q &= \frac{f_{\parallel} - f_{\perp}}{2} \approx G(x) \frac{\Theta_{\parallel} - \Theta_{\perp} + \Theta_{\parallel}^2 - \Theta_{\perp}^2}{2} + Y(x) \frac{\Theta_{\parallel}^2 - \Theta_{\perp}^2}{4}. \end{aligned}$$

Now, identifying the right anisotropies associated to each Stokes parameter,  $\Theta_I = (\Theta_{\parallel} + \Theta_{\perp})/2$  and  $\Theta_Q = (\Theta_{\parallel} - \Theta_{\perp})/2$ , we find

$$\begin{aligned} f_I &\approx B(x) + G(x) \left( \Theta_I + \Theta_I^2 + \Theta_Q^2 \right) + Y(x) \frac{\Theta_I^2 + \Theta_Q^2}{2}, \\ f_Q &\approx G(x) \left( \Theta_Q + 2\Theta_I \Theta_Q \right) + Y(x) \Theta_I \Theta_Q. \end{aligned}$$

This shows that also the phase space associated to the  $Q$  parameter gets a temperature shift and a y-distortion.

To generalize this result to a generic distortion we can simply consider the phase space distribution  $f_U$ , by a change of basis this can be rotated into  $f_Q$  (as a rotation changes  $U \rightarrow Q$ ). This means that the above calculations holds also for  $f_U$  (since the distribution is itself a scalar) and just by rotating everything back we get the final result

$$\mathcal{F} = f_I \hat{1} + f_Q \sigma_3 + f_U \sigma_1 \quad (3.28a)$$

$$f_I \approx B(x) + G(x) \left( \Theta_I + \Theta_I^2 + \Theta_Q^2 + \Theta_U^2 \right) + Y(x) \frac{\Theta_I^2 + \Theta_Q^2 + \Theta_U^2}{2}, \quad (3.28b)$$

$$f_Q \approx G(x) \left( \Theta_Q + 2\Theta_I \Theta_Q \right) + Y(x) \Theta_I \Theta_Q, \quad (3.28c)$$

$$f_U \approx G(x) \left( \Theta_U + 2\Theta_I \Theta_U \right) + Y(x) \Theta_I \Theta_U, \quad (3.28d)$$



where we obtained  $f_u \sigma_1$  by the change of basis. Overall, the y-distortion can be read by averaging the phase space distributions

$$f \stackrel{\text{def}}{=} \frac{1}{2} \text{Tr}(\mathcal{F}) = B(x) + G(x) \left( \Theta_I + \Theta_I^2 + \Theta_Q^2 + \Theta_U^2 \right) + Y(x) \frac{\Theta_I^2 + \Theta_Q^2 + \Theta_U^2}{2}$$

and then by taking the spatial average over the temperature anisotropies (recall  $\langle \Theta \rangle = 0$  as in section 3.3.1)

$$\begin{aligned} \langle f \rangle &= B(x) + G(x) \left\langle \Theta_I^2 + \Theta_Q^2 + \Theta_U^2 \right\rangle + Y(x) \left\langle \frac{\Theta_I^2 + \Theta_Q^2 + \Theta_U^2}{2} \right\rangle \\ \Rightarrow \quad &\boxed{y = \frac{1}{2} \left\langle \Theta_I^2 + \Theta_Q^2 + \Theta_U^2 \right\rangle}. \end{aligned} \tag{3.29}$$

### 3.3.4 Dissipation of acoustic waves

We introduced *Silk damping* as the process that, through the mixing of blackbodies and their eventual successive Comptonization, dissipates the primordial perturbations that reentered the Hubble horizon. Now that we are familiar with these two processes, it is time to understand how the dissipation take place: we will begin by analyzing the dissipation of acoustic waves (which are the perturbations in the plasma induced by primordial scalar perturbation).



# Appendix A

## Differential geometry tools

### A.1 Maximally symmetric spaces

Consider  $\mathbb{R}^n$ , this space is highly symmetric: it is isotropic and homogeneous, or, in a simpler way, every point and every direction "look" the same.

This means that  $\mathbb{R}^n$  is symmetric under every rotation and translation: in  $n$ -dimensions there are  $n$  possible translations (along the  $n$  axes) and  $n\frac{n-1}{2}$  possible rotations (for each axis we can rotate it towards  $n-1$  other axes and to avoid double counting  $x \rightarrow y$  and  $y \rightarrow x$  we divide by 2), for a total number of symmetries equals to

$$n + n\frac{n-1}{2} = n\frac{n+1}{2}.$$

An  $n$ -dimensional manifold is said to be **maximally symmetric** if it possesses the same number of symmetries of  $\mathbb{R}^n$ . In the differential geometry language, a symmetry is defined through isometries, that are diffeomorphisms under which the metric tensor is invariant. For each symmetry of the metric we can define a **Killing vector**, which satisfies the Killing equation

$$0 = (\mathcal{L}_{\vec{K}}g)_{\mu\nu} = \nabla_\mu K_\nu + \nabla_\nu K_\mu, \quad (\text{A.1})$$

where  $\mathcal{L}_{\vec{K}}$  is the Lie derivative along  $\vec{K}$ , which is the Killing vector.

We now want to show that a maximally symmetric space really possesses the maximum number of symmetries, namely the maximum number of independent<sup>1</sup> Killing vectors. Consider the defining equation of the Riemann tensor applied to a 1-form

$$R^\mu_{\nu\rho\sigma}K_\mu = -[\nabla_\rho, \nabla_\sigma]K_\nu, \quad (\text{A.2})$$

this definition, combined with the algebraic Bianchi identity, ( $R^\mu_{\nu\rho\sigma} + R^\mu_{\rho\sigma\nu} + R^\mu_{\sigma\nu\rho} = 0$ ) implies that each Killing vector must satisfy

$$\nabla_\rho \nabla_\sigma K_\nu - \nabla_\sigma \nabla_\rho K_\nu + \nabla_\sigma \nabla_\nu K_\rho - \nabla_\nu \nabla_\sigma K_\rho + \nabla_\nu \nabla_\rho K_\sigma - \nabla_\rho \nabla_\nu K_\sigma = 0.$$

---

<sup>1</sup>Linearly independent here means that  $\exists$  a set of constants  $c_n$  such that

$$\sum_n c_n K_\mu^{(n)}(P) = 0 \quad \forall P \in \mathcal{M}.$$

## Appendix A. Differential geometry tools

---

This equation can be simplified by the Killing equation (A.1): using this relation we can sum pairs of terms obtaining

$$2(\nabla_\rho \nabla_\sigma K_\nu - \nabla_\sigma \nabla_\rho K_\nu - \nabla_\nu \nabla_\sigma K_\rho) = 0,$$

that using (A.2) turns out to be the following

$$R_{\nu\rho\sigma}^\mu K_\mu = \nabla_\nu \nabla_\sigma K_\rho. \quad (\text{A.3})$$

This equation shows that the second covariant derivative acts on Killing vectors just as a linear application. In this way we can determine every derivative of a Killing vector in a specific point, just by knowing its value and the value of its first covariant derivative, at the same point.

If we now Taylor expand the Killing vector around a point  $P$ , we will obtain some kind of expansion that depends on the value in  $P$  of all covariant derivatives of all orders, however we showed that we can evaluate those just knowing  $K_\mu(P)$  and  $\nabla_\nu K_\mu(P)$ . This means that we can express the Killing vector field as a combination of two functions that do not depend on the Killing vector itself or on its derivatives:

$$K_\mu(x) = A_\mu{}^\lambda(x, P) K_\lambda(P) + B_\mu{}^{\lambda\nu}(x, P) \nabla_\nu K_\lambda(P),$$

these functions depend only on  $x$ , the point  $P$ , and the metric, through the Riemann tensor. For this reason these must be the same functions for all Killing vectors:

$$K_\mu^{(n)}(x) = A_\mu{}^\lambda(x, P) K_\lambda^{(n)}(P) + B_\mu{}^{\lambda\nu}(x, P) \nabla_\nu K_\lambda^{(n)}(P). \quad (\text{A.4})$$

The above equation tells us that a given Killing vector is determined by  $K_\lambda^{(n)}(P)$ , which has  $N$  possible independent values, and by  $\nabla_\nu K_\lambda^{(n)}(P)$ , which has  $N \frac{N-1}{2}$  independent values, due to its antisymmetry (which is a consequence of the Killing equation (A.1)). In this way we have shown that the maximum number of independent Killing vectors in an  $N$ -dimensional manifold is exactly the same number that possesses  $\mathbb{R}^N$

$$N + N \frac{N-1}{2} = N \frac{N+1}{2}.$$

We want to conclude deriving the form that has the Riemann tensor in a maximally symmetric space.

In general, equation (A.3) must hold for every Killing vector, furthermore it also must be consistent with the commutator of covariant derivatives (A.2). This requirement and the fact that we have the maximum number of linearly independent Killing vectors will determine the form of  $R_{\nu\rho\sigma}^\mu$ . Consider (A.2) applied to the two indices tensor

$$[\nabla_\sigma, \nabla_\nu] \nabla_\mu K_\rho = -R_{\mu\sigma\nu}^\lambda \nabla_\lambda K_\rho - R_{\rho\sigma\nu}^\lambda \nabla_\mu K_\lambda,$$

the equation (A.3) can be used to obtain

$$\begin{aligned} \nabla_\sigma (R_{\nu\rho\mu}^\lambda K_\lambda) - \nabla_\nu (R_{\sigma\rho\mu}^\lambda K_\lambda) &= \\ &= \nabla_\sigma R_{\nu\rho\mu}^\lambda K_\lambda - \nabla_\nu R_{\sigma\rho\mu}^\lambda K_\lambda + R_{\nu\rho\mu}^\lambda \nabla_\sigma K_\lambda - R_{\sigma\rho\mu}^\lambda \nabla_\nu K_\lambda = -R_{\mu\sigma\nu}^\lambda \nabla_\lambda K_\rho - R_{\rho\sigma\nu}^\lambda \nabla_\mu K_\lambda. \end{aligned}$$

Now, Killing equation (A.1) allows us to move the index  $\lambda$  to the covariant derivative in each term, then, using a bunch of Kronecker deltas we get

$$(\nabla_\sigma R_{\nu\rho\mu}^\lambda - \nabla_\nu R_{\sigma\rho\mu}^\lambda) K_\lambda = (R_{\nu\rho\mu}^\lambda \delta_\sigma{}^\alpha - R_{\sigma\rho\mu}^\lambda \delta_\nu{}^\alpha + R_{\mu\sigma\nu}^\lambda \delta_\rho{}^\alpha - R_{\rho\sigma\nu}^\lambda \delta_\mu{}^\alpha) \nabla_\lambda K_\alpha.$$

This relation must hold for every Killing vector. We have the maximum number of independent Killing vectors, thus we can generate any other Killing vector from a combination of these. The general expansion (A.4) shows that a Killing vector field that vanishes in  $P$ , while its derivatives does not, can exist, and we surely can obtain it from a linear combination of the others. The above equation holds also for this one in  $P$  only if the right-hand side vanishes too, this can happen only if the term in parentheses is symmetric in  $\lambda \alpha$  (so that it vanishes when contracted with  $\nabla_\lambda K_\alpha$  that is antisymmetric)

$$R_{\nu\rho\mu}^\lambda \delta_\sigma^\alpha - R_{\sigma\rho\mu}^\lambda \delta_\nu^\alpha + R_{\mu\sigma\nu}^\lambda \delta_\rho^\alpha - R_{\rho\sigma\nu}^\lambda \delta_\mu^\alpha = R_{\nu\rho\mu}^\alpha \delta_\sigma^\lambda - R_{\sigma\rho\mu}^\alpha \delta_\nu^\lambda + R_{\mu\sigma\nu}^\alpha \delta_\rho^\lambda - R_{\rho\sigma\nu}^\alpha \delta_\mu^\lambda.$$

Contracting  $\mu$  and  $\alpha$ , recalling that  $R_{\nu\mu\rho}^\mu = R_{\nu\rho}$  and  $R_{\mu\nu\rho}^\mu = 0$ , we find

$$R_{\nu\rho\sigma}^\lambda - R_{\sigma\rho\nu}^\lambda + R_{\rho\sigma\nu}^\lambda - N R_{\rho\sigma\nu}^\lambda = -R_{\nu\rho} \delta_\sigma^\lambda + R_{\sigma\rho} \delta_\nu^\lambda - R_{\rho\sigma\nu}^\lambda,$$

here we recognize that, from the algebraic Bianchi identity,

$$R_{\sigma\rho\nu}^\lambda = -R_{\sigma\nu\rho}^\lambda = R_{\nu\rho\sigma}^\lambda + R_{\rho\sigma\nu}^\lambda,$$

which cancels two terms in the previous equation, that now reads, after having lowered one index,

$$(N-1)R_{\lambda\rho\sigma\nu} = R_{\nu\rho}g_{\sigma\lambda} - R_{\sigma\rho}g_{\nu\lambda}. \quad (\text{A.5})$$

Notice that the above equation must be antisymmetric in  $\lambda \rho$  (due to the properties of the Riemann tensor),

$$R_{\nu\rho}g_{\sigma\lambda} - R_{\sigma\rho}g_{\nu\lambda} = -R_{\nu\lambda}g_{\sigma\rho} + R_{\sigma\lambda}g_{\nu\rho},$$

contracting  $\lambda \nu$ , this relation becomes

$$R_{\sigma\rho} - N R_{\sigma\rho} = -R g_{\sigma\rho} + R_{\sigma\rho}, \quad \Rightarrow \quad \boxed{R_{\sigma\rho} = \frac{R}{N} g_{\sigma\rho}}, \quad (\text{A.6})$$

inserting this one into the (A.5) we get our final result

$$\boxed{R_{\lambda\rho\sigma\nu} = \frac{R}{N(N-1)}(g_{\nu\rho}g_{\lambda\sigma} - g_{\sigma\rho}g_{\lambda\nu})}. \quad (\text{A.7})$$



# Appendix B

## Thermodynamics tools

### B.1 Phase space distribution and thermodynamics observable

#### B.1.1 Small chemical potential approximation

In this appendix we will show how to approximate the energy and number densities for a gas of photons in the presence of a small chemical potential. The goal is to obtain corrections to

$$\rho = a_R T^4, \quad n = b_R T^3,$$

that are obtained from the Planck distribution.

Let's start from the number density, analogous calculations will then give the result for the energy density. From the definition we have

$$\begin{aligned} n &= \frac{g}{(2\pi)^3} \int d^3p \frac{1}{\exp(\frac{\nu}{k_B T} + \mu) - 1} = \frac{g}{2\pi^2} \int_0^\infty dp \frac{p^2}{\exp(\frac{\nu}{k_B T} + \mu) - 1} \\ &\quad \downarrow \quad p = \nu, \quad x \stackrel{\text{def}}{=} \frac{\nu}{k_B T} \\ &= \frac{g}{2\pi^2} (k_B T)^3 \int_0^\infty dx \frac{x^2}{\exp(x + \mu) - 1} = \frac{g}{2\pi^2} (k_B T)^3 \int_0^\infty dx \frac{x^2 e^{-(x+\mu)}}{1 - e^{-(x+\mu)}} \\ &= \frac{g}{2\pi^2} (k_B T)^3 \int_0^\infty dx x^2 e^{-(x+\mu)} \sum_{n=0}^\infty e^{-n(x+\mu)} = \frac{g}{2\pi^2} (k_B T)^3 \sum_{n=0}^\infty \int_0^\infty dx x^2 e^{-(n+1)(x+\mu)} \\ &= \frac{g}{2\pi^2} (k_B T)^3 \sum_{n=0}^\infty \frac{2}{(n+1)^3} e^{-(n+1)\mu} \approx \frac{g}{2\pi^2} (k_B T)^3 \sum_{n=0}^\infty 2 \frac{1 - (n+1)\mu}{(n+1)^3} \\ &\quad \downarrow \quad \zeta(z) \stackrel{\text{def}}{=} \sum_{n=1}^\infty \left(\frac{1}{n}\right)^z \quad \text{Riemann zeta function} \\ &= \frac{g}{\pi^2} (k_B T)^3 [\zeta(3) - \mu \zeta(2)] = b_R T^3 \left[ 1 - \mu \frac{\zeta(2)}{\zeta(3)} \right] \end{aligned} \tag{B.1}$$

where in the last line we defined  $b_R \stackrel{\text{def}}{=} \frac{g}{\pi^2} k_B^3 \zeta(3)$  with  $g = 2$ .

## Appendix B. Thermodynamics tools

The same calculation can be applied to the energy density, we just need to pay attention to the extra  $\nu$  factor in the integrand: ultimately this will lead to a different integral inside the series expansion, hence different points of the zeta function will appear. Again from the definition and preceding as before

$$\begin{aligned}\rho &= \frac{g}{(2\pi)^3} \int d^3p \frac{E}{\exp(\frac{\nu}{k_B T} + \mu) - 1} = \frac{g}{2\pi^2} \int_0^\infty dp \frac{p^3}{\exp(\frac{\nu}{k_B T} + \mu) - 1} \\ &= \frac{g}{2\pi^2} (k_B T)^4 \sum_{n=0}^\infty \int_0^\infty dx x^3 e^{-(n+1)(x+\mu)} = \frac{g}{2\pi^2} (k_B T)^4 \sum_{n=0}^\infty \frac{6}{(n+1)^4} e^{-(n+1)\mu} \\ &\approx \frac{g}{2\pi^2} (k_B T)^4 \sum_{n=0}^\infty 6 \frac{1 - (n+1)\mu}{(n+1)^4} = \frac{3g}{\pi^2} (k_B T)^4 [\zeta(4) - \mu\zeta(3)] = a_R T^4 \left[ 1 - \mu \frac{\zeta(3)}{\zeta(4)} \right] \quad (\text{B.2})\end{aligned}$$

where we defined  $a_R \stackrel{\text{def}}{=} \frac{3g}{\pi^2} k_B^4 \zeta(4) = \frac{\pi^2}{15} k_B^4$  with  $g = 2$ .

## B.2 Scalar perturbed Liouville operator

In this appendix we will show how to obtain the perturbed Liouville operator, at first order, for the photon phase space in the presence of scalar perturbations. Since we are interested only in first order perturbations, in the next calculations, we will always neglect higher order contributions by Taylor expanding every function of the perturbations. We will work with the perturbed metric in the conformal Newtonian gauge, which is given by

$$ds^2 = a^2(\eta) \left[ -(1 + 2\Psi)d\tau^2 + (1 - 2\Phi)\delta_{ij}dx^i dx^j \right].$$

The Liouville operator, defined in , reads

$$\hat{\mathbf{L}}[f] = \frac{df}{d\tau} = \frac{\partial f}{\partial \tau} + \frac{\partial f}{\partial x^i} \frac{dx^i}{d\tau} + \frac{\partial f}{\partial p} \frac{dp}{d\tau} + \frac{\partial f}{\partial \hat{p}^i} \frac{d\hat{p}^i}{d\tau},$$

where  $p^i = p \hat{p}^i$  (with  $\hat{p}^i \hat{p}^j \delta_{ij} = 1$ ) is the local 3-momentum of the photon, and we already considered that the local energy and the 3-momentum are not independent due to the mass-shell condition. We also assume that  $f$  can also be expanded on a background, which corresponds to the black body radiation, plus a first order perturbation (see section 2.2 for more on this expansion). Note that, since the blackbody radiation is isotropic and homogeneous (it does not depend on  $x^i$  or  $\hat{p}^i$ ) the two factors  $\frac{\partial f}{\partial x^i}$  and  $\frac{\partial f}{\partial \hat{p}^i}$  are only first order contributions. This observation will simplify our calculations later on since it implies that  $\frac{dx^i}{d\tau}$  and  $\frac{d\hat{p}^i}{d\tau}$  are needed only at order zero.

Let's spend some time discussing local energy and momentum. The local energy is defined as the energy of a photon in the local rest frame of an observer, thus for a static observer ( $U^\mu = (\frac{1-\Psi}{a}, 0, 0, 0)$ ) it reads

$$E = -U_\mu P^\mu = a(1 + 2\Psi)P^0(1 - \Psi) \approx aP^0(1 + \Psi).$$

The local momentum defined in the same way, therefore it must satisfy the usual Minkowskian mass-shell relation  $E = \sqrt{p^i p^j \delta_{ij}}$ . Using the mass-shell condition for the 4-momentum of



the photon  $P^\mu P_\mu = 0$ , we can write

$$\begin{aligned} P^\mu P_\mu &= -a^2(1+2\Psi)(P^0)^2 + a^2(1+2\Phi)P^i P^j \delta_{ij} = 0, \\ \Rightarrow P^0 &= \sqrt{\frac{1+2\Phi}{1+2\Psi}} P^i P^j \delta_{ij} \approx (1+\Phi-\Psi)\sqrt{P^i P^j \delta_{ij}}, \\ E &= \sqrt{p^i p^j \delta_{ij}} = aP^0(1+\Psi) = a(1+\Phi)\sqrt{P^i P^j \delta_{ij}}. \end{aligned}$$

In this way we identify  $p^i = a(1+\Phi)P^i$  as the local 3-momentum. Note that it follows from  $E = \sqrt{p^i p^j \delta_{ij}}$  that decomposing  $p^i = p \hat{p}^i$  then  $p = E$ , as we expect in the local reference frame.

We are now ready to determine all the contribution to the Liouville operator. First, from the above discussion on the local energy and momentum, we recognize that

$$\frac{dx^i}{d\tau} = \frac{P^i}{P^0} = \frac{(1-\Phi)p^i}{(1+\Psi)E} \approx \hat{p}^i(1-\Psi-\Phi). \quad (\text{B.3})$$

Then we have to evaluate

$$\frac{dp}{d\tau} = \frac{d}{d\tau} aP^0(1+\Psi) = \mathcal{H}p + a(1+\Psi)\frac{dP^0}{d\tau} + p\Psi',$$

therefore we need to compute  $\frac{dP^0}{d\tau}$ . This can be accomplished by using the geodesic equation

$$\frac{dP^0}{d\tau} = \frac{dP^0}{d\lambda} \frac{1}{P^0} = -\frac{\Gamma_{\mu\nu}^0}{P^0} P^\mu P^\nu,$$

in the conformal Newtonian gauge the relevant Christoffel symbols are

$$\Gamma_{00}^0 = \mathcal{H} + \Psi', \quad \Gamma_{0i}^0 = \Psi_{,i}, \quad \Gamma_{ij}^0 = \left[ \mathcal{H}(1+2\Phi-2\Psi) + \Phi' \right] \delta_{ij}.$$

In this way we get

$$\begin{aligned} \frac{dp}{d\tau} &= (\mathcal{H} + \Psi')p - a(1+\Psi) \times \\ &\quad \times \left[ (\mathcal{H} + \Psi')P^0 + P^i \Psi_{,i} + \left( \mathcal{H}(1+2\Phi-2\Psi) + \Phi' \right) \frac{P^i P^j \delta_{ij}}{P^0} \right] \\ &\approx \mathcal{H}p - \mathcal{H}p + \Psi'p - \Psi'p - p^i \Psi_{,i} - \mathcal{H}p - \Phi'p \\ &= -\mathcal{H}p - \Phi'p - p^i \Psi_{,i} \end{aligned} \quad (\text{B.4})$$

We now have to obtain

$$\frac{d\hat{p}^i}{d\tau} = \frac{d}{d\tau} \frac{p^i}{p} = \frac{dp^i}{d\tau} \frac{1}{p} - \frac{dp}{d\tau} \frac{p^i}{p^2},$$

in which we can get  $\frac{dp^i}{d\tau}$  by (B.4) noting

$$\frac{dp}{d\tau} = \frac{d}{d\tau} \sqrt{p^i p^j \delta_{ij}} = \frac{p^j}{p} \frac{dp^i}{d\tau} \delta_{ij}.$$

These two simple calculations, with equation (B.4), show that  $\frac{d\hat{p}^i}{d\tau}$  has no zeroth order contributions, but only first order ones. Therefore, when multiplied by  $\frac{\partial f}{\partial \hat{p}^i}$  a second order, in perturbations, term is generated, and for this reason we will neglect its contributions.

Inserting equations (B.3) and (B.4) into the Liouville operator we end up with

$$\begin{aligned} \hat{\mathbf{L}}[f] &= \frac{\partial f}{\partial \tau} + \hat{p}^i \frac{\partial f}{\partial x^i} - p \left( \mathcal{H} - \frac{\partial \Phi}{\partial \tau} + \frac{\partial \Phi}{\partial x^i} \hat{p}^i \right) \frac{\partial f}{\partial p}, \\ &\quad \downarrow \text{moving to cosmic time } dt = a \, d\tau, \\ \hat{\mathbf{L}}[f] &= \frac{\partial f}{\partial t} + \frac{\hat{p}^i}{a} \frac{\partial f}{\partial x^i} - p \left( H - \frac{\partial \Phi}{\partial t} + \frac{\partial \Phi}{\partial x^i} \frac{\hat{p}^i}{a} \right) \frac{\partial f}{\partial p} \end{aligned} \quad (\text{B.5})$$

### B.3 Collision term

### B.4 Tensor perturbed Liouville operator

Previously, we considered how scalar perturbations of the metric (which are in general the most studied) contributes to the evolution of the phase space associated to photons. Now, we are going to follow the same steps to study instead the effects of tensor perturbations. Again keep in mind that we will only consider first order perturbations and higher contributions will be neglected.

Tensor perturbations are described by the transverse traceless tensor  $h_{ij}$ , which happens to be gauge invariant (section ). At first order in perturbation theory the tensor perturbed metric thus reads

$$ds^2 = a^2(-d\tau^2 + (\delta_{ij} + h_{ij})dx^i dx^j).$$

The Liouville operator, as usual, is defined as

$$\hat{\mathbf{L}}[f] = \frac{df}{d\tau} = \frac{\partial f}{\partial \tau} + \frac{\partial f}{\partial x^i} \frac{dx^i}{d\tau} + \frac{\partial f}{\partial p} \frac{dp}{d\tau} + \frac{\partial f}{\partial \hat{p}^i} \frac{d\hat{p}^i}{d\tau},$$

where  $p^i = p \hat{p}^i$  is again the local 3-momentum, note that even though its definition (as the momentum observed by a static observer) won't change, its relation to the 4-momentum is changed due to the different metric considered. Now, indeed the local energy is

$$U^\mu = (a^{-1}, 0, 0, 0) \Rightarrow E = -U_\mu P^\mu = aP^0$$

and then requiring that  $E = \sqrt{p^i p^j \delta_{ij}} = p$  we observe that the form of the local 3-momentum should be

$$\begin{aligned} P^\mu P_\mu &= -a^2(P^0)^2 + a^2(\delta_{ij} + h_{ij})P^i P^j = 0 \Rightarrow (P^0)^2 = (\delta_{ij} + h_{ij})P^i P^j \\ E^2 &= p_i p_j \delta_{ij} = (aP^0)^2 = a^2(\delta_{ij} + h_{ij})P^i P^j \Rightarrow p_i = a(\delta_{ij} + \frac{1}{2}h_{ij})P^j, \end{aligned}$$

where we used that there is no difference between covariant e contravariant vectors for the local momentum since in the local reference frame the spatial metric is the identity.

We can now proceed and evaluate the first contribution to the Liouville operator  $\frac{dx^i}{d\tau}$ , keeping in mind that (as in appendix B.2) we only need order zero contributions.

$$\frac{dx^i}{d\tau} = \frac{P^i}{P^0} = \frac{p_j}{E}(\delta^{ij} - \frac{1}{2}h^{ij}) \approx \frac{p^i}{E}. \quad (\text{B.6})$$

The second factor is instead needed up to the first order. We start by evaluating

$$\frac{dp}{d\tau} = \frac{d}{d\tau} a P^0 = \mathcal{H}p + a \frac{dP^0}{d\tau} = \mathcal{H}p - \frac{a}{P^0} \Gamma_{\mu\nu}^0 P^\mu P^\nu,$$

where in the last step we used the geodesic equation. With the metric in consideration the relevant Christoffel symbols read:

$$\Gamma_{00}^0 = \mathcal{H}, \quad \Gamma_{0i}^0 = 0, \quad \Gamma_{ij}^0 = \mathcal{H}(\delta_{ij} + h_{ij}) + \frac{1}{2} h'_{ij}.$$

With these, recalling that  $p^2 = a^2(\delta_{ij} + h_{ij})P^i P^j$  and that at order zero  $p^\mu = aP^\mu$ , we finally get

$$\frac{dp}{d\tau} = -\frac{a}{P^0} \left[ \mathcal{H}(\delta_{ij} + h_{ij}) - \frac{1}{2} h'_{ij} \right] P^i P^j = -\mathcal{H}p - \frac{1}{2} h'_{ij} \hat{p}^i \hat{p}^j. \quad (\text{B.7})$$

We are left with  $\frac{d\hat{p}^i}{d\tau}$  to be evaluated, however as in appendix B.2, we can show that this gives no zeroth order contribution, generating in the Liouville operator a second order term (since  $\frac{\partial f}{\partial \hat{p}^i}$  has to be of first order too since the unperturbed distribution is isotropic) that can be neglected.

Summing all up we get that the Liouville operator now reads

$$\begin{aligned} \hat{\mathbf{L}}[f] &= \frac{\partial f}{\partial \tau} + \hat{p}^i \frac{\partial f}{\partial x^i} - \frac{1}{2} \frac{\partial f}{\partial \tau} h'_{ij} \hat{p}^i \hat{p}^j \\ &\quad \downarrow \text{moving to cosmic time } dt = a \, d\tau, \\ \hat{\mathbf{L}}[f] &= \frac{\partial f}{\partial t} + \frac{\hat{p}^i}{a} \frac{\partial f}{\partial x^i} - \frac{1}{2} \frac{\partial f}{\partial t} \dot{h}_{ij} \hat{p}^i \hat{p}^j. \end{aligned} \quad (\text{B.8})$$



# Bibliography

- [1] J. R. Bond and G. Efstathiou. The statistics of cosmic background radiation fluctuations. *Monthly Notices of the Royal Astronomical Society*, 226(3):655–687, 06 1987.
- [2] J. Chluba. Green’s function of the cosmological thermalization problem. *Monthly Notices of the Royal Astronomical Society*, 434(1):352–357, June 2013.
- [3] Jens Chluba, Liang Dai, Daniel Grin, Mustafa A. Amin, and Marc Kamionkowski. Spectral distortions from the dissipation of tensor perturbations. *Monthly Notices of the Royal Astronomical Society*, 446(3):2871–2886, November 2014.
- [4] Scott Dodelson and Fabian Schmidt. *Modern Cosmology*. Academic Press, 2nd edition, 2020.
- [5] D. J. Fixsen, E. S. Cheng, J. M. Gales, J. C. Mather, R. A. Shafer, and E. L. Wright. The cosmic microwave background spectrum from the full coBE FIRS data set. *The Astrophysical Journal*, 473:576–587, 1996.
- [6] Wayne Hu and Martin White. CMB anisotropies: Total angular momentum method. *Physical Review D*, 56(2):596–615, July 1997.
- [7] Edwin Hubble. A Relation between Distance and Radial Velocity among Extra-Galactic Nebulae. *Proceedings of the National Academy of Science*, 15(3):168–173, March 1929.
- [8] R. Khatri, R. A. Sunyaev, and J. Chluba. Mixing of blackbodies: entropy production and dissipation of sound waves in the early universe. *Astronomy and Astrophysics*, 543:A136, July 2012.
- [9] Matteo Lucca, Nils Schöneberg, Deanna C. Hooper, Julien Lesgourgues, and Jens Chluba. The synergy between CMB spectral distortions and anisotropies. *Journal of Cosmology and Astroparticle Physics*, 2020(02):026–026, February 2020.
- [10] Y. B. Zeldovich, A. F. Illarionov, and R. A. Sunyaev. Influence of Energy Release on the Radiation Spectrum in the Hot Model of the Universe. *Zhurnal Eksperimentalnoi i Teoreticheskoi Fiziki*, 68:1217, January 1972.